

Role of scrambling and noise in temporal information processing with quantum systems

Weijie Xiong,^{1,2} Zoë Holmes,^{1,2} Armando Angrisani,^{1,2}
Yudai Suzuki,^{1,2} Thiparat Chotibut,³ and Supanut Thanasilp^{1,2,3}

¹*Institute of Physics, Ecole Polytechnique Fédérale de Lausanne (EPFL), Lausanne, Switzerland*

²*Centre for Quantum Science and Engineering, Ecole Polytechnique Fédérale de Lausanne (EPFL), Lausanne, Switzerland*

³*Chula Intelligent and Complex Systems Lab, Department of Physics,
Faculty of Science, Chulalongkorn University, Bangkok, Thailand*

(Dated: May 21, 2025)

Scrambling quantum systems have been demonstrated as effective substrates for temporal information processing. While their role in providing rich feature maps has been widely studied, a theoretical understanding of their performance in temporal tasks is still lacking. Here we consider a general quantum reservoir processing framework that captures a broad range of physical computing models with quantum systems. We examine the scalability and memory retention of the model with scrambling reservoirs modelled by high-order unitary designs in both noiseless and noisy settings. In the former regime, we show that measurement readouts become exponentially concentrated with increasing reservoir size, yet strikingly do not worsen with the reservoir iterations. Thus, while repeatedly reusing a small scrambling reservoir with quantum data might be viable, scaling up the problem size deteriorates generalization unless one can afford an exponential shot overhead. In contrast, the memory of early inputs and initial states decays exponentially in *both* reservoir size and reservoir iterations. In the noisy regime, we also prove exponential memory decays with iterations for local noisy channels. Proving these results required us to introduce new proof techniques for bounding concentration in temporal quantum learning models.

I. INTRODUCTION

Physical computing is an emerging computational paradigm in which the native, continuous dynamics of a physical substrate is used directly as part of a computational process, rather than being fully abstracted into digital logic. This approach can offer adaptability and, in some implementations, substantial energy savings, both of which are critical for large-scale artificial intelligence [1–3]. Among such substrates, quantum systems are especially appealing due to their large Hilbert spaces and the complex spatio-temporal correlations they naturally generate, making them well-suited for information processing tasks involving spatially or temporally correlated data [4, 5]. Recent experiments indeed show that reusing a quantum system repeatedly can enhance performance in time-series prediction, suggesting a *recurrent* or *iterative* mode of operation that interleaves these quantum systems with streams of quantum data [6, 7].

Quantum reservoir processing (QRP) [8–13] exemplifies this iterative physical computing paradigm. Building upon the input-feedback strategy in classical reservoir computing [14–16], this approach has recently gained considerable attention as a compelling non-variational framework for leveraging quantum substrates for temporal information processing [8–13]. At its core, QRP processes input states using a fixed quantum evolution (the *reservoir*) to generate a rich feature map. The reservoir-processed states are then

read out via quantum measurements and the resulting vector of expectation values are trained classically via linear regression to solve a given learning task. This approach can tackle not only standard machine learning problems with classical data [17–21], but also intrinsically quantum problems such as state discrimination and tomography [11, 22–26] and quantum dynamics prediction [27]. Experimental realizations across various platforms further highlight QRP’s viability [7, 12, 28–31], while a growing benchmarking studies chart its performance [4, 6, 8, 9, 11, 19, 30, 32–43] and hints towards the potential to rival large classical neural networks [17, 19, 44].

Many QRP schemes utilize quantum scrambling under chaotic dynamics as a quantum reservoir to create a natural, high-dimensional feature map for input data [8, 9, 35]. Numerous studies highlight correlations between the degree of scrambling of the reservoir and the QRP performance [25, 31, 34, 35, 45]. Yet existing work is confined to small problem sizes [7, 12, 17, 19, 28–30], thus it remains unclear whether these promising results survive when the reservoir size enters the regime where real quantum advantages might appear. In the absence of large-scale, high-quality quantum hardware, theoretical analysis is the only viable avenue to study these phenomena on larger scales.

In this work, we idealize scrambling reservoirs as unitaries drawn from a high-order design ensemble, to capture the extreme-scrambling limit while enable rigorous theoretical analysis with Haar integration [46, 47]. Related tech-

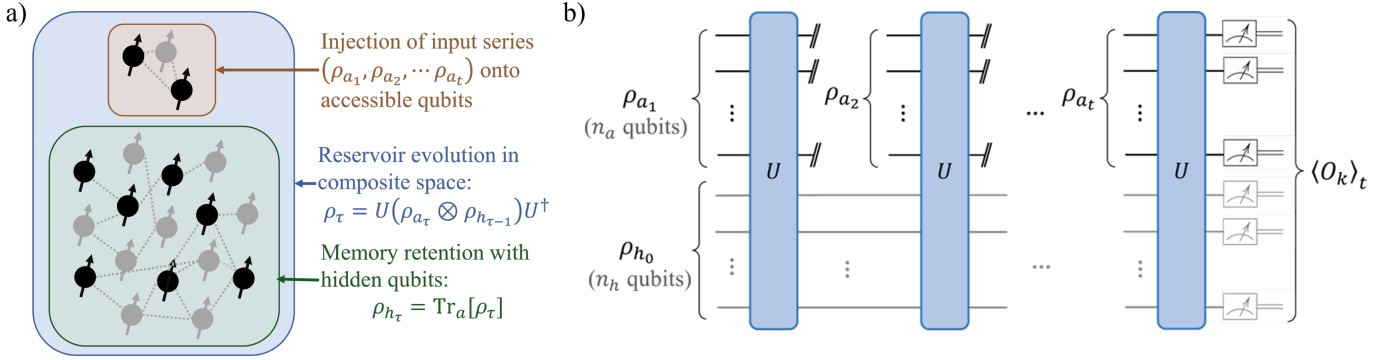


Figure 1. **Framework of QRP (a) and its circuit diagram (b).** The quantum reservoir consists of $n = n_a + n_h$ qubits. n_a denotes the number of accessible qubits, which are used for data uploading; and n_h the number of hidden qubits. After injecting the input states into accessible qubits, the reservoir dynamics, described by some unitary U , will be applied to the composite system of accessible and hidden qubits. The key component of a RC system is its memory. In QRP, while the accessible qubits will be initialized after each iteration and subsequently be encoded with data of next time step, the hidden qubits will never be initialized and their state are obtained from the reduced state of the last reservoir evolution in hidden space. Thus, the hidden qubits play the role of quantum memory and store the information of previous inputs.

niques already establish scalability barriers for variational quantum algorithms [48, 49], quantum kernels [50], and quantum extreme learning machines (QELMs), the single-pass variant of QRP such that the reservoir evolution is applied only once [51, 52]. By contrast, the full QRP protocol is much more demanding: a fixed reservoir repeatedly interleaves with a stream of input time-series. This temporal correlation between reservoir iterations hinders standard analytical techniques. To address this challenge, we apply tensor-diagram approaches to unroll multi-step QRP into a single high-moment Haar integral amenable for scalability analysis.

With this approach, we derive an asymptotic concentration bound for the QRP's output magnitudes. The bound reveals the exponential concentration of the output with increasing reservoir size (i.e., the number of qubits), yet incurs no further concentration over successive reservoir iterations. On the one hand, this exponential concentration presents a scalability barrier- their outputs for distinct inputs become effectively data independent for large scale problems. On the other hand, as reservoir iterations cost no further concentration, repeatedly reusing a modest-sized scrambling reservoir remains effective with a feasible number of measurement shots. This potentially leaves room for practical data processing advantages for quantum data in the spirit of physical computing.

We also examine how a scrambling reservoir retains memory of its past. For this, we introduce a *memory indicator* that quantifies how strongly outputs depend on earlier inputs or initial reservoir states. Previous studies

have indicated that the memory of QRP generally decays exponentially over reservoir iterations [30, 53]. Here we compute the exact rate of memory decay for a fully scrambling reservoir. Viewed positively, this decay reflects the Fading Memory Property (FMP) and Echo State Property (ESP) - behaviors necessary for operational QRP. However, the memory indicators also exponentially decay, ultimately rendering the model input-insensitive at large reservoir sizes. Thus, while modest scale QRP with fully scrambling reservoirs could remain viable, QRP with large highly scrambling reservoirs will be unusable in practice as it becomes input-agnostic and its memory fades exponentially fast. This highlights the need for caution when relying solely on standard FMP and ESP for designing scalable QRP.

Realizing QRP on near-term quantum devices unavoidably involves hardware noise. We further extend our analysis to scrambling reservoirs with both unital and non-unital noises. We derive upper bounds showing that the reservoir loses the memory of an initial state exponentially with increasing temporal iterations. While recent evidence suggests certain forms of dissipation or decoherence can be used as a computational resource for improved performance on small QRP [38, 54–58], our analysis explicitly shows how generic noise channels can compound concentration effects over multiple iteration steps, leading to vanishing memory and scalability barrier for QRP in the presence of noise.

Finally, to explore how one might sidestep these scalability barriers, we examine two *moderate-scrambling* reservoirs: (i) alternating layer circuits and (ii) chaotic Ising

evolutions, with intermediate depth and evolution time respectively. We observe only *polynomial* rather than exponential output concentration, albeit at the cost of reduced expressive power and potentially classical simulability. These examples suggest that carefully controlling the degree of scrambling may provide a middle-ground to engineer quantum reservoirs to remain sufficiently expressive while avoiding exponential resource overheads.

II. PRELIMINARIES

A. Framework of QRP

To systematically examine quantum reservoir processing (QRP) across diverse experimental platforms, we recast it in a unified framework that naturally accommodates both quantum and classical inputs. This abstraction captures the essential structure encompassing most current proposals for quantum reservoir computing, allowing for the applicability of our results across quantum substrates.

Concretely, we will consider a dataset \mathcal{S} containing D time series, each of length t , denoted by $\{\rho_{a_t}^{(l)}\}_{l=1}^D$. Every sequence of input quantum states $\rho_{a_t}^{(l)} = (\rho_{a_1}^{(l)}, \rho_{a_2}^{(l)}, \dots, \rho_{a_t}^{(l)})$ is associated with a target output sequence $\mathbf{y}_t^{(l)} = (y_1^{(l)}, \dots, y_t^{(l)})$. The input sequences can be intrinsic quantum data such as time-dependent density matrices generated from quantum dynamics [59], or they can arise from classical data s_τ (e.g. Mackey-Glass chaotic sequences) that have been encoded through a unitary $U_{\text{enc}}(s_\tau)$ acting on a fixed reference state.

Given a training subset $\mathcal{S}_{\text{tr}} = \{(\rho_{a_t}^{(l)}, \mathbf{y}_t^{(l)})\}_{l=1}^{D_{\text{tr}}} \subseteq \mathcal{S}$, our goal is to predict an output y_τ associated with a previously unseen input $\rho_{a_\tau} \notin \mathcal{S}_{\text{tr}}$. For simplicity, we assume the output is scalar, though it may generally be vector-valued.

Concretely, the quantum reservoir architecture consists of

- n_a *accessible qubits*, onto which each new input ρ_{a_τ} is loaded at time τ (replacing the previous accessible-qubit state),
- n_h *hidden qubits*, which accumulate information from past inputs and hidden-qubit states. We denote their initial state by ρ_{h_0} , and throughout the reservoir iterations is never reinitialized.

At each time step τ , the QRP model recursively processes the data stream as follows (see Fig. 1):

- (i) **Data injection:** Replace the state of the n_a accessible qubits by the new input ρ_{a_τ} . The hidden qubits

remain in the state carried over from the previous iteration.

- (ii) **Reservoir evolution:** Apply a *fixed* reservoir evolution U acting on all $n_a + n_h$ qubits (here we assume a unitary channel for simplicity, although we will consider more general noisy channels in subsequent sections.):

$$\rho_\tau = U(\rho_{a_\tau} \otimes \rho_{h_{\tau-1}})U^\dagger, \quad (1)$$

where $\rho_{h_{\tau-1}} = \text{Tr}_a[\rho_{\tau-1}]$ is the hidden-qubit state from the previous time step, and ρ_{h_0} denotes the initial hidden-qubit state.

After processing the input sequence by repeating (i) and (ii) up to time step $\tau \leq t$, one can choose to perform measurement readout to obtain QRP outputs.

- (iii) **Measurement readout:** Measures a fixed set of observables $\{O_k\}_{k=1}^M$ on the state ρ_τ . The QRP output associated with the k^{th} component of the total readout is then

$$\langle O_k \rangle_\tau = \text{Tr}[O_k \rho_\tau], \quad (2)$$

leading to the ideal (shot noise-free) readout of the form

$$\mathbf{r}_\tau = (\text{Tr}[O_1 \rho_\tau], \dots, \text{Tr}[O_M \rho_\tau]). \quad (3)$$

In practice, however, these outputs are estimated with finite measurement shots leading to limited precision due to shot noise [13].

- (iv) **Classical post-processing:** To approximate the label y_τ , one typically forms a linear combination of these measured QRP observables, namely

$$f_\tau(\rho_{a_\tau}; \boldsymbol{\eta}) = \sum_{k=1}^M \eta_k \text{Tr}[O_k \rho_\tau], \quad (4)$$

where $\rho_{a_\tau} = (\rho_{a_1}, \rho_{a_2}, \dots, \rho_{a_\tau})$ and $\tau \leq t$ specifies the number of iterations of QRP, $\boldsymbol{\eta} = (\eta_1, \dots, \eta_M) \in \mathbb{R}^M$ are trainable weights and we recall that ρ_τ implicitly depends on ρ_{a_τ} .

The optimal weights are then obtained by classically minimising an empirical loss, $\boldsymbol{\eta}^* = \arg \min_{\boldsymbol{\eta}} [\mathcal{L}(\boldsymbol{\eta})]$, which, for suitable choices of the loss \mathcal{L} (e.g. regularised least-squares), reduces to standard linear regression and therefore admits a closed-form solution. For example, one could use the mean-squared error loss

$$\mathcal{L}(\boldsymbol{\eta}) = \frac{1}{|\mathcal{T}_{\text{tr}}|} \sum_{\tau \in \mathcal{T}_{\text{tr}}} \mathcal{L}_\tau(\boldsymbol{\eta}), \quad (5)$$

where $\mathcal{T}_{\text{tr}} \subseteq [t]$ specifies the time steps used for training – typically those after a wash-out period, $\mathcal{T}_{\text{tr}} = \{t_w, t_w + 1, \dots\}$ with $t_w \gg 1$ [4] – and

$$\mathcal{L}_{\tau}(\boldsymbol{\eta}) = \frac{1}{D_{\text{tr}}} \sum_{(\boldsymbol{\rho}_{a_t}^{(l)}, \mathbf{y}_t^{(l)}) \in \mathcal{S}_{\text{tr}}} \left(f_{\tau}(\boldsymbol{\rho}_{a_t}^{(l)}; \boldsymbol{\eta}) - y_t^{(l)} \right)^2, \quad (6)$$

where $\boldsymbol{\rho}_{a_t}^{(l)}$ is a subseries of element $\boldsymbol{\rho}_{a_t}^{(l)}$ of the training set \mathcal{S}_{tr} . With that loss form, one obtains closed-form optimal weights $\boldsymbol{\eta}^*$ [8]. Then, the trained model $f_{\boldsymbol{\eta}^*}(\cdot)$ can be used to predict or classify unseen time-series data.

The special case $t = 1$, involving a single reservoir evolution and a single input datum, corresponds to the *quantum extreme learning machine* (QELM) framework, of which Fourier expressivity and scalability barriers were analyzed in Ref. [51]. In contrast, the multi-step QRP protocol boosts expressivity by repeatedly interleaving fresh inputs into the reservoir dynamics, yet this recurrent coupling introduces scalability analysis challenges.

B. Memory properties of reservoirs

Here we review relevant memory properties of reservoirs, which have been widely studied in the context of theory of dynamical systems [8, 10, 60]. Two fundamental memory properties, that are necessary for reservoir computing to be operational (though by themselves insufficient to guarantee strong predictive performance) are:

1. *Fading Memory Property (FMP)*: A reservoir has the FMP if the influence of inputs fed *far in the past* on the present output *fades away* in time. In other words, perturbations in the input $\rho_{a_{t-\tau}}$ for large τ cause only a negligible difference in the current output y_t . FMP ensures that the reservoir focuses on the relevant recent history of the input and is not overwhelmed by far past information.
2. *Echo State Property (ESP)*: A reservoir has the ESP if the reservoir state ρ_{h_t} at large t depends only on the driving inputs $\{\rho_{a_{\tau}}\}_{\tau \leq t}$ and *not* on the reservoir's initial condition, i.e., the initial state of hidden qubits ρ_{h_0} . The ESP thus guarantees that, after a long washout (burn-in) period, the reservoir state becomes a function of only input sequences, and of only recent inputs if the reservoir also has FMP, but *independent* of how the reservoir was initially prepared. Without ESP, the output could spuriously depend on arbitrary past state preparations, making the system ill-defined for consistent time series processing.

Both properties are necessary conditions for the QRP model to be operative [10, 60]. Moreover, by properly choosing a reservoir, such as a sufficiently large Echo State Network (ESN), certain QRP models with such properties can achieve a *universal approximation* of fading memory maps and possess short-term sequence-modelling capabilities [60, 61].

C. Exponential concentration

The exponentially large Hilbert space, if not properly handled, can hinder the scalability of QML models. In variational quantum models, this curse of dimensionality manifests itself as the Barren Plateau (BP) phenomena [48, 49], where loss landscapes become exponentially flat with system size, prohibiting training. In contrast, the curse of dimensionality appears differently in *non-variational* QML approaches such as quantum kernel methods [50, 62], and QELMs [51]. In these classically trainable, non-variational QML models, the exponential concentration results in data-insensitive models that generalize poorly.

We now review the definition of exponential concentration

Definition 1 (Probabilistic exponential concentration). *Consider a quantity $Q(\boldsymbol{\alpha})$ that depends on some variable $\boldsymbol{\alpha}$ which can be estimated from an n -qubit quantum computer as an expectation value of some observable. $Q(\boldsymbol{\alpha})$ is said to probabilistically exponentially concentrate around an input-independent value μ if*

$$\Pr_{\boldsymbol{\alpha}}[|Q(\boldsymbol{\alpha}) - \mu| \geq \delta] \leq \frac{\beta}{\delta^2}, \quad \beta \in \mathcal{O}(1/b^n), \quad (7)$$

for some $b > 1$. That is, the probability that $Q(\boldsymbol{\alpha})$ deviates from μ by a small amount δ is exponentially small for all $\boldsymbol{\alpha}$.

The above definition is rather general and can be applied to many instances. In the context of QRP, we will consider $Q(\boldsymbol{\alpha}) = \langle O \rangle_t$, where O can be any one of the observables out of the set used for training. In this case, the probability in Eq. (7), as well as variance and mean of $\langle O \rangle_t$, would be taken over the set of all inputs \mathcal{X} or over an ensemble from which the reservoir U is drawn. We note that in Eq. (7), by applying Chebyshev's inequality, β can readily be associated to $\text{Var}_{\boldsymbol{\alpha}}[Q(\boldsymbol{\alpha})]$ with $\mu = \mathbb{E}_{\boldsymbol{\alpha}}[Q(\boldsymbol{\alpha})]$.

Reservoir Dynamics	Output	Memory
Scrambling	Theorem 1 <ul style="list-style-type: none"> • Exp. concentration in system size • No concentration in iterations 	Theorem 2 <ul style="list-style-type: none"> • Exp. decay in system size • Exp. decay in iterations
Local Noise	Refs. [50, 51, 63] <ul style="list-style-type: none"> • Exp. concentration in system size (Pauli noise) 	Theorem 3 / Theorem 4 <ul style="list-style-type: none"> • Exp. decay in iterations (and also in system size with non-unital noise)

Table I. **Summary of this work.** The analytical results of the paper are summarized in this table. We analyse the scaling of the variance of output observables and indicators of the memory of the reservoir for two types of reservoir dynamics – scrambling and noise.

III. RESULTS

A. Extreme scrambling reservoir dynamics

Here we study the effect of using scramblers as the quantum reservoir. A highly scrambling process at long times can be modelled by typical (pseudo) random unitaries [46, 47, 64]. This approach for modelling the scrambling reservoir has the added benefit of allowing us to adopt tools from Haar integration for analytical treatments [65]. Concretely, for t time steps, we suppose that the scrambling unitary is drawn from a distribution that agrees with the (Haar) random distribution of unitaries up to the $2t$ -th moment. That is, we consider reservoirs to form $2t$ -design over the unitary group of $d_a d_h$ dimensions $\mathcal{U}(d_a d_h)$ with $d_a = 2^{n_a}$ and $d_h = 2^{n_h}$.

1. Concentration in output's magnitude

We start with the impact of extreme scrambling reservoirs on the scalability. The scrambling dynamics from the reservoir spreads out local information encoded from the input injection steps onto the exponentially large Hilbert space, making the information inaccessible in the large system size limit. Consequently, this effect manifests itself as the exponential concentration of the QRP output with respect to the reservoir size and is formalized as the vanishing variance in the following theorem.

Theorem 1 (Vanishing variance of QRP output with extreme scrambling reservoir). *Given that a reservoir is sampled from a $2t$ -design on $\mathcal{U}(d_a d_h)$, the variance of a QRP's outputs vanish exponentially with the system size. For-*

mally, the variance is given by

$$\text{Var}_{U \sim \mathcal{U}(d_a d_h)}[\langle O \rangle_t] = \frac{\text{Tr}[O^2](1 + \beta)}{d_a^2 d_h^3}, \quad (8)$$

with $\beta \in \mathcal{O}(\frac{1}{d_a d_h})$.

By using Chebyshev's inequality, we straightforwardly obtain the probabilistic exponential concentration as in Definition 1 with the average $\mathbb{E}_{U \sim \mathcal{U}(d_a d_h)}[\langle O \rangle_t] = \frac{\text{Tr}[O](1+\beta)}{d_a d_h}$ as the concentration value, which is also independent of either reservoir or input states. The proof and a formal version of Theorem 1 is presented in Appendix A 3.

Proving Theorem 1 is non-trivial and involves going beyond the standard proof technique commonly used to show exponential concentration. In particular, while the same instance of the quantum reservoir is employed for every time step, the entire composite system becomes larger with every time step due to the input state injection process. This prompts the question of whether the randomness generated by the same scrambling instance is sufficient to cause concentration. The proof of Theorem 1 relies on expressing the whole QRP dynamics as a tensor diagram. One then carefully works with the recursive expression of expectation values in Eq. (2) by writing in the effectively extended space such that the first and second moments of the expectation transformed to a standard Haar integral with $2t$ -design. This alternative form of the QRP output is presented in Supplemental Proposition 1.

We remark that our assumption that the reservoir is drawn from a unitary $2t$ -design is stronger than typically required for similar concentration bounds in QELM or quantum kernel methods [50, 51], where a 2-design ensemble is sufficient. Whether this is also a necessary condition, or just a relic of our proof techniques, remains an open question.

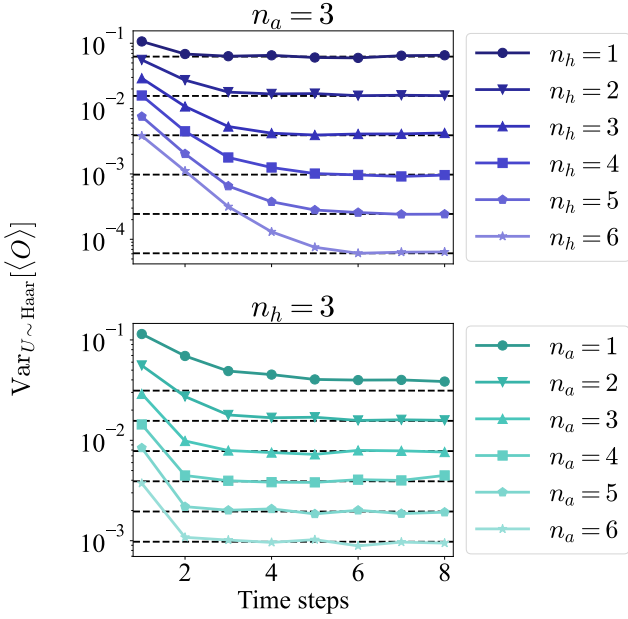


Figure 2. **Concentration induced by reservoir dynamics.** The variance of reservoir output over Haar random reservoirs are plotted against number of time steps for different numbers of hidden qubits (top) and accessible qubits (bottom). The observables are Pauli strings. The dashed horizontal lines represent the leading terms $\frac{1}{d_a d_h^2}$ obtained analytically. Note that the classical input are sequences of independent random numbers uniformly drawn from $[0, 1]$ and the exponential encoding strategy is employed to encode the data.

A numerical simulation of the variance scaling with the scrambling reservoir is illustrated in Fig. 2, as a function of n_a and n_h . While the dominant term of the variance (for large d) in Theorem 1 does not depend on the time steps, one indeed observes some discrepancy at the early time steps. However, after some reservoir iterations, the variance quickly saturates to the predicted value which depends only on the number of qubits. The convergence rate is empirically observed to depend on the ratio n_h/n_a , which reflects the interplay of the injection of new data and the accumulated scrambling due to reservoir dynamics.

Practical consequences. Exponential concentration does not prevent the training of a QRP model, as the optimisation over readout weights is a classical convex optimization problem. However, due to the intrinsically probabilistic nature of quantum hardware, the observables read-out can only be estimated with measurement shots. For large system sizes, one typically can only afford a polynomial number of measurements to estimate these

observables. As a consequence of the concentration phenomena, these estimates become statistically indistinguishable from input-independent random variables. Training on these estimates therefore yields an *input-insensitive* QRP with poor generalisation. Thus, while trainability is guaranteed, the scalability of generalisation is not.

The following proposition formalizes this notion for QRP output.

Proposition 1. *Consider the same assumptions as Theorem 1 and further suppose that O is a Pauli string. After polynomial measurement shots $N \in \mathcal{O}(\text{poly}(n))$, the estimate of $\langle O \rangle_t$ is statistically indistinguishable, with probability exponentially close to 1, from an input-independent random variable of the form*

$$\widehat{O}_{\text{rand}} = \frac{1}{N} \sum_{i=1}^N z_i, \quad (9)$$

where each z_i takes a value ‘+1’ and ‘-1’ with an equal probability.

The formal version of this statement is presented in Supplemental Theorem 1 using hypothesis testing tools. In addition, Supplemental Corollary 1 also formally presents an explicit connection to trainability and unseen model predictions. We refer the readers to Appendix B 2 for further technical discussions and the proof.

While the above implications arise in the regime of large system size, for *small* reservoirs one can afford sufficient shots to obtain accurate estimates of observables. Together with the fact that the prediction variance in Theorem 1 does not further decrease with time, this leaves a window of opportunity in which an *extreme-scrambling QRP on modest system sizes might offer a polynomial advantage over standard tomography approaches when processing quantum data.*

Other concentration sources. With the detrimental implications of concentration being unfolded, it is crucial to identify other potential factors. While the concentration due to hardware noise will be discussed in Section III B, other sources of exponential concentration of QRP –such as entanglement and global measurement– can be shown directly using the same proof strategies as for QELM [51] –we can simply view the initial state of QELM as the state of QRP ($\rho_{a_t} \otimes \rho_{h_{t-1}}$) before the reservoir evolution of the last step t .

2. Exponential decay of memory indicators

A viable QRP must not only remember useful information about past inputs, but also should eventually forget

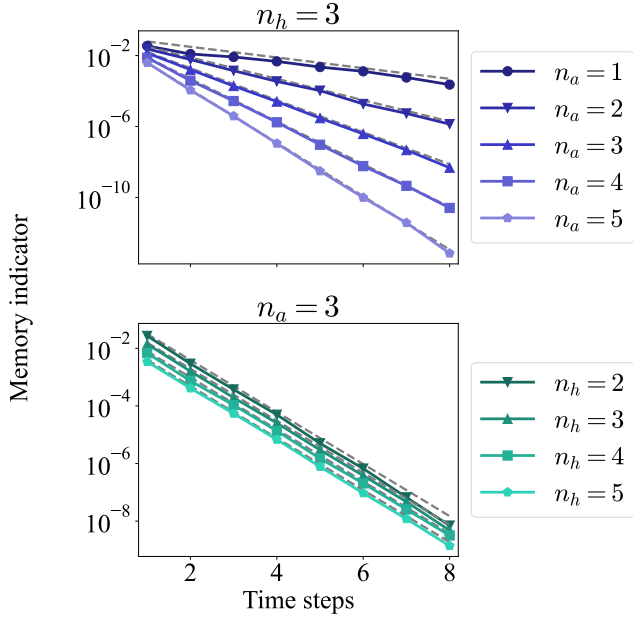


Figure 3. **Memory indicator of the early input.** The dependence of outputs on inputs of t steps early $\mathcal{M}_a(t; \mathcal{S}_a, \mathcal{U})$ are plotted for different qubit numbers. Here both the reservoir and the first input state are Haar random. The grey lines indicate the bounds given in Theorem 2.

older inputs and older reservoir states, so that the current outputs are not dominated by the far past history. In classical reservoir computing (RC), these two requirements are commonly encapsulated by the *Fading Memory Property* (FMP) and the *Echo State Property* (ESP) [10, 60]. As reviewed in Section II B, FMP requires that the effect of inputs fed far in the past fades away, while ESP demands that the reservoir’s internal state eventually becomes independent of its initial state.

To capture these forgetting characteristics of QRP, we define two *memory indicators* that quantify how much the output depends on an early state: one for the *accessible qubits* (input channel) and one for the *hidden qubits* (reservoir’s internal state).

Definition 2 (Memory of input τ). *Let us denote the distribution of input states at step τ , which we assume is independent of inputs at other time steps, by $\rho_{a\tau} \sim \mathcal{S}(d_a)$. Let us suppose the reservoir is drawn from $\mathcal{U}(d_a d_h)$. We define the memory of the input at step τ after t time steps have passed as*

$$\mathcal{M}_a(t; \mathcal{S}_a, \mathcal{U}) := \mathbb{E}_{U \sim \mathcal{U}} \left[\text{Var}_{\rho_{a\tau} \sim \mathcal{S}_a} \left[\langle O \rangle_{(t+\tau)} \right] \right]. \quad (10)$$

Definition 3 (Memory of initial condition). *Given the distribution of initial state of the hidden qubits $\rho_{h0} \sim \mathcal{S}(d_h)$, given the distribution of reservoirs $U \sim \mathcal{U}(d_a d_h)$, we define the memory of the initial state at step t as*

$$\mathcal{M}_h(t; \mathcal{S}_h, \mathcal{U}) := \mathbb{E}_{U \sim \mathcal{U}} \left[\text{Var}_{\rho_{h0} \sim \mathcal{S}_h} \left[\langle O \rangle_t \right] \right]. \quad (11)$$

If $\mathcal{M}_h(t)$ is significant, the final output is still sensitive to how one prepared the hidden qubits long ago. Similarly, if $\mathcal{M}_a(t)$ is large, the output significantly depends on input states fed into the accessible qubits many steps earlier. These memory indicators provide an operational measure of whether a QRP is retaining or forgetting old information at time t , *on average*.

We now state the bounds on these memory indicators (with the proof presented in Appendix A 4).

Theorem 2 (Upper bound of memory of arbitrary early input and initial state ensemble). *For extreme scrambling reservoirs and an arbitrary ensemble of inputs \mathcal{S}_a , we have*

$$\mathcal{M}_a(t; \mathcal{S}_a, \mathcal{U}) \in \mathcal{O} \left(\frac{1}{d_h d_a^t} \right). \quad (12)$$

Similarly, for an arbitrary ensemble of initial reservoir states \mathcal{S}_h , we have

$$\mathcal{M}_h(t; \mathcal{S}_h, \mathcal{U}) \in \mathcal{O} \left(\frac{1}{d_h d_a^t} \right). \quad (13)$$

In essence, Theorem 2 indicates that extreme-scrambling unitaries behave too chaotically to store memories at scale. Early injected states get scrambled in the large Hilbert space and their signals decay exponentially fast. For certain tasks requiring longer memory, this exponential forgetting may be prohibitive.

While such forgetting behaviors are reminiscent of the FMP and ESP used in classical RC theory [60], our exponential concentration-based statements are inherently *averaged* over random reservoirs or random inputs, and thus are not necessarily strict analogs of the traditional deterministic properties in formal RC. Nonetheless, they ensure with high probability that typically these reservoirs do not retain obsolete information indefinitely, which is crucial for most time-series processing tasks in QRP. In Appendix D, we provide further discussion and formalize the relation of our vanishing memory indicators to FMP-like and ESP-like behaviours (see Supplemental Theorem 3 and Supplemental Theorem 4, respectively). In addition, we also remark on the connection to the universality of fading memory maps.

B. Noisy reservoir dynamics

Here we study the impact of hardware noise in two different settings: (i) unital noise where local Pauli noise acts between different noiseless reservoir dynamics, and (ii) noisy scrambling reservoir where the reservoir itself consists of local scrambling unitaries intervened with arbitrary local non-unitary noise.

1. Unital noise

To study how the noise between each time steps of noiseless reservoir evolutions affects the memory, we consider the state after reservoir evolution as

$$\rho_{\tau+1} = \mathcal{N}(U(\rho_{a_{\tau+1}} \otimes \rho_{h_{\tau}})U^\dagger), \quad (14)$$

where $\mathcal{N}(\cdot)$ is a noise channel which implements a tensor product of local Pauli noise on each individual qubits i.e., $\mathcal{N} = \mathcal{N}_1 \otimes \dots \otimes \mathcal{N}_{n_a+n_h}$ with

$$\mathcal{N}_j(\sigma) = q_\sigma \sigma, \quad (15)$$

acting on the j^{th} qubit. Here, $\sigma \in \{X, Y, Z\}$ is one of the non-trivial single-qubit Pauli operators and q_σ is an associated noise coefficient. We further define the characteristic noise parameter $q := \max\{|q_X|, |q_Y|, |q_Z|\}$.

With the above setting, the following theorem holds.

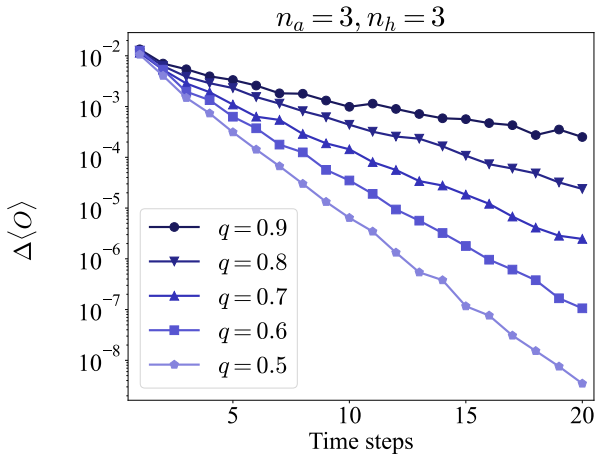


Figure 4. **Noisy reservoir induced concentration.** The averaged deviation of two outputs of QRP with randomly sampled pairs of initial states and first inputs are plotted for different noise factors.

Theorem 3 (Memory erasure induced by unital noise). *Consider a QRP with noisy layers between noiseless reservoir evolutions as defined in Eq. (15), with $q < 1$. Then, for time step t , the expectation value of the observable will become independent of the initial condition and early inputs, exponentially in number of steps t . Formally, given two initial states of hidden qubits ρ_{h_0} and σ_{h_0} , given two inputs ρ_{a_1} and σ_{a_1} at the first time step, given the same series of input states $[\rho_{a_\tau}]_{\tau=2}^t = [\sigma_{a_\tau}]_{\tau=2}^t$ from the second step, then the deviation of the corresponding outputs*

$$\Delta O \leq \|O\|_\infty \sqrt{2 \ln 2 q^{b(t-1)}} \cdot \left(S_2(\rho_{a_1} \| \sigma_{a_1}) + S_2(\rho_{h_0} \| \sigma_{h_0}) \right)^{1/2} \quad (16)$$

$$\in \mathcal{O}(\exp(-t)), \quad (17)$$

where $\Delta O = |\langle O \rangle_t^{(\rho_{h_0}, \rho_{a_1})} - \langle O \rangle_t^{(\sigma_{h_0}, \sigma_{a_1})}|$, $b = 1/\ln 2$ and $S_2(\cdot \| \cdot)$ denotes the sandwiched 2-Rényi relative entropy.

This upper bound indicates that the difference between outputs from different initial states shrinks exponentially with the number of time steps. Thus at long times the QRP is effectively insensitive to the initial state. Numerics in Fig. 4 demonstrates these effects. The proof of this Theorem is provided in Appendix C3.

On another note, when input data are classical, noise can act also during the input-data encoding stage. We proved in Appendix C2 that noisy encoding can solely drive exponential concentration in QRP's outputs, extending the noisy-encoding bounds previously obtained for QELMs [51].

2. Non-unital noise

In this section, we investigate how *arbitrary* local noise – possibly significantly deviating from the Pauli noise model considered above – erase memory of early inputs and reservoir's initial state. In particular, we extend our analysis to include non-unital noise, which exhibits markedly different behaviors. Unlike unital noise, non-unital noise does not leave the maximally mixed state invariant. Instead, it can reduce the entropy of a quantum system, thereby providing a potential resource for computation. This property has been exploited in various contexts, including fault-tolerant quantum computing [66] and QRP [55]

In the case of non-unital noise it is not possible to derive bounds for generic reservoirs because with careful engineering (essentially sneaking in error correction) arbitrary circuits can be realized despite non-unital noise [66]. Instead, we here we focus on *typical* noisy reservoirs. Specifically,

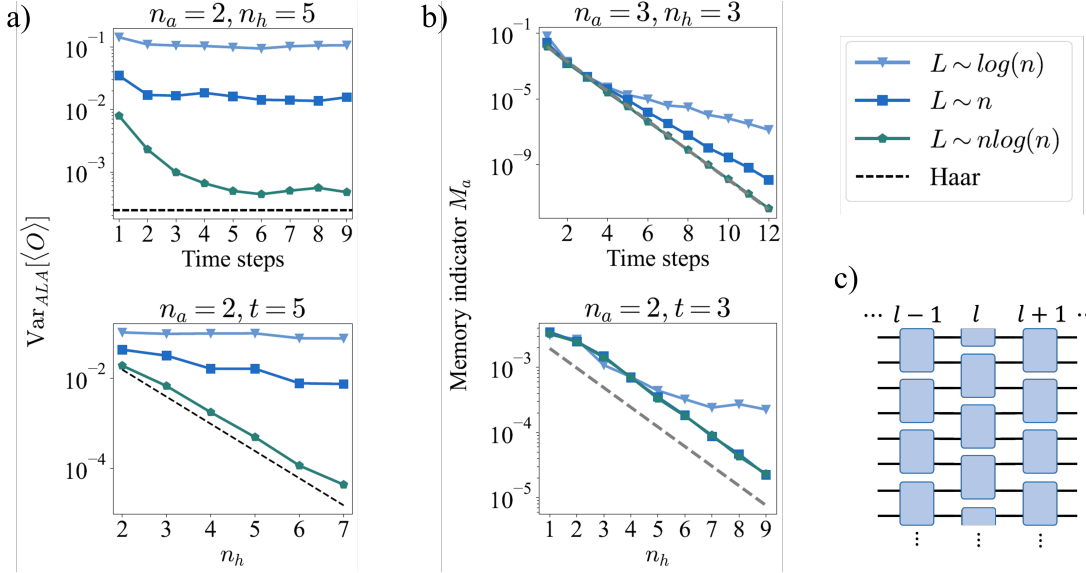


Figure 5. **Absence of exponential concentration in QRP with alternating layered reservoirs.** Here we consider reservoir consisting of L such alternating layers, as illustrated in **c)**. Each layer is given by tensor products of 2-local blocks of neighbouring qubits, and in the next layer each qubit is connected with another neighbouring qubit. The blocks are independent and randomly sampled from Haar measure. The variance of output over reservoirs and the memory indicator M_a for QRP with alternating layers are plotted for different depth, and compare with Haar random reservoir, in **a)** and **b)**. In the top sub figures, the qubit numbers are fixed and the variance and memory indicator are plotted against number of time step. In the bottom one, we fix instead the number of accessible qubits and the time step, to plot both quantities against the number of hidden qubits.

following Refs. [67, 68], we model the reservoir \mathcal{U} as sequence of L random unitary layers interleaved by arbitrary local noise $\mathcal{N}^{\otimes n}$:

$$\mathcal{U} = \mathcal{U}_L \circ \mathcal{N}^{\otimes n} \circ \mathcal{U}_{L-1} \circ \dots \circ \mathcal{N}^{\otimes n} \circ \mathcal{U}_1 \circ \mathcal{N}^{\otimes n}. \quad (18)$$

We assume that each \mathcal{U}_j is sampled from a “locally scrambling” distribution [69–71], e.g. \mathcal{U}_j can be Brickwall layer with local Haar-random gates, and we let the depth L be at least linear in system size.

One intuitively expects noisy QRP, even with non-unital noise, to be insensitive to its early states due to the noise destroying their information. The following theorem formalizes this notion.

Theorem 4 (Memory erasure induced by non-unital noise). *Given a noisy reservoir \mathcal{U} as in Eq. (18), let \mathcal{N} be an arbitrary non-unitary channel with constant noise rate and let $L \geq c \cdot (n_a + n_h)$ for a sufficiently large constant $c > 0$. Given two initial states of hidden qubits ρ_{h_0} and σ_{h_0} , given two inputs ρ_{a_1} and σ_{a_1} at the first time step, given the same series of input states $[\rho_{a_\tau}]_{\tau=2}^t = [\sigma_{a_\tau}]_{\tau=2}^t$ from the second step, the corresponding output states satisfies*

$$\|\rho_t - \sigma_t\|_1 \in \exp(-\Omega((n_a + n_h)t)), \quad (19)$$

with probability at least $1 - \exp(-\Omega((n_a + n_h)))$. In particular, for any observable O it holds that

$$\Delta O \in \exp(-\Omega((n_a + n_h)t)) \|O\|_\infty, \quad (20)$$

with probability at least $1 - \exp(-\Omega((n_a + n_h)))$, where we define $\Delta O = |\langle O \rangle_t^{(\rho_{h_0}, \rho_{a_1})} - \langle O \rangle_t^{(\sigma_{h_0}, \sigma_{a_1})}|$.

Our bounds imply that for reservoirs with arbitrary local noise, possibly non-unital, the dependence of reservoir states on early input states and the initial state of hidden qubits vanishes exponentially in number of time steps. This leads to FMP- and ESP-like characteristics, such that QRP forgets the influence of the distant past and remains responsive to recent inputs (see Appendix D). Nevertheless, if the decay of memory indicator is too strong the capability of QRP for processing long time series will be limited. While previous results on concentration (and lack thereof) for non-unital dynamics rely on i.i.d. assumptions, our setting involves repeated application of the same noisy reservoir. To establish our result, we extend the analytical framework developed in Refs. [67, 68].

C. Practical reservoirs with less concentration

In this section we analyze more moderately scrambling reservoirs. In particular, we consider two types of physical reservoirs with limited dynamics: (i). 2-local alternating layered random circuits and (ii). chaotic Ising model—that may avoid exponential concentration. We numerically compare the memory decay of both types of reservoirs with different parameters and discuss their useful regimes.

(i). *2-local random circuits with alternating layered structure:* Here we consider an alternating layered structure of quantum circuits. In each layer the qubits are connected with a neighbouring qubit, and in the next layer they are connected with another neighbouring qubit. In terms of circuit diagram, as shown in panel c) of Fig. 5, each layer consists of 2-local circuit blocks, that are independently and randomly sampled from Haar measure. The dynamics of the reservoir can be controlled by number of alternating layers. A variational quantum circuit with the alternating layered Ansatz does not exhibit exponential concentration if the number of layers L is in $\mathcal{O}(\log(n))$ [72].

As illustrated in Fig. 5, we numerically demonstrate that for alternating layered reservoirs with low depth $L \in \mathcal{O}(\log(n))$, the exponential concentration of outputs and memory indicator in qubit number can be avoided. However, for reservoirs with more than linearly many layers, the reservoir dynamics approximates Haar random and the memory indicator becomes exponentially concentrated in system size.

(ii). *Chaotic Ising model:* Ising model is a typical class of physical platform for QRP [10, 34, 45, 73–77]. Here we focus on a chaotic Ising model, rather than an integrable Ising model, as these have been found to be more expressive [51]. Here we numerically study the exponential concentration of QRP with chaotic Ising model as reservoir. As shown in Fig. 6, when the evolution time is increased, the memory indicator decays faster with the number of time steps and becomes closer to the behavior of a Haar random reservoir.

IV. DISCUSSION

In this work, we analytically study the scalability and memory properties of scrambling quantum systems used for temporal information processing, by considering QRP as a general framework, with an extreme scrambling reservoir modeled as a high-order unitary design. We introduce a tensor-diagram technique that unrolls the sequence of identical reservoir dynamics, casting it into a single-step higher-order moment integration. Our scalability analysis shows

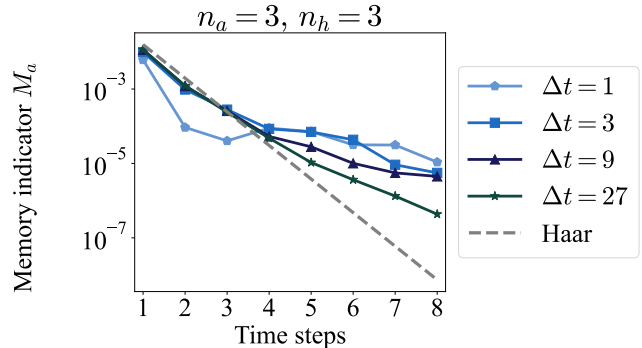


Figure 6. **Memory indicator of Ising reservoirs.** The dependence M_a of outputs on inputs are plotted against number of time steps for different reservoirs. We consider reservoirs with different dynamics—sampled from Haar random unitaries and Ising models with different evolution times Δt , where the Hamiltonian is $H_{\text{Ising}} = J \sum_{i=1}^{n-1} Z_i Z_{i+1} + B_z \sum_i Z_i + B_x \sum_i X_i$, with $J = -1$, $B_x = 0.7$, $B_z = 1.5$.

that QRP outputs concentrate exponentially with increasing reservoir size, hindering the use of extreme scramblers in the large-system size limit.

However, once the concentration saturates it no longer worsens with increasing iterations. This provides a small window of opportunity in which QRP might yield a polynomial advantage, compared to standard tomography, on temporal tasks that process quantum data in a sufficiently small number of qubits. In particular, the sampling complexity of performing quantum tomography followed by classical post-processing could be saved by processing the states directly within the QRP framework. This could be specifically relevant for input state ensembles with high rank, e.g. states generated from complex many-body systems, since tomography requires $\Omega(\text{rank}(\rho)d/\epsilon)$ samples [78]. These insights thus suggest an opportunity to utilize moderate-sized noisy quantum systems as a substrate for physical computing [79, 80] and hint towards the possibility of achieving practical information processing advantages [6].

One potential approach to successfully scale QRPs to larger problem sizes is to incorporate symmetry into the construction of QRP. An analytical analysis on a single reservoir iteration has shown that working in the low dimensional symmetric subspace avoids exponential concentration [52], in direct analogy with the case for variational quantum algorithms [81, 82]. Proving this for multiple reservoir iterations requires integrating over the symmetric group with the unrolled form of the QRP output [83].

Nonetheless, it is important to note that variational QML models which provably avoid exponential concentration are susceptible to classical surrogatability (i.e., they can be classically simulated after performing some form of state tomography) [84]. A similar relation is also expected in QRP.

In addition, we have analyzed the memory properties of extreme-scrambling reservoirs. By introducing *memory indicators* to capture the characteristics reminiscent of Echo State Property (ESP) and Fading Memory Property (FMP) *on average*, we applied the tensor-diagram technique to show that these indicators indeed decay exponentially with the time step. This rapid decay reflects the expected forgetting behaviour associated with ESP and FMP. However, taken together with the scalability barrier, our results provide an explicit example of a QRP that satisfies averaged ESP- and FMP-like characteristics yet remains practically non-operational (input-independent and poor generalization) at large scale. Thus, achieving these memory properties alone is insufficient, and scalable QRP design requires a broader set of considerations.

Lastly, there is still much to explore when it comes to moderate scramblers as reservoirs. Our numerical studies suggest that it is possible to have scrambling reservoirs without the concentration, and provide a direction towards designing the reservoir with scalability guarantees. This same relation is also expected in QRP although the technical details remain to be pinned down. Making theoretical progress with moderate reservoirs to understand its scalability and more generally other QRP-related properties probably requires us to come up with new theoretical tools combining the existing analytical frameworks in the field of quantum many-body physics such as Eigenstate Thermalization Hypothesis [85] together with those in the field of machine learning.

Related work: During the preparation of manuscript, we

became aware of a related independent work [52] which also studied exponential concentration in QRP but with a different focus. While our analytical results have focussed on general QRP models with time correlated reservoir dynamics, Ref. [52]’s analytical results focus on a single reservoir iteration and explores the effect of symmetry.

V. ACKNOWLEDGEMENTS

The authors are indebted to Marco Cerezo, who showed us how to handle time correlated Haar random unitaries while waiting for tacos. The authors also gratefully acknowledge Rodrigo Martínez-Peña for valuable feedback on an earlier draft of this paper, and further acknowledge interesting discussions with Matthew Duschene, Giorgio Facelli, Gian Luca Giorgi, Daniel Stilck França, Jonas Landman, Martin Larocca, Sacha Lerch, Hela Mhiri, Juan-Pablo Ortega, Barry Sanders, Mehrad Sahebi, Antonio Sannia, and Roberta Zambrini.

WX acknowledges the funding support from NCCR SPIN, a National Centre of Competence in Research, funded by the Swiss National Science Foundation (grant number 225153). ZH, AA, and ST acknowledge support from the Sandoz Family Foundation-Monique de Meuron program for Academic Promotion. TC and ST acknowledge the funding support from the NSRF via the Program Management Unit for Human Resources & Institutional Development, Research and Innovation [grant number B39G680007]. ST also acknowledges the grants for development of new faculty staff, Ratchadaphiseksomphot Fund, Chulalongkorn University [grant number 3230120336 DNS_68_052_2300_012].

-
- [1] G. Wetzstein, A. Ozcan, S. Gigan, S. Fan, D. Englund, M. Soljačić, C. Denz, D. A. Miller, and D. Psaltis, Inference in artificial intelligence with deep optics and photonics, *Nature* **588**, 39 (2020).
 - [2] H. Seok, D. Lee, S. Son, H. Choi, G. Kim, and T. Kim, Beyond von neumann architecture: Brain-inspired artificial neuromorphic devices and integrated computing, *Advanced Electronic Materials* **10**, 2300839 (2024).
 - [3] J. Hasler and E. Black, Physical computing: Unifying real number computation to enable energy efficient computing, *Journal of Low Power Electronics and Applications* **11**, 14 (2021).
 - [4] Y. Suzuki, Q. Gao, K. C. Pradel, K. Yasuoka, and N. Yamamoto, Natural quantum reservoir computing for temporal information processing, *Scientific reports* **12**, 1353 (2022).
 - [5] J. Chen, H. I. Nurdin, and N. Yamamoto, Temporal information processing on noisy quantum computers, *Physical Review Applied* **14**, 024065 (2020).
 - [6] A. Senanian, S. Prabhu, V. Kremenetski, S. Roy, Y. Cao, J. Kline, T. Onodera, L. G. Wright, X. Wu, V. Fatemi, and P. L. McMahon, Microwave signal processing using an analog quantum reservoir computer, *Nature Communications* **15**, 7490 (2024).
 - [7] M. Kornjača, H.-Y. Hu, C. Zhao, J. Wurtz, P. Weinberg, M. Hamdan, A. Zhdanov, S. H. Cantu, H. Zhou, R. A. Bravo, *et al.*, Large-scale quantum reservoir learning with an analog quantum computer, arXiv preprint

- arXiv:2407.02553 [10.48550/arXiv.2407.02553](#) (2024).
- [8] K. Fujii and K. Nakajima, Harnessing disordered-ensemble quantum dynamics for machine learning, *Physical Review Applied* **8**, 024030 (2017).
 - [9] K. Nakajima, K. Fujii, M. Negoro, K. Mitarai, and M. Kitagawa, Boosting computational power through spatial multiplexing in quantum reservoir computing, *Physical Review Applied* **11**, 034021 (2019).
 - [10] P. Mujal, R. Martí nez-Peña, J. Nokkala, J. García-Beni, G. L. Giorgi, M. C. Soriano, and R. Zambrini, Opportunities in quantum reservoir computing and extreme learning machines, *Advanced Quantum Technologies* **4**, 2100027 (2021).
 - [11] S. Ghosh, A. Opala, M. Matuszewski, T. Paterek, and T. C. Liew, Reconstructing quantum states with quantum reservoir networks, *IEEE Transactions on Neural Networks and Learning Systems* **32**, 3148 (2020).
 - [12] L. Govia, G. Ribeill, G. Rowlands, H. Krovi, and T. Ohki, Quantum reservoir computing with a single nonlinear oscillator, *Physical Review Research* **3**, 013077 (2021).
 - [13] F. Hu, G. Angelatos, S. A. Khan, M. Vives, E. Türeci, L. Bello, G. E. Rowlands, G. J. Ribeill, and H. E. Türeci, Tackling sampling noise in physical systems for machine learning applications: Fundamental limits and eigentasks, *Physical Review X* **13**, 041020 (2023).
 - [14] H. Jaeger, The “echo state” approach to analysing and training recurrent neural networks-with an erratum note, Bonn, Germany: German National Research Center for Information Technology GMD Technical Report **148**, 13 (2001).
 - [15] W. Maass, T. Natschläger, and H. Markram, Real-time computing without stable states: A new framework for neural computation based on perturbations, *Neural computation* **14**, 2531 (2002).
 - [16] M. Lukoševičius and H. Jaeger, Reservoir computing approaches to recurrent neural network training, *Computer Science Review* **3**, 127 (2009).
 - [17] A. Burgess and M. Florescu, Quantum reservoir computing implementations for classical and quantum problems, arXiv preprint arXiv:2211.08567 [10.48550/arXiv.2211.08567](#) (2022).
 - [18] J. Settino, L. Salatino, L. Mariani, M. Channab, L. Bozzolo, S. Vallisa, P. Barillà, A. Policicchio, N. L. Gullo, A. Giordano, *et al.*, Memory-augmented hybrid quantum reservoir computing, arXiv preprint arXiv:2409.09886 [10.48550/arXiv.2409.09886](#) (2024).
 - [19] P. Pfeffer, F. Heyder, and J. Schumacher, Hybrid quantum-classical reservoir computing of thermal convection flow, *Physical Review Research* **4**, 033176 (2022).
 - [20] O. Ahmed, F. Tennie, and L. Magri, Prediction of chaotic dynamics and extreme events: A recurrence-free quantum reservoir computing approach, *Physical Review Research* **6**, 043082 (2024).
 - [21] C.-F. Chen, J. Docter, M. Xu, A. Bouland, and P. Hayden, Efficient unitary t-designs from random sums, arXiv preprint arXiv:2402.09335 (2024).
 - [22] G. Angelatos, S. A. Khan, and H. E. Türeci, Reservoir computing approach to quantum state measurement, *Physical Review X* **11**, 041062 (2021).
 - [23] K. Kobayashi, K. Fujii, and N. Yamamoto, Feedback-driven quantum reservoir computing for time-series analysis, *PRX Quantum* **5**, 040325 (2024).
 - [24] Y. Li, S. Ghosh, J. Shang, Q. Xiong, and X. Zhang, Estimating many properties of a quantum state via quantum reservoir processing, *Physical Review Research* **6**, 013211 (2024).
 - [25] M. Vetrano, G. Lo Monaco, L. Innocenti, S. Lorenzo, and G. M. Palma, State estimation with quantum extreme learning machines beyond the scrambling time, *npj Quantum Information* **11**, 20 (2025).
 - [26] J. Nokkala, G. L. Giorgi, and R. Zambrini, Retrieving past quantum features with deep hybrid classical-quantum reservoir computing, *Machine Learning: Science and Technology* **5**, 035022 (2024).
 - [27] A. Sornsaeng, N. Dangniam, and T. Chotibut, Quantum next generation reservoir computing: an efficient quantum algorithm for forecasting quantum dynamics, *Quantum Machine Intelligence* **6**, 57 (2024).
 - [28] T. Yasuda, Y. Suzuki, T. Kubota, K. Nakajima, Q. Gao, W. Zhang, S. Shimono, H. I. Nurdin, and N. Yamamoto, Quantum reservoir computing with repeated measurements on superconducting devices, arXiv preprint arXiv:2310.06706 [10.48550/arXiv.2310.06706](#) (2023).
 - [29] J. Dudas, B. Carles, E. Plouet, F. A. Mizrahi, J. Grollier, and D. Marković, Quantum reservoir computing implementation on coherently coupled quantum oscillators, *npj Quantum Information* **9**, 64 (2023).
 - [30] J. García-Beni, G. L. Giorgi, M. C. Soriano, and R. Zambrini, Scalable photonic platform for real-time quantum reservoir computing, *Physical Review Applied* **20**, 014051 (2023).
 - [31] F. Hu, S. A. Khan, N. T. Bronn, G. Angelatos, G. E. Rowlands, G. J. Ribeill, and H. E. Türeci, Overcoming the coherence time barrier in quantum machine learning on temporal data, *nature communications* **15**, 7491 (2024).
 - [32] W. Kalfus, G. Ribeill, G. Rowlands, H. Krovi, T. Ohki, and L. Govia, Hilbert space as a computational resource in reservoir computing, *Physical Review Research* **4**, 033007 (2022).
 - [33] S. A. Khan, F. Hu, G. Angelatos, and H. E. Türeci, Physical reservoir computing using finitely-sampled quantum systems, arXiv preprint arXiv:2110.13849 [10.48550/arXiv.2110.13849](#) (2021).
 - [34] R. Martínez-Peña, J. Nokkala, G. L. Giorgi, R. Zambrini, and M. C. Soriano, Information processing capacity of spin-based quantum reservoir computing systems, *Cognitive Computation* , 1 (2020).
 - [35] R. Martínez-Peña, G. L. Giorgi, J. Nokkala, M. C. Soriano, and R. Zambrini, Dynamical phase transitions in quantum reservoir computing, *Physical Review Letters* **127**, 100502 (2021).
 - [36] J. Nokkala, R. Martínez-Peña, G. L. Giorgi, V. Parigi, M. C. Soriano, and R. Zambrini, Gaussian states of continuous-variable quantum systems provide univer-

- sal and versatile reservoir computing, *Communications Physics* **4**, 53 (2021).
- [37] D. Fry, A. Deshmukh, S. Y.-C. Chen, V. Rastunkov, and V. Markov, Optimizing quantum noise-induced reservoir computing for nonlinear and chaotic time series prediction, arXiv preprint arXiv:2303.05488 [10.48550/arXiv.2303.05488](#) (2023).
- [38] R. Martínez-Peña and J.-P. Ortega, Quantum reservoir computing in finite dimensions, *Physical Review E* **107**, 035306 (2023).
- [39] L. G. Wright and P. L. McMahon, The capacity of quantum neural networks, in *CLEO: Science and Innovations* (Optica Publishing Group, 2020) pp. JM4G–5.
- [40] L. C. Govia, G. J. Ribeill, G. E. Rowlands, and T. A. Ohki, Nonlinear input transformations are ubiquitous in quantum reservoir computing, *Neuromorphic Computing and Engineering* **2**, 014008 (2022).
- [41] T. Kubota, Y. Suzuki, S. Kobayashi, Q. H. Tran, N. Yamamoto, and K. Nakajima, Temporal information processing induced by quantum noise, *Phys. Rev. Res.* **5**, 023057 (2023).
- [42] L. Domingo, G. Carlo, and F. Borondo, Taking advantage of noise in quantum reservoir computing, *Scientific Reports* **13**, 8790 (2023).
- [43] T. Kubota, H. Takahashi, and K. Nakajima, Unifying framework for information processing in stochastically driven dynamical systems, *Physical Review Research* **3**, 043135 (2021).
- [44] K. Fujii, H. Kobayashi, T. Morimae, H. Nishimura, S. Tamate, and S. Tani, Power of Quantum Computation with Few Clean Qubits, *43rd International Colloquium on Automata, Languages, and Programming (ICALP 2016) Leibniz International Proceedings in Informatics (LIPIcs)*, **55**, 13:1 (2016).
- [45] A. Palacios, R. Martínez-Peña, M. C. Soriano, G. L. Giorgi, and R. Zambrini, Role of coherence in many-body quantum reservoir computing, *Communications Physics* **7**, 369 (2024).
- [46] Z. Holmes, A. Arrasmith, B. Yan, P. J. Coles, A. Albrecht, and A. T. Sornborger, Barren plateaus preclude learning scramblers, *Physical Review Letters* **126**, 190501 (2021).
- [47] D. A. Roberts and B. Yoshida, Chaos and complexity by design, *Journal of High Energy Physics* **2017**, 121 (2017).
- [48] J. R. McClean, S. Boixo, V. N. Smelyanskiy, R. Babbush, and H. Neven, Barren plateaus in quantum neural network training landscapes, *Nature Communications* **9**, 1 (2018).
- [49] M. Larocca, S. Thanasilp, S. Wang, K. Sharma, J. Biamonte, P. J. Coles, L. Cincio, J. R. McClean, Z. Holmes, and M. Cerezo, A review of barren plateaus in variational quantum computing, *Nature Reviews Physics* **3**, 625–644 (2025).
- [50] S. Thanasilp, S. Wang, M. Cerezo, and Z. Holmes, Exponential concentration in quantum kernel methods, *Nature Communications* **15**, 5200 (2024).
- [51] W. Xiong, G. Facelli, M. Sahebi, O. Agnel, T. Chotibut, S. Thanasilp, and Z. Holmes, On fundamental aspects of quantum extreme learning machines, *arXiv preprint arXiv:2312.15124* (2023).
- [52] A. Sannia, G. L. Giorgi, and R. Zambrini, Exponential concentration and symmetries in quantum reservoir computing, to be published on arXiv.
- [53] A. Sannia, R. R. Rodríguez, G. L. Giorgi, and R. Zambrini, Non-markovianity and memory enhancement in quantum reservoir computing, arXiv preprint arXiv:2505.02491 [10.48550/arXiv.2505.02491](#) (2025).
- [54] R. Martínez-Peña and J.-P. Ortega, Input-dependence in quantum reservoir computing, arXiv preprint arXiv:2412.08322 [10.48550/arXiv.2412.08322](#) (2024).
- [55] A. Sannia, R. Martínez-Peña, M. C. Soriano, G. L. Giorgi, and R. Zambrini, Dissipation as a resource for quantum reservoir computing, *Quantum* **8**, 1291 (2024).
- [56] K. Cheamsawat and T. Chotibut, Dissipation alters modes of information encoding in small quantum reservoirs near criticality, *Entropy* **27**, [10.3390/e27010088](#) (2025).
- [57] F. Monzani, E. Ricci, L. Nigro, and E. Prati, Leveraging non-unital noise for gate-based quantum reservoir computing, arXiv preprint arXiv:2409.07886 [10.48550/arXiv.2409.07886](#) (2024).
- [58] A. Yosifov, A. Iyer, and V. Vedral, Dissipation-induced quantum homogenization for temporal information processing, *Phys. Rev. A* **111**, 012622 (2025).
- [59] M. Cerezo, G. Verdon, H.-Y. Huang, L. Cincio, and P. J. Coles, Challenges and opportunities in quantum machine learning, *Nature Computational Science* [10.1038/s43588-022-00311-3](#) (2022).
- [60] L. Grigoryeva and J.-P. Ortega, Echo state networks are universal, *Neural Networks* **108**, 495 (2018).
- [61] L. Gonon and J.-P. Ortega, Fading memory echo state networks are universal, *Neural Networks* **138**, 10 (2021).
- [62] Y. Suzuki, H. Kawaguchi, and N. Yamamoto, Quantum fisher kernel for mitigating the vanishing similarity issue, *Quantum Science and Technology* **9**, 035050 (2024).
- [63] S. Wang, E. Fontana, M. Cerezo, K. Sharma, A. Sone, L. Cincio, and P. J. Coles, Noise-induced barren plateaus in variational quantum algorithms, *Nature Communications* **12**, 1 (2021).
- [64] J. Tangpanitanon, S. Thanasilp, M.-A. Lemonde, N. Dangniam, and D. G. Angelakis, Signatures of a sampling quantum advantage in driven quantum many-body systems, *Quantum Science and Technology* **8**, 025019 (2023).
- [65] A. A. Mele, Introduction to haar measure tools in quantum information: A beginner’s tutorial, *Quantum* **8**, 1340 (2024).
- [66] M. Ben-Or, D. Gottesman, and A. Hassidim, Quantum refrigerator, *arXiv preprint arXiv:1301.1995* (2013).
- [67] A. A. Mele, A. Angrisani, S. Ghosh, S. Khatri, J. Eisert, D. S. França, and Y. Quek, Noise-induced shallow circuits and absence of barren plateaus, *arXiv preprint arXiv:2403.13927* (2024).
- [68] A. Angrisani, A. A. Mele, M. S. Rudolph, M. Cerezo, and Z. Holmes, Simulating quantum circuits with arbitrary local noise using pauli propagation, arXiv preprint arXiv:2501.13101 [10.48550/arXiv.2501.13101](#) (2025).
- [69] M. C. Caro, H.-Y. Huang, N. Ezzell, J. Gibbs, A. T. Sorn-

- borger, L. Cincio, P. J. Coles, and Z. Holmes, Out-of-distribution generalization for learning quantum dynamics, *Nature Communications* **14**, 3751 (2023).
- [70] H.-Y. Huang, S. Chen, and J. Preskill, Learning to predict arbitrary quantum processes, *PRX Quantum* **4**, 040337 (2023).
- [71] A. Angrisani, A. Schmidhuber, M. S. Rudolph, M. Cerezo, Z. Holmes, and H.-Y. Huang, Classically estimating observables of noiseless quantum circuits, *arXiv preprint arXiv:2409.01706* (2024).
- [72] M. Cerezo, A. Sone, T. Volkoff, L. Cincio, and P. J. Coles, Cost function dependent barren plateaus in shallow parametrized quantum circuits, *Nature Communications* **12**, 1 (2021).
- [73] L. Domingo, M. Grande, G. Carlo, F. Borondo, and J. Borondo, Optimal quantum reservoir computing for market forecasting: An application to fight food price crises, *arXiv preprint arXiv:2401.03347* 10.48550/arXiv.2401.03347 (2023).
- [74] L. Domingo, G. Carlo, and F. Borondo, Optimal quantum reservoir computing for the noisy intermediate-scale quantum era, *Physical Review E* **106**, L043301 (2022).
- [75] K. Kobayashi and Y. Motome, Quantum reservoir probing: an inverse paradigm of quantum reservoir computing for exploring quantum many-body physics, *arXiv preprint arXiv:2308.00898* 10.48550/arXiv.2308.00898 (2023).
- [76] K. Kobayashi and Y. Motome, Quantum reservoir probing of quantum phase transitions, *arXiv preprint arXiv:2402.07097* 10.48550/arXiv.2402.07097 (2024).
- [77] A. Kutvonen, K. Fujii, and T. Sagawa, Optimizing a quantum reservoir computer for time series prediction, *Scientific Reports* **10**, 14687 (2020).
- [78] H. Yuen, An improved sample complexity lower bound for (fidelity) quantum state tomography, *Quantum* **7**, 890 (2023).
- [79] J. Preskill, Quantum computing in the NISQ era and beyond, *Quantum* **2**, 79 (2018).
- [80] Z. Zimborás, B. Koczor, Z. Holmes, E.-M. Borrelli, A. Gilyén, H.-Y. Huang, Z. Cai, A. Acín, L. Aolita, L. Banchi, *et al.*, Myths around quantum computation before full fault tolerance: What no-go theorems rule out and what they don't, *arXiv preprint arXiv:2501.05694* <https://doi.org/10.48550/arXiv.2501.05694> (2025).
- [81] E. Fontana, D. Herman, S. Chakrabarti, N. Kumar, R. Yalovetzky, J. Heredge, S. H. Sureshbabu, and M. Pistoia, Characterizing barren plateaus in quantum ansätze with the adjoint representation, *Nature Communications* **15**, 7171 (2024).
- [82] M. Ragone, B. N. Bakalov, F. Sauvage, A. F. Kemper, C. Ortiz Marrero, M. Larocca, and M. Cerezo, A lie algebraic theory of barren plateaus for deep parameterized quantum circuits, *Nature Communications* **15**, 7172 (2024).
- [83] W. Xiong, Z. Holmes, A. Angrisani, Y. Suzuki, T. Chotibut, and S. Thanasilp, Quantum temporal processing with symmetry, to be published on arXiv.
- [84] M. Cerezo, M. Larocca, D. García-Martín, N. L. Diaz, P. Braccia, E. Fontana, M. S. Rudolph, P. Bermejo, A. Ijaz, S. Thanasilp, *et al.*, Does provable absence of barren plateaus imply classical simulability? Or, why we need to rethink variational quantum computing, *arXiv preprint arXiv:2312.09121* (2023).
- [85] T. Mori, T. N. Ikeda, E. Kaminishi, and M. Ueda, Thermalization and prethermalization in isolated quantum systems: a theoretical overview, *Journal of Physics B: Atomic, Molecular and Optical Physics* **51**, 112001 (2018).
- [86] D. García-Martín, M. Larocca, and M. Cerezo, Deep quantum neural networks form gaussian processes, *arXiv preprint arXiv:2305.09957* (2023).
- [87] C. King and M. Ruskai, Minimal entropy of states emerging from noisy quantum channels, *IEEE Trans. Inf. Th.* **47**, 192–209 (2001).
- [88] A. Müller-Hermes, D. Stilck França, and M. M. Wolf, Relative entropy convergence for depolarizing channels, *Journal of Mathematical Physics* **57**, 022202 (2016).
- [89] C. Hirche, C. Rouzé, and D. S. França, On contraction coefficients, partial orders and approximation of capacities for quantum channels, *Quantum* **6**, 862 (2022).
- [90] Y. Quek, D. S. França, S. Khatri, J. J. Meyer, and J. Eisert, Exponentially tighter bounds on limitations of quantum error mitigation, *arXiv preprint arXiv:2210.11505* (2022).
- [91] C. Hirche, C. Rouzé, and D. S. França, On contraction coefficients, partial orders and approximation of capacities for quantum channels, *Quantum* **6**, 862 (2022).
- [92] I. B. Yildiz, H. Jaeger, and S. J. Kiebel, Re-visiting the echo state property, *Neural Networks* **35**, 1 (2012).
- [93] S. Kobayashi, Q. H. Tran, and K. Nakajima, Extending echo state property for quantum reservoir computing, *Phys. Rev. E* **110**, 024207 (2024).
- [94] S. Kobayashi, Q. H. Tran, and K. Nakajima, Coherence influx is indispensable for quantum reservoir computing (2024), *arXiv:2409.12693* [quant-ph].
- [95] A. Sannia, F. Tacchino, I. Tavernelli, G. L. Giorgi, and R. Zambrini, Engineered dissipation to mitigate barren plateaus, *arXiv preprint arXiv:2310.15037* (2023).
- [96] L. Innocenti, S. Lorenzo, I. Palmisano, A. Ferraro, M. Paternostro, and G. M. Palma, Potential and limitations of quantum extreme learning machines, *Communications Physics* **6**, 118 (2023).

Appendices

Table of Contents

A	Extreme scrambling reservoir dynamics	15
1	Preliminaries	16
2	Unrolling QRP dynamics with tensor-diagram	17
3	Proof of Theorem 1: Exponential concentration	20
4	Proof of Theorem 2: Exponential memory decay	26
B	Practical consequences of exponential concentration on QRP	32
1	Preliminaries: Hypothesis testing	32
2	Main results: Statistical indistinguishability in QRP	34
3	Proofs of analytical results	36
C	Role of noise in output concentration and memory retention in QRP	38
1	Preliminaries on noise channels	38
2	Noisy input-data encoding induces concentration in the output	39
3	Memory erasure induced by reservoir with depolarizing-like noise	41
4	Memory erasure induced by reservoir with arbitrary noise	42
D	Memory indicators, and relations to standard metrics for reservoir computing	44
1	Background: echo state and fading memory properties in reservoir computing	44
2	Exponential decay of $\mathcal{M}_a(t)$ implies Fading Memory Property (FMP)-like characteristics in QRP	45
3	Exponential decay of $\mathcal{M}_h(t)$ implies Echo State Property (ESP)-like characteristics in QRP	47
4	Discussions on reservoir universality and the role of dissipation	48

Appendix A: Extreme scrambling reservoir dynamics

In this section, we provide technical details regarding the impact of the extreme scrambling reservoirs on the scalability and memory properties of QRP, including the proofs of Theorem 1 and Theorem 2.

Setting and technical challenge. For the input time series of length t , we model the extreme scrambling reservoir as an instance drawn from a $2t$ -design unitary ensemble of dimensions $d_a d_h$. Formally, we define the ensemble of the t -order extreme scrambling reservoirs $\mathcal{U}_S^{(t)}(d_a d_h)$ such that it satisfies

$$\int_{U \sim \mathcal{U}_S^{(t)}(d_a d_h)} (U \otimes U^\dagger)^{\otimes 2t} d\mu(U) = \int_{U \sim \mathcal{U}(d_n d_h)} (U \otimes U^\dagger)^{\otimes 2t} d\mu_H(U), \quad (\text{A1})$$

where $d\mu(U)$ and $d\mu_H(U)$ denote the measure associated with $\mathcal{U}_S^{(t)}(d_a d_h)$ and the Haar measure, respectively.

Modelling the extreme reservoirs with Eq. (A1) enables the Haar integral tools to analytically analyse the QRP dynamics. Nevertheless, the technical challenge stands due to the temporal correlations of the reservoir dynamics at different time steps. To see this, recall that the recursive relations of the QRP states at two consecutive time steps in Eq. (1)

$$\rho_\tau = U(\rho_{a_\tau} \otimes \rho_{h_{\tau-1}})U^\dagger. \quad (\text{A2})$$

In particular, for all time steps, the reservoir dynamic U is identical. This recursive temporal form hinders us from directly applying the standard Haar integral formulae.

Overview of our technical contributions. To tackle the above challenge, we express the QRP output in an alternative analytical form as a single time-step on a larger dimension which is achieved by systematically unrolling multiple time step with the tensor-diagram approach, as shown in Appendix A2. Then, we perform high-order Haar integration and carefully keep track of dominant terms for asymptotic scaling analysis of QRP to show exponential concentration of the outputs and exponential memory vanishing. In particular, the subsections are structured as:

- In Appendix A1, we provide existing theoretical results necessary to perform high-order Haar integration.
- In Appendix A2, we present the alternative form of QRP output unrolled as a single reservoir iteration on an extended space in Supplemental Proposition 1 together with the detailed proof.
- In Appendix A3, we prove Theorem 1 which shows the vanishing variance of QRP output.
- In Appendix A4, we prove Theorem 2 which shows the exponential vanishing of memory in QPP.

1. Preliminaries

We present the preliminary results which allow us to perform high moment Haar integration. This is a necessary tool for identifying dominant contributions for scalability and memory analysis.

Lemma 1 (Leading term of k -th moment of Haar integral (Lemma 3 of Ref. [86])). *Let X be an operator in $\mathcal{B}(\mathcal{H}^{\otimes k})$, the twirl of X over $\mathbb{U}(d)$, defined as*

$$\mathcal{T}_{\mathbb{U}(d)}^{(k)}[X] := \int_{\mathbb{U}(d)} d\mu(U) U^{\otimes k} X (U^\dagger)^{\otimes k}, \quad (\text{A3})$$

equals

$$\mathcal{T}_{\mathbb{U}(d)}^{(k)}[X] = \frac{1}{d^k} \sum_{\sigma \in P_d(S_k)} \text{Tr}[X\sigma] \sigma^{-1} + \frac{1}{d^k} \sum_{\sigma, \pi \in P_d(S_k)} c_{\sigma, \pi} \text{Tr}[X\sigma] \pi, \quad (\text{A4})$$

where $P_d(S_k)$ is the set of permutation operators applied on the copies of spaces with dimension d induced by the elements of symmetric group S_k , and the constants $c_{\sigma, \pi}$ are in $\mathcal{O}(1/d)$.

Remark: The elements in the symmetric group S_k can be denoted as collection of distinct tuples of indices from $[k]$. In the representation for the operators, these elements are essentially presented as SWAP operators between different copies/subsystems. More specifically, consider two subsystems A and B ; each of dimensions d with orthonormal basis $\{|i\rangle\}_{i=1}^d$, the SWAP operator is defined as $\text{SWAP}_{A,B} = \sum_{i,j} |i\rangle\langle j|_A \otimes |j\rangle\langle i|_B$. For two operators O_A and O_B on the subsystems A and B respectively, one useful identity follows

$$\text{Tr}[(O_A \otimes O_B) \text{SWAP}_{A,B}] = \text{Tr}[O_A O_B]. \quad (\text{A5})$$

Here we further provide examples of S_k and the induced $\text{Tr}[X\sigma]$ with $\sigma \in P_d(S_k)$ for small k 's:

- $k = 1$: $S_1 = \{(1)\}$.
For $s = (1)$, we have $\sigma = P_d(s) = \mathcal{I}$, and hence $\text{Tr}[X\sigma] = \text{Tr}[X]$.
- $k = 2$: $S_2 = \{(1)(2), (21)\}$.
For $s = (1)(2)$, we have $\sigma = P_d(s) = \mathcal{I} \otimes \mathcal{I}$, and hence $\text{Tr}[(X_{h_1} \otimes X_{h_2})\sigma] = \text{Tr}[X_{h_1}] \text{Tr}[X_{h_2}]$.
If $s = (21)$, then $\sigma = P_d(s) = \text{SWAP}$, and $\text{Tr}[(X_{h_1} \otimes X_{h_2})\sigma] = \text{Tr}[X_{h_1} X_{h_2}]$.

- $k = 3$: $S_3 = \{(1)(2)(3), (1)(23), (12)(3), (13)(2), (123), (132)\}$.
 If $s = (1)(23)$, then $\sigma = P_d(s) = \mathcal{I}_1 \otimes \text{SWAP}_{23}$, and $\text{Tr}[(X_{h_1} \otimes X_{h_2} \otimes X_{h_3})\sigma] = \text{Tr}[X_{h_1}] \text{Tr}[X_{h_2} X_{h_3}]$.
 If $s = (123)$, then $\sigma = P_d(s) = (\mathcal{I}_1 \otimes \text{SWAP}_{23})(\text{SWAP}_{12} \otimes \mathcal{I}_3)$, and $\text{Tr}[(X_{h_1} \otimes X_{h_2} \otimes X_{h_3})\sigma] = \text{Tr}[X_{h_1} X_{h_2} X_{h_3}]$.
 If $s = (132)$, then $\sigma = P_d(s) = (\text{SWAP}_{12} \otimes \mathcal{I}_3)(\mathcal{I}_1 \otimes \text{SWAP}_{23})$, and $\text{Tr}[(X_{h_1} \otimes X_{h_2} \otimes X_{h_3})\sigma] = \text{Tr}[X_{h_1} X_{h_3} X_{h_2}]$.
- Arbitrary k : $S_k = \{(\alpha_{1,1}, \alpha_{1,2}, \dots, \alpha_{1,n_1}), (\alpha_{2,1}, \alpha_{2,2}, \dots, \alpha_{2,n_2}), \dots, (\alpha_{m,1}, \alpha_{m,2}, \dots, \alpha_{m,n_m})\}$ where $\sum_{k=1}^m n_k = k$ and $\cup_{k=1}^m (\cup_{l=1}^{n_k} \alpha_{k,l} = [k])$

For more details about the symmetric group and the induced permutation, we refer the readers to Supplemental Information A of Ref. [86], and the references therein.

2. Unrolling QRP dynamics with tensor-diagram

We recall the QRP output at time step t for the state ρ_t in Eq. (A2) and an observable O is written in the recursive form as

$$\langle O \rangle_t = \text{Tr}[O \rho_t] \quad (\text{A6})$$

$$= \text{Tr}[OU(\rho_{a_t} \otimes \text{Tr}_a(\rho_{t-1}))U^\dagger] . \quad (\text{A7})$$

The following statement presents an alternative form of QRP output as a single iteration on a larger $(n_a + n_h)t$ composite system. A sketch of the proof of this statement is provided in Fig. 7.

Supplemental Proposition 1. Consider a QRP model with the reservoir U , the initial reservoir state ρ_{h_0} which recursively processes the input states $\rho_{a_t} = (\rho_{a_1}, \dots, \rho_{a_t})$. The QRP output at the time step t in Eq. (A7) can be expressed as

$$\langle O \rangle_t = \sum_{\mathbf{X}_{h_{t-1}}} \text{Tr}[(X_{h_1}, \mathcal{I}_a; X_{h_2}, \mathcal{I}_a; \dots; X_{h_{t-1}}, \mathcal{I}_a; O) U^{\otimes t}(\rho_{h_0}, \rho_{a_1}; X_{h_1}, \rho_{a_2}; X_{h_2}, \rho_{a_3}; \dots; X_{h_{t-1}}, \rho_{a_t}) (U^\dagger)^{\otimes t}] , \quad (\text{A8})$$

where $\mathbf{X}_{h_{t-1}} = (X_{h_1}, \dots, X_{h_{t-1}})$ and $X_{h_\tau} \in \mathcal{B}_h$ with \mathcal{B}_h being the orthonormal basis over the operator space of the subsystem h_τ with dimensions d_h . Here, “,” denotes the tensor products of operators in accessible and hidden space, and “;” denotes the tensor products of composite operators in different copies of the composite space. In addition, \mathcal{I}_a is an identity matrix on the accessible subsystem with dimensions d_a .

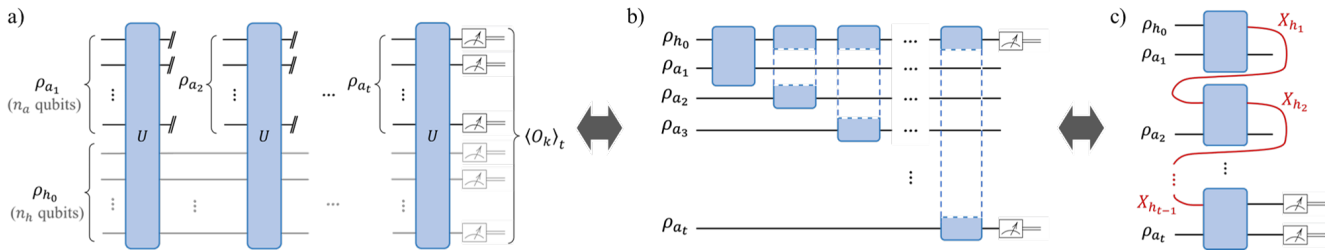


Figure 7. **Sketch of proof for unrolling the multiple step QRP output.** First, from panel a) to b), we simplify the recursive expression of expectation values in Eq. (2) and write it in the effectively extended space of $(t \cdot n_a + n_h)$ qubits. Second, from panel b) to c), we further extend the system to $t \cdot (n_a + n_h)$ qubits, such that the integral for QRP with arbitrary t -steps can be transformed to a standard Haar integral of $2t$ 'th moment. Finally, we calculate the leading term of observables' variance and find its lower bound using Lemma 3 of Ref. [86].

Proof. We consider the QRP output at time step t in Eq. (A7) and recursively unroll the early time step QRP states with Eq. (A2). Our first crucial remark is that throughout the proof we explicitly write the subscripts for all the reservoirs

to keep track of which subsystems they act on. For example, at the last time step t , we have U_{a_th} which indicates that the reservoir U acts on the accessible subsystem “ a_t ” (corresponding to the one being injected by the input ρ_{a_t}) and the hidden subsystem “ h ”. Note that the observable O acts on the subsystems “ a_t ” and “ h ”.

Now, our strategy is to absorb the partial trace with respect to the hidden space into a trace of larger dimension by using the “trace-partial-trace-identity”, i.e. $\text{Tr}_{AB}[(X_A \otimes \mathcal{I}_B)Y_{AB}] = \text{Tr}_A[X_A \text{Tr}_B(Y_{AB})]$ for any operators X_A in subspace A , Y_{AB} in composite space AB and \mathcal{I}_B is an identity on the subspace B . Let us exemplify the above process by unrolling the last 3 consecutive time steps, namely $t, t-1$ and $t-2$.

$$\langle O \rangle_t = \text{Tr}_{ha_t} [O U_{a_th} (\rho_{a_t} \otimes \text{Tr}_{a_{t-1}}(\rho_{t-1})) U_{a_th}^\dagger] \quad (\text{A9})$$

$$= \text{Tr}_{ha_t a_{t-1}} [(O \otimes \mathcal{I}_{a_{t-1}}) (U_{a_th} \otimes \mathcal{I}_{a_{t-1}}) (\rho_{a_t} \otimes \rho_{t-1}) (U_{a_th}^\dagger \otimes \mathcal{I}_{a_{t-1}})] \quad (\text{A10})$$

$$= \text{Tr}_{ha_t a_{t-1}} [(O \otimes \mathcal{I}_{a_{t-1}}) (U_{a_th} \otimes \mathcal{I}_{a_{t-1}}) (\rho_{a_t} \otimes [U_{a_{t-1}h} (\rho_{a_{t-1}} \otimes \text{Tr}_{a_{t-2}}[\rho_{t-1}]) U_{a_{t-1}h}^\dagger]) (U_{a_th}^\dagger \otimes \mathcal{I}_{a_{t-1}})] \quad (\text{A11})$$

$$= \text{Tr}_{ha_t \dots a_{t-2}} [(O \otimes \mathcal{I}_{a_{t-1}, a_{t-2}}) (U_{a_th} \otimes \mathcal{I}_{a_{t-1}, a_{t-2}}) (\rho_{a_t} \otimes \mathcal{I}_{h, a_{t-1}, a_{t-2}}) (U_{a_{t-1}h} \otimes \mathcal{I}_{a_t, a_{t-2}}) (\rho_{a_{t-1}} \otimes \rho_{t-2} \otimes \mathcal{I}_{a_t}) (U_{a_{t-1}h}^\dagger \otimes \mathcal{I}_{a_t, a_{t-2}}) (U_{a_th}^\dagger \otimes \mathcal{I}_{a_{t-1}, a_{t-2}})] \quad (\text{A12})$$

$$= \text{Tr}_{ha_t \dots a_{t-2}} [(O \otimes \mathcal{I}_{a_{t-1}, a_{t-2}}) (U_{a_th} \otimes \mathcal{I}_{a_{t-1}, a_{t-2}}) (U_{a_{t-1}h} \otimes \mathcal{I}_{a_t, a_{t-2}}) (\rho_{a_t} \otimes \rho_{a_{t-1}} \otimes \rho_{t-2}) (U_{a_{t-1}h}^\dagger \otimes \mathcal{I}_{a_t, a_{t-2}}) (U_{a_th}^\dagger \otimes \mathcal{I}_{a_{t-1}, a_{t-2}})] \quad (\text{A13})$$

where to reach the last equality we commute $(\rho_{a_t} \otimes \mathcal{I}_{h, a_{t-1}, a_{t-2}})$ and $(U_{a_{t-1}h} \otimes \mathcal{I}_{a_t, a_{t-2}})$, as their non-identity parts are in different subspaces, and then do $(\rho_{a_t} \otimes \mathcal{I}_{h, a_{t-1}, a_{t-2}}) (\rho_{a_{t-1}} \otimes \rho_{t-2} \otimes \mathcal{I}_{a_t}) = (\rho_{a_t} \otimes \rho_{a_{t-1}} \otimes \rho_{t-2})$. We remark that in the equalities above, the subscripts of traces denote the subspaces that the trace operator is acting upon.

By repeating the above procedure until the first time step, we obtain

$$\langle O \rangle_t = \text{Tr}_{h, a_t, \dots, a_1} [(O \otimes \mathcal{I}_{a_{t-1}, \dots, a_1}) U_t \dots U_1 (\rho_{h_0} \otimes \rho_{a_t} \otimes \dots \rho_{a_1}) U_1^\dagger \dots U_t^\dagger] \quad (\text{A14})$$

where, for all $\tau = 1, \dots, t$, we denote $U_\tau = U_{a_\tau h} \otimes \mathcal{I}_{\{a_t, \dots, a_1\} \setminus a_\tau}$ which indicates that U_τ acts non-trivially on the hidden space and the accessible space of the τ -th iteration, and acts trivially on the other subsystems.

Our next step is to further extend the space. To do so, it is convenient to work in the vectorized form. Using the identity $\text{Tr}[OU\rho U^\dagger] = \langle O|U \otimes U^*|\rho\rangle$ where $|\rho\rangle$ and $|O\rangle$ are vectorized forms of ρ and O respectively, we obtain

$$\langle O \rangle_t = \langle O \otimes \mathcal{I}_{a_{t-1}, \dots, a_1} | (U_t \dots U_1) \otimes (U_t^* \dots U_1^*) | \rho_{h_0} \otimes \rho_{a_t} \otimes \dots \rho_{a_1} \rangle \quad (\text{A15})$$

$$= \langle O \otimes \mathcal{I}_{a_{t-1}, \dots, a_1} | W_{a_th} \dots W_{a_1 h} | \rho_{h_0} \otimes \rho_{a_t} \otimes \dots \rho_{a_1} \rangle \quad (\text{A16})$$

where $W_{a_\tau h} := U_{a_\tau h} \otimes U_{a_\tau h}^* \otimes \mathcal{I}_{\{a_t, \dots, a_1\} \setminus a_\tau}^{\otimes 2}$. We note that here the order of spaces and subspaces are interchangeable.

To further proceed, it is crucial to notice that for distinct τ and τ' , $U_{a_\tau h}$ and $U_{a_{\tau'} h}$ (as well as $W_{a_\tau h}$ and $W_{a_{\tau'} h}$) only overlap in the hidden subsystem but never in the accessible subsystems, as illustrated in Fig. 7(b). Inspired by this, let us first consider the simplified version with only three subsystems A, B and C and the following quantity $\langle \tilde{O} \rangle_{ABC}$ of the form

$$\langle \tilde{O} \rangle_{ABC} = \langle O_{AB} \otimes O_C | (W_{AB} \otimes \mathcal{I}_C^{\otimes 2}) (W_{AC} \otimes \mathcal{I}_B^{\otimes 2}) | \rho_A \otimes \rho_B \otimes \rho_C \rangle \quad (\text{A17})$$

where W_{AB} and W_{AC} are some operators acting on the subsystems AB and AC respectively. Crucially, they both act on subsystem A . In addition, O_{AB} is an arbitrary observable on the subsystems AB while O_C is an observable on the subsystem C . Similarly, ρ_A, ρ_B, ρ_C are some arbitrary states on the subsystems A, B, C respectively.

By using the Hilbert-Schmidt resolution of identities on the common subsystem, the following computation steps hold (or, alternatively, are illustrated in Fig. 8 with tensor diagrams):

$$\langle \tilde{O} \rangle_{ABC} = (\langle O_{AB} | W_{AB} \otimes \mathcal{I}_C^{\otimes 2}) (\mathcal{I}_A^{\otimes 2} \otimes |\rho_B\rangle \otimes \langle O_C |) (W_{AC} \otimes \mathcal{I}_B^{\otimes 2} | \rho_A \otimes \rho_C \rangle) \quad (\text{A18})$$

$$= (\langle O_{AB} | W_{AB} \otimes \mathcal{I}_C^{\otimes 2}) \left[\sum_{X \in B_A} |X\rangle \langle X| \right] \otimes |\rho_B\rangle \otimes \langle O_C | (\mathcal{I}_A^{\otimes 2} \otimes W_{CB} | \rho_A \otimes \rho_C \rangle) \quad (\text{A19})$$

$$= \sum_{X \in B_A} \langle O_{AB} | W_{AB} | X \otimes \rho_B \rangle \langle X \otimes O_C | W_{AC} | \rho_A \otimes \rho_C \rangle \quad (\text{A20})$$

where the sum is taken over $X \in B_A$ where B_A is a complete orthonormal basis in the operator space of the subsystem A under the Hilbert-Schmidt norm. For instance, we could choose a set of singleton matrices $B_A = \{|i\rangle\langle j| : i, j = 0, \dots, d_A - 1\}$ such that $\{|X\rangle\rangle : X \in B_A\}$ forms the computational basis; alternatively we could also use Pauli strings, if space A is qubit-defining, such that their vectorizations are Bell states.

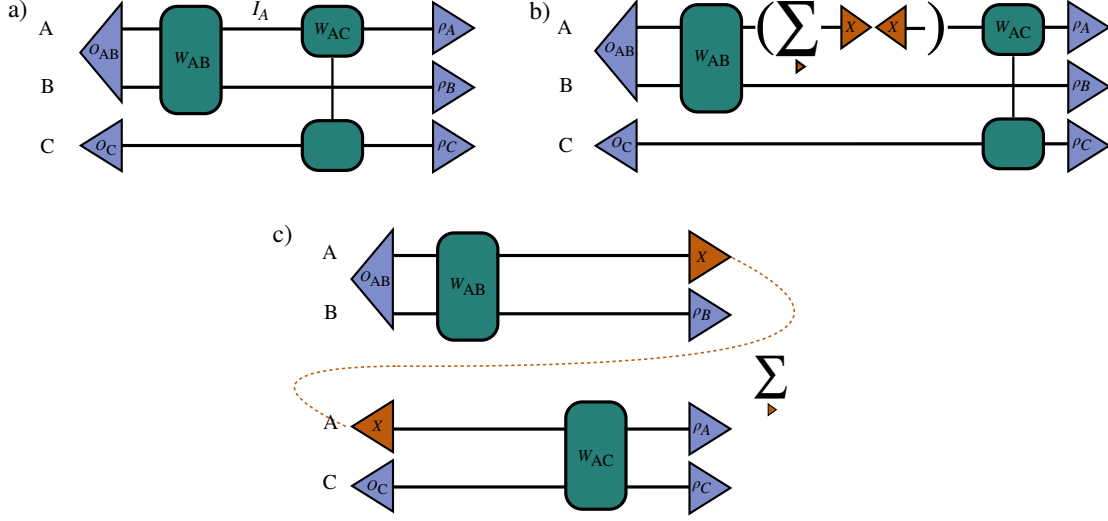


Figure 8. **Tensor diagram for proving Eq (A20)**. Unrolling multiple step QRP output relies on recursively applying this tensor diagram for different time steps (with appropriately assigned subsystems A , B and C).

We are now ready to tackle the QRP output $\langle O \rangle_t$ in Eq. (A16) by recursively applying Eq. (A20). This is done by systematically identifying what the subsystems A , B and C are for each iteration.

For the time step t . We choose A in Eq. (A20) to be the hidden subsystem h_0 , choose B to be the subsystem a_t and choose C to be the rest i.e., a_{t-1}, \dots, a_1 .

With this selection, we have $O_{AB} = O$, $O_C = \mathcal{I}_{a_{t-1}, \dots, a_1}$, as well as $\rho_A = \rho_{h_0}$, $\rho_B = \rho_{a_t}$, $\rho_C = \rho_{a_{t-1}} \otimes \dots \otimes \rho_{a_1}$, leading to

$$\langle O \rangle_t = \sum_{X_{h_{t-1}} \in B_h} \langle\langle O | W_{a_t h} | X_{h_{t-1}} \otimes \rho_{a_t} \rangle\rangle \langle\langle X_{h_{t-1}} \otimes \mathcal{I}_{a_{t-1}, \dots, a_1} | W_{a_{t-1} h} \dots W_{a_1 h} | \rho_{h_0} \otimes \rho_{a_{t-1}} \dots \rho_{a_1} \rangle\rangle, \quad (\text{A21})$$

where we introduce the subscript h_t to indicate that $X_{h_{t-1}}$ acts on the expanded hidden subspace.

For the time step $t-1$. We only apply Eq. (A20) to the term $\langle\langle X_{h_{t-1}} \otimes \mathcal{I}_{a_{t-1}, \dots, a_1} | W_{a_{t-1} h} \dots W_{a_1 h} | \rho_{h_0} \otimes \rho_{a_{t-1}} \dots \rho_{a_1} \rangle\rangle$ in Eq. (A21). Here, we choose A to be the hidden subsystem h_0 , choose B to be $\rho_{a_{t-1}}$ and choose C to be the rest i.e., a_{t-2}, \dots, a_1 (excluding a_t).

With this selection, we have $O_{AB} = X_{h_{t-1}} \otimes \mathcal{I}_{a_{t-1}}$, $O_C = \mathcal{I}_{a_{t-2}, \dots, a_1}$, and $\rho_A = \rho_{h_0}$, $\rho_B = \rho_{a_{t-1}}$, $\rho_C = \rho_{a_{t-2}} \otimes \dots \otimes \rho_{a_1}$, leading to

$$\langle O \rangle_t = \sum_{X_{h_{t-1}}, X_{h_{t-2}}} \langle\langle O | W_{a_t h} | X_{h_{t-1}} \otimes \rho_{a_t} \rangle\rangle \langle\langle X_{h_{t-1}} \otimes \mathcal{I}_{a_{t-1}} | W_{a_{t-1} h} | X_{h_{t-2}} \otimes \rho_{a_{t-1}} \rangle\rangle \langle\langle X_{h_{t-2}} \otimes \mathcal{I}_{a_{t-2}, \dots, a_1} | W_{a_{t-2} h} \dots W_{a_1 h} | \rho_{h_0} \otimes \rho_{a_{t-2}} \dots \rho_{a_1} \rangle\rangle \quad (\text{A22})$$

$$= \sum_{X_{h_{t-1}}, X_{h_{t-2}}} \langle\langle O \otimes X_{h_{t-1}} \otimes \mathcal{I}_{a_{t-1}} | W_{a_t h} \otimes W_{a_{t-1} h} | X_{h_{t-1}} \otimes \rho_{a_t} \otimes X_{h_{t-2}} \otimes \rho_{a_{t-1}} \rangle\rangle \langle\langle X_{h_{t-2}} \otimes \mathcal{I}_{a_{t-2}, \dots, a_1} | W_{a_{t-2} h} \dots W_{a_1 h} | \rho_{h_0} \otimes \rho_{a_{t-2}} \dots \rho_{a_1} \rangle\rangle, \quad (\text{A23})$$

where in the second equality we use $\langle\langle A | B | C \rangle\rangle \langle\langle A' | B' | C' \rangle\rangle = \langle\langle A \otimes A' | B \otimes B' | C \otimes C' \rangle\rangle$.

By recursively doing this procedure, we eventually obtain

$$\langle O \rangle_t = \sum_{\mathbf{X}_{h_{t-1}}} \langle\langle O; X_{h_{t-1}}, \mathcal{I}_{a_{t-1}}; \cdots; X_{h_1}, \mathcal{I}_{a_1} | W_{a_t h}; W_{a_{t-1} h}; \cdots; W_{a_1 h} | X_{h_{t-1}}, \rho_{a_t}; \cdots; X_{h_1}, \rho_{a_2}; \rho_{h_0}, \rho_{a_1} \rangle\rangle \quad (\text{A24})$$

$$= \sum_{\mathbf{X}_{h_{t-1}}} \text{Tr}[(X_{h_1}, \mathcal{I}_{a_1}; X_{h_2}, \mathcal{I}_{a_2}; \cdots; X_{h_{t-1}}, \mathcal{I}_{a_{t-1}}; O) U^{\otimes t}(\rho_{h_0}, \rho_{a_1}; X_{h_1}, \rho_{a_2}; X_{h_2}, \rho_{a_3}; \cdots; X_{h_{t-1}}, \rho_{a_t}) (U^\dagger)^{\otimes t}] , \quad (\text{A25})$$

where $\mathbf{X}_{h_{t-1}} = (X_{h_{t-1}}, \cdots, X_{h_1})$ with each X_k being sum over all the basis. Here in the above equations, “,” denotes the tensor products of operators in accessible and hidden space, and “;” denotes the tensor products of composite operators in different copies of the composite space. In the last equality, we undo the vectorization together with explicitly writing the reservoir U (instead of $W_{a_\tau h}$). \square

3. Proof of Theorem 1: Exponential concentration

In this section, we provide a formal version of Theorem 1 addressing the concentration of QRP’s output and its detailed proof.

Theorem 1 (Vanishing variance of QRP output with extreme scrambling reservoir, formal). *Given that a reservoir is sampled from a $2t$ -design on $\mathbb{U}(d_a d_h)$, the variance of QRP output with some observable O at time step t vanishes exponentially with the number of accessible n_a and hidden n_h qubits. The scaling depends on neither the input states nor the time step t . Formally, the variance is given by*

$$\text{Var}_{U \sim \mathbb{U}(d_a d_h)}[\langle O \rangle_t] = \frac{\text{Tr}[O^2](1 + \beta)}{d_a^2 d_h^3} , \quad (\text{A26})$$

with $\beta \in \mathcal{O}(\frac{1}{d_a d_h})$. In addition, the QRP output exponentially concentrates as

$$\Pr_{U \sim \mathbb{U}(d_a d_h)} (|\langle O \rangle_t - \mathbb{E}_U[\langle O \rangle_t]| \geq \delta) \leq \frac{\text{Tr}[O^2]}{\delta^2 d_a^2 d_h^3} , \quad (\text{A27})$$

where the concentration point is independent of the reservoir and the input states

$$\mathbb{E}_{\mathbb{U}(d_a d_h)}[\langle O \rangle] = \frac{\text{Tr}[O]}{d_a d_h} (1 + \beta') , \quad (\text{A28})$$

with $\beta' \in \mathcal{O}(\frac{1}{d_a d_h})$.

Proof: By Supplemental Proposition 1, we obtain the standard form of t -th moment for QRP’s output, which enables Haar integral. Our proof strategy is by applying Lemma 1 to find the leading term of the variance of QRP output.

We first recall the expression of reservoir output from Supplemental Proposition 1

$$\langle O \rangle_t = \sum_{\mathbf{X}_{h_{t-1}}} \text{Tr}[(X_{h_1}, \mathcal{I}_a; X_{h_2}, \mathcal{I}_a; \cdots; X_{h_{t-1}}, \mathcal{I}_a; O) U^{\otimes t}(\rho_{h_0}, \rho_{a_1}; X_{h_1}, \rho_{a_2}; X_{h_2}, \rho_{a_3}; \cdots; X_{h_{t-1}}, \rho_{a_t}) (U^\dagger)^{\otimes t}] . \quad (\text{A29})$$

Here, “,” denotes the tensor products of operators in accessible and hidden space, and “;” denotes the tensor products of composite operators in different copies of the composite space. Then, the square of the quantity is given by

$$\begin{aligned} \langle O \rangle_t^2 &= \sum_{\mathbf{X}_{h_{t-1}}, \mathbf{Y}_{h_{t-1}}} \text{Tr}[(X_{h_1}, \mathcal{I}_a; X_{h_2}, \mathcal{I}_a; \cdots; X_{h_{t-1}}, \mathcal{I}_a; O) U^{\otimes t}(\rho_{h_0}, \rho_{a_1}; X_{h_1}, \rho_{a_2}; X_{h_2}, \rho_{a_3}; \cdots; X_{h_{t-1}}, \rho_{a_t}) (U^\dagger)^{\otimes t}] \\ &\quad \cdot \text{Tr}[(Y_{h_1}, \mathcal{I}_a; Y_{h_2}, \mathcal{I}_a; \cdots; Y_{h_{t-1}}, \mathcal{I}_a; O) U^{\otimes t}(\rho_{h_0}, \rho_{a_1}; Y_{h_1}, \rho_{a_2}; Y_{h_2}, \rho_{a_3}; \cdots; Y_{h_{t-1}}, \rho_{a_t}) (U^\dagger)^{\otimes t}] \end{aligned} \quad (\text{A30})$$

$$\begin{aligned} &= \sum_{\mathbf{X}_{h_{t-1}}, \mathbf{Y}_{h_{t-1}}} \text{Tr}[(X_{h_1}, \mathcal{I}_a; X_{h_2}, \mathcal{I}_a; \cdots; X_{h_{t-1}}, \mathcal{I}_a; O; Y_{h_1}, \mathcal{I}_a; Y_{h_2}, \mathcal{I}_a; \cdots; Y_{h_{t-1}}, \mathcal{I}_a; O) U^{\otimes 2t} \\ &\quad \cdot (\rho_{h_0}, \rho_{a_1}; X_{h_1}, \rho_{a_2}; X_{h_2}, \rho_{a_3}; \cdots; X_{h_{t-1}}, \rho_{a_t}; \rho_{h_0}, \rho_{a_1}; Y_{h_1}, \rho_{a_2}; Y_{h_2}, \rho_{a_3}; \cdots; Y_{h_{t-1}}, \rho_{a_t}) (U^\dagger)^{\otimes 2t}] \end{aligned} \quad (\text{A31})$$

To obtain the variance, we proceed by determining the leading terms of first and second moments, respectively.

a. First moment

We first determine the leading term of the expectation value of QRP's output:

$$\mathbb{E}_{\mathbb{U}(d_a d_h)} [\langle O \rangle_t] \quad (\text{A32})$$

$$= \sum_{\mathbf{X}_{h_{t-1}}} \int d\mu(U) \text{Tr}[(X_{h_1}, \mathcal{I}_a; X_{h_2}, \mathcal{I}_a; \dots; X_{h_{t-1}}, \mathcal{I}_a; O) U^{\otimes t} (\rho_{h_0}, \rho_{a_1}; X_{h_1}, \rho_{a_2}; X_{h_2}, \rho_{a_3}; \dots; X_{h_{t-1}}, \rho_{a_t}) (U^\dagger)^{\otimes t}] \quad (\text{A33})$$

$$= \frac{1}{(d_a d_h)^t} \sum_{\mathbf{X}_{h_{t-1}}} \left(\sum_{\sigma \in P_{d_a d_h}(S_t)} \text{Tr}[(X_{h_1}, \mathcal{I}_a; X_{h_2}, \mathcal{I}_a; \dots; X_{h_{t-1}}, \mathcal{I}_a; O) \sigma] \text{Tr}[(\rho_{h_0}, \rho_{a_1}; X_{h_1}, \rho_{a_2}; X_{h_2}, \rho_{a_3}; \dots; X_{h_{t-1}}, \rho_{a_t}) \sigma^{-1}] \right. \\ \left. + \sum_{\sigma, \pi \in P_{d_a d_h}(S_t)} c_{\sigma, \pi} \text{Tr}[(X_{h_1}, \mathcal{I}_a; X_{h_2}, \mathcal{I}_a; \dots; X_{h_{t-1}}, \mathcal{I}_a; O) \sigma] \text{Tr}[(\rho_{h_0}, \rho_{a_1}; X_{h_1}, \rho_{a_2}; X_{h_2}, \rho_{a_3}; \dots; X_{h_{t-1}}, \rho_{a_t}) \pi] \right), \quad (\text{A34})$$

where the last equality is obtained using Lemma 1, and the prefactors $c_{\sigma, \pi} \in \mathcal{O}((d_a d_h)^{-1})$ which are exponentially small in number of qubits. We further note that both sums have polynomially many terms. Hence for the leading order terms we have:

$$\mathbb{E}_{\mathbb{U}(d_a d_h)} [\langle O \rangle_t] = \frac{1}{(d_a d_h)^t} (1 + \mathcal{O}((d_a d_h)^{-1})) \sum_{\mathbf{X}_{h_{t-1}}} \sum_{\sigma \in P_{d_a d_h}(S_t)} \text{Tr}[(X_{h_1}, \mathcal{I}_a; X_{h_2}, \mathcal{I}_a; \dots; X_{h_{t-1}}, \mathcal{I}_a; O) \sigma] \text{Tr}[(\rho_{h_0}, \rho_{a_1}; X_{h_1}, \rho_{a_2}; X_{h_2}, \rho_{a_3}; \dots; X_{h_{t-1}}, \rho_{a_t}) \sigma^{-1}] \quad (\text{A35})$$

$$\text{Tr}[(X_{h_1}, \mathcal{I}_a; X_{h_2}, \mathcal{I}_a; \dots; X_{h_{t-1}}, \mathcal{I}_a; O) \sigma] \text{Tr}[(\rho_{h_0}, \rho_{a_1}; X_{h_1}, \rho_{a_2}; X_{h_2}, \rho_{a_3}; \dots; X_{h_{t-1}}, \rho_{a_t}) \sigma^{-1}] \quad (\text{A36})$$

$$= \frac{1}{(d_a d_h)^t} (1 + \mathcal{O}((d_a d_h)^{-1})) \sum_{\sigma \in P_{d_a d_h}(S_t)} g_\sigma^{(1)}(O), \quad (\text{A37})$$

where we denote

$$g_\sigma^{(1)}(O) := \sum_{\mathbf{X}_{h_{t-1}}} \text{Tr}[(X_{h_1}, \mathcal{I}_a; X_{h_2}, \mathcal{I}_a; \dots; X_{h_{t-1}}, \mathcal{I}_a; O) \sigma] \text{Tr}[(\rho_{h_0}, \rho_{a_1}; X_{h_1}, \rho_{a_2}; X_{h_2}, \rho_{a_3}; \dots; X_{h_{t-1}}, \rho_{a_t}) \sigma^{-1}]. \quad (\text{A38})$$

In what follows, our argument hinges on two fundamental observations:

1. $g_\sigma^{(1)}(O)$ with the identity operator $\sigma = \otimes_{i=1}^t \mathcal{I}_{a_i} \otimes \mathcal{I}_{h_i}$ is the dominant term in Eq. (A37).
2. Other $g_\sigma^{(1)}(O)$ (with other permutation operators $\sigma \neq \otimes_{i=1}^t \mathcal{I}_{a_i} \otimes \mathcal{I}_{h_i}$) are smaller than the dominant term by at least one order of $d_a d_h$.

Proving them is indeed not straight forward. We proceed by first gaining some intuition with the toy example for $t = 2$, and then consider the general setting with arbitrary t time steps by performing the computation with the identity element as well as arguing that other permutation elements give smaller contribution.

Toy example with $t = 2$ and a separable observable. We gain some intuitive understanding regarding the dominant term with a simple example¹. Let us consider $t = 2$ and $O = O_h \otimes O_a$ with some observables O_h and O_a acting on hidden and accessible subsystems respectively. In this setting, $g_\sigma^{(1)}(O)$ is of the form

$$g_\sigma^{(1)}(O) = \sum_{\mathbf{X}_{h_1} \in \{|i\rangle\}_{i,j=1}^{d_h}} \text{Tr}[(X_{h_1}, \mathcal{I}_a; O_h, O_a) \sigma] \text{Tr}[(\rho_{h_0}, \rho_{a_1}; X_{h_1}, \rho_{a_2}) \sigma]. \quad (\text{A39})$$

¹ – just like how other physics problems start to get solved with a simple harmonic oscillator –

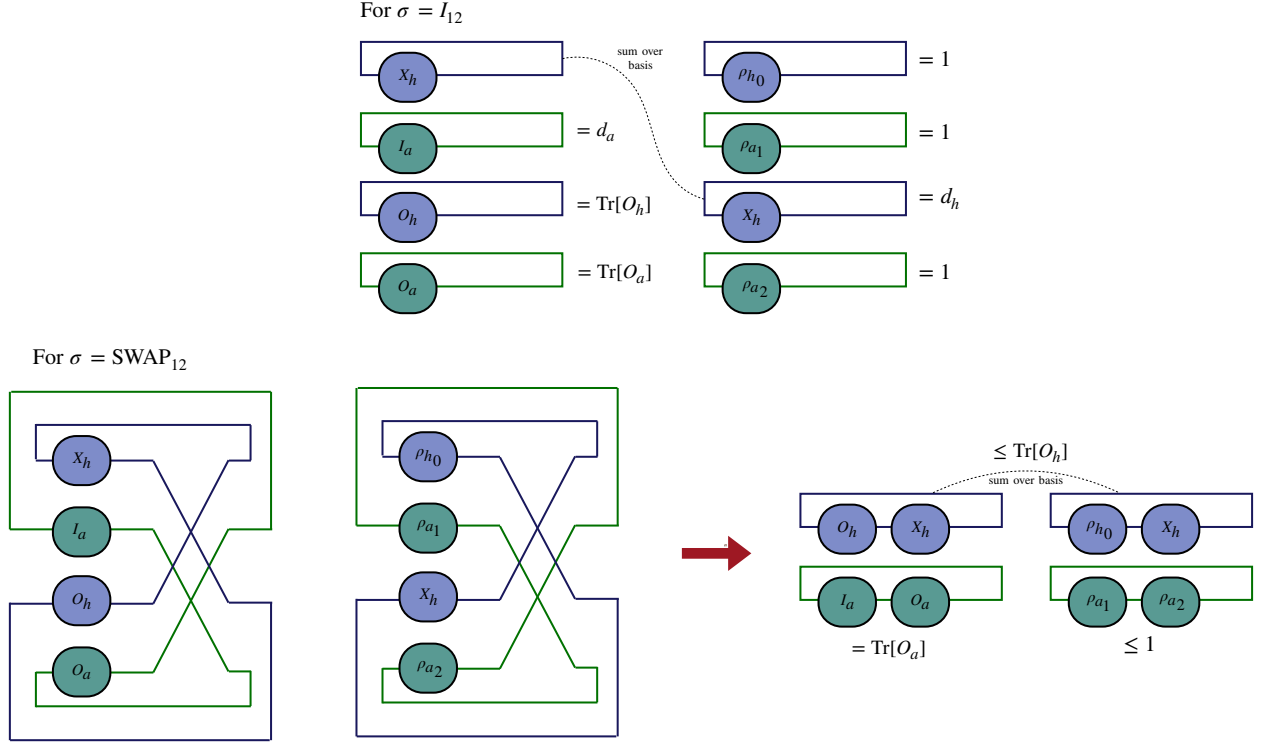


Figure 9. **Tensor diagrams of $g_\sigma^{(1)}(O)$ for the toy example with $t = 2$.** We illustrate the tensor diagrams for $g_\sigma^{(1)}(O)$ in Eq. (A39) associated with identity and SWAP operators. The effect of the SWAP operator is such that the factor of $d_a d_h$ vanishes, and hence $g_\sigma^{(1)}(O)$ with $\sigma = I_{12}$ is the dominant term.

Here, the set of permutation operators is $\sigma \in \{I_{12}, \text{SWAP}_{12}\}$ with $I_{12} = (\mathcal{I}_a \otimes \mathcal{I}_{h_0})^{\otimes 2}$. We now compute $g_\sigma^{(1)}(O)$ for these two operators and compare their values. Fig. 9 illustrates this computation with tensor network diagrams.

For $\sigma = I_{12}$, we have

$$g_\sigma^{(1)}(O) = \sum_{\mathbf{X}_{h_1} \in \{|i\rangle\langle j|\}_{i,j=1}^{d_h}} \text{Tr}[(X_{h_1}, \mathcal{I}_a; O_h, O_a) I_{12}] \text{Tr}[(\rho_{h_0}, \rho_{a_1}; X_{h_1}, \rho_{a_2}) I_{12}] \quad (\text{A40})$$

$$= \sum_{\mathbf{X}_{h_1} \in \{|i\rangle\langle j|\}_{i,j=1}^{d_h}} \text{Tr}[X_{h_1}] \text{Tr}[\mathcal{I}_a] \text{Tr}[O_h] \text{Tr}[O_a] \text{Tr}[X_{h_1}] \quad (\text{A41})$$

$$= \sum_{i,j=1}^{d_h} \delta_{ij}^2 d_a \text{Tr}[O] \quad (\text{A42})$$

$$= d_h d_a \text{Tr}[O], \quad (\text{A43})$$

where we use $\text{Tr}[X_{h_1}] = \delta_{ij}$ together with $\delta_{ij}^2 = \delta_{ij}$, $\text{Tr}[O_h] \text{Tr}[O_a] = \text{Tr}[O]$ and $\text{Tr}[\rho] = 1$ for any quantum state ρ .

On the other hand, for $\sigma = \text{SWAP}_{12}$ we have

$$g_{\sigma}^{(1)}(O) = \sum_{\mathbf{X}_{h_1} \in \{|i\rangle\langle j|\}_{i,j=1}^{d_h}} \text{Tr}[(X_{h_1}, \mathcal{I}_a; O_h, O_a) \text{SWAP}_{12}] \text{Tr}[(\rho_{h_0}, \rho_{a_1}; X_{h_1}, \rho_{a_2}) \text{SWAP}_{12}] \quad (\text{A44})$$

$$= \sum_{\mathbf{X}_{h_1} \in \{|i\rangle\langle j|\}_{i,j=1}^{d_h}} \text{Tr}[X_h O_h] \text{Tr}[\mathcal{I}_a O_a] \text{Tr}[\rho_{h_0} X_{h_1}] \text{Tr}[\rho_{a_1} \rho_{a_2}] \quad (\text{A45})$$

$$= \sum_{i,j=1}^{d_h} \langle j|O_h|i\rangle \text{Tr}[O_a] \langle j|\rho_{h_0}|i\rangle \text{Tr}[\rho_{a_1} \rho_{a_2}] \quad (\text{A46})$$

$$\leq \sum_{i,j=1}^{d_h} \langle j|O_h|i\rangle \text{Tr}[O_a] \delta_{ij} \quad (\text{A47})$$

$$= \text{Tr}[O], \quad (\text{A48})$$

where in the second equality we have used $\text{Tr}[(P_1 \otimes P_2) \text{SWAP}_{12}] = \text{Tr}[P_1 P_2]$ with P_1 and P_2 being some operators on the first and second copies. The inequality is from $\text{Tr}[\rho_{h_0} X_{h_1}] \leq \|\rho_{h_0}\|_{\infty} \|X\|_1 \leq \delta_{ij}$ (with $\|\rho_{h_0}\|_{\infty} \leq 1$), and $\text{Tr}[\rho_{a_1} \rho_{a_2}] \leq 1$.

Hence, we observe that $g_{\sigma}^{(1)}(O)$ with σ being the identity is the leading term and larger than the other term by the factor $d_a d_h$. This can be intuitively understood from the role of SWAP operator. In particular, we observe that

1. The disappear of d_a is due to the fact that the SWAP operation leads to $\text{Tr}[\mathcal{I}_a O_a] = \text{Tr}[O_a]$ (instead of $\text{Tr}[\mathcal{I}_a] \text{Tr}[O_a] = d_a \text{Tr}[O_a]$ with the identity).
2. The disappear of d_h is due to the fact that the SWAP operation leads to the upper bound of $\sum_{i,j} \langle j|O_h|i\rangle \delta_{ij} = \text{Tr}[O_h]$ (instead of the double Kronecker deltas $\sum_{i,j} \text{Tr}[O_h] \delta_{ij}^2 = d_h \text{Tr}[O_h]$ with the identity).

This intuitive understanding of how the SWAP operator can impact the terms does indeed carry out to more general setting. We argue this more thoroughly in the coming step.

General setting with arbitrary time steps. We now compute $g_{\sigma}^{(1)}(O)$ in Eq. (A38) with the symmetric group element $s = ((1)(2)\dots(t))$ for which $\sigma = \bigotimes_{i=1}^t \mathcal{I}_{a_i} \otimes \mathcal{I}_{h_i}$ leading to

$$g_{\sigma}^{(1)}(O) = \sum_{\mathbf{X}_{h_{t-1}}} \text{Tr} \left[(X_{h_1}, \mathcal{I}_a; X_{h_2}, \mathcal{I}_a; \dots; X_{h_{t-1}}, \mathcal{I}_a; O) \bigotimes_{i=1}^t \mathcal{I}_{a_i} \otimes \mathcal{I}_{h_i} \right] \text{Tr} \left[(\rho_{h_0}, \rho_{a_1}; X_{h_1}, \rho_{a_2}; X_{h_2}, \rho_{a_3}; \dots; X_{h_{t-1}}, \rho_{a_t}) \bigotimes_{i=1}^t \mathcal{I}_{a_i} \otimes \mathcal{I}_{h_i} \right] \quad (\text{A49})$$

$$= \sum_{\mathbf{X}_{h_{t-1}}} \text{Tr}[X_{h_1}]^2 \dots \text{Tr}[X_{h_{t-1}}]^2 \text{Tr}[I_a]^{t-1} \text{Tr}[O] \quad (\text{A50})$$

$$= d_a^{t-1} \text{Tr}[O] \sum_{i_1, j_1; \dots; i_{t-1}, j_{t-1} \in \{1, \dots, d_h\}} \text{Tr}[|i_1\rangle\langle j_1|]^2 \dots \text{Tr}[|i_{t-1}\rangle\langle j_{t-1}|]^2 \quad (\text{A51})$$

$$= d_a^{t-1} \text{Tr}[O] \sum_{i_1, j_1; \dots; i_{t-1}, j_{t-1} \in \{1, \dots, d_h\}} \delta_{i_1, j_1}^2 \dots \delta_{i_{t-1}, j_{t-1}}^2 \quad (\text{A52})$$

$$= d_a^{t-1} \text{Tr}[O] \sum_{i_1, \dots, i_{t-1} \in \{1, \dots, d_h\}} 1 \quad (\text{A53})$$

$$= d_a^{t-1} d_h^{t-1} \text{Tr}[O], \quad (\text{A54})$$

where in the second line we ignore the traces of states as they equal 1.

We next claim that this is the leading order term. This is justified with two arguments.

(i). The scaling with respect to d_a is maximized with the identity. That is, for all permutations, only s consisting of identities leads the term in Eq. (A38) to $\text{Tr}[I_a]^{t-1} = d_a^{t-1}$. Similar to the toy example presented above, other permutations containing “SWAP” operations between copies of spaces ranging from 1 to $(t-1)$ will lead to terms containing $\text{Tr}[\mathcal{I}_a \cdot \mathcal{I}_a] =$

$\text{Tr}[\mathcal{I}_a] = d_a$, while with identities permutation we will obtain $\text{Tr}[\mathcal{I}_a] \text{Tr}[\mathcal{I}_a] = \text{Tr}[\mathcal{I}_a]^2 = d_a^2$. We also remark that with the SWAP operators the terms get smaller by at least a factor of d_a .

(ii). The scaling with respect to d_h is maximized with the identity. Consider the summation over all the operators $X_{h_1}, \dots, X_{h_{t-1}}$, when computing product of their traces, we see that the identity permutation will maximize the number of identical delta functions, which is the situation when the number of d_h factors is maximal. To better illustrate this argument, we further provide an example:

Consider X_1 and X_2 with $X_k = |i_k\rangle\langle j_k|$ and $i_k, j_k = 0, \dots, d_h - 1$, then we calculate two quantities

- Case 1:

$$\sum_{X_1, X_2} \text{Tr}[X_1] \text{Tr}[X_2] \text{Tr}[X_1 X_2] = \sum_{i_1, j_1, i_2, j_2} \text{Tr}[|i_1\rangle\langle j_1|] \text{Tr}[|i_2\rangle\langle j_2|] \text{Tr}[|i_1\rangle\langle j_1| \langle j_2| \langle i_2|] \quad (\text{A55})$$

$$= \sum_{i_1, j_1, i_2, j_2} \delta_{i_1, j_1} \delta_{i_2, j_2} \delta_{i_1, j_2} \delta_{i_2, j_1} \quad (\text{A56})$$

$$= \sum_{i_1} 1 \quad (\text{A57})$$

$$= d_h \quad (\text{A58})$$

- Case 2:

$$\sum_{X_1, X_2} \text{Tr}[X_1]^2 \text{Tr}[X_2]^2 = \sum_{i_1, j_1, i_2, j_2} \text{Tr}[|i_1\rangle\langle j_1|]^2 \text{Tr}[|i_2\rangle\langle j_2|]^2 \quad (\text{A59})$$

$$= \sum_{i_1, j_1, i_2, j_2} \delta_{i_1, j_1}^2 \delta_{i_2, j_2}^2 \quad (\text{A60})$$

$$= \sum_{i_1, j_1, i_2, j_2} \delta_{i_1, j_1} \delta_{i_2, j_2} \quad (\text{A61})$$

$$= \sum_{i_1, i_2} 1 \quad (\text{A62})$$

$$= d_h^2 \quad (\text{A63})$$

We see that case 2 leads to a larger scaling than case 1, since in case 2 the product traces in Eq. (A59) eventually lead to only 2 distinct Kronecker delta functions. In contrast, in case 1 although the degree in operators are the same, the traces in Eq (A55) induce 4 distinct delta functions and hence the magnitude of the sum is smaller.

More generally. Given a set of operators $\{X_k\}_{k=1}^K$ with $X_k = |i_k\rangle\langle j_k|$ and $i_k, j_k = 0, \dots, d_h - 1$, given two sets of indices $\{a_k\}_{k=1}^p = \{b_k\}_{k=1}^p \subseteq [K]$ which are identical sets but the elements could be in different order, i.e. not necessarily $a_k = b_k$, then the traces of their products are

$$\text{Tr}[M_{a_1} \dots M_{a_p}] = \delta_{j_{a_p}, i_{a_1}} \delta_{j_{a_1}, i_{a_2}} \dots \delta_{j_{a_{p-1}}, i_{a_p}} \quad (\text{A64})$$

and

$$\text{Tr}[M_{b_1} \dots M_{b_p}] = \delta_{j_{b_p}, i_{b_1}} \delta_{j_{b_1}, i_{b_2}} \dots \delta_{j_{b_{p-1}}, i_{b_p}}. \quad (\text{A65})$$

And the product of both traces is

$$\text{Tr}[M_{a_1} \dots M_{a_p}] \text{Tr}[M_{b_1} \dots M_{b_p}] = \delta_{j_{a_p}, i_{a_1}} \delta_{j_{a_1}, i_{a_2}} \dots \delta_{j_{a_{p-1}}, i_{a_p}} \delta_{j_{b_p}, i_{a_1}} \delta_{j_{b_1}, i_{b_2}} \dots \delta_{j_{b_{p-1}}, i_{b_p}}. \quad (\text{A66})$$

Summing over all the i_k and j_k , where $k \in \{a_l\}_{l=1}^p = \{b_l\}_{l=1}^p$, we obtain

$$\sum_{\substack{i_k, j_k \in \{0, \dots, d-1\} \\ \forall k \in \{a_l\}_{l=1}^p = \{b_l\}_{l=1}^p}} \text{Tr}[M_{a_1} \dots M_{a_p}] \text{Tr}[M_{b_1} \dots M_{b_p}] = \frac{d_h^{2p}}{d_h^{r_1}} \quad (\text{A67})$$

$$= \frac{d_h^{2p}}{d_h^{2p-r_2}} \quad (\text{A68})$$

$$= d_h^{r_2}, \quad (\text{A69})$$

where r_1 denotes the number of distinct Kronecker delta functions since $\delta_{i,j}^2 = \delta_{i,j} \forall i, j$ and r_2 is the number of identical pairs $(a_k, a_{k+1}) = (b_k, b_{k'+1})$ among all $k \in [p]$. Consequently, to maximize the sum above, one has to maximize the number of identical pairs of indices r_2 . In addition, we note that failing to maximize the scaling leads to at least one order of d_h magnitude smaller. Together with the d_a case, we have that the less dominant terms are at least $d_a d_h$ smaller than the leading term.

Altogether, We insert Eq. (A54) into Eq. (A37) and obtain an asymptotic form of the first moment as

$$\mathbb{E}_{\mathbb{U}(d_a d_h)}[\langle O \rangle_t] = \frac{\text{Tr}[O]}{d_a d_h} \left(1 + \mathcal{O}\left(\frac{1}{d_a d_h}\right) \right). \quad (\text{A70})$$

b. Second moment

We then similarly calculate the second moment of the QRP output at time step t :

$$\begin{aligned} & \mathbb{E}_{\mathbb{U}(d_a d_h)}[\langle O \rangle^2] \\ &= \sum_{\mathbf{X}_{h_{t-1}}, \mathbf{Y}_{h_{t-1}}} \int d\mu(U) \text{Tr}[(X_{h_1}, \mathcal{I}_a; X_{h_2}, \mathcal{I}_a; \dots; X_{h_{t-1}}, \mathcal{I}_a; O) U^{\otimes t} (\rho_{h_0}, \rho_{a_1}; X_{h_1}, \rho_{a_2}; X_{h_2}, \rho_{a_3}; \dots; X_{h_{t-1}}, \rho_{a_t}) (U^\dagger)^{\otimes t}] \\ & \quad \cdot \text{Tr}[(Y_{h_1}, \mathcal{I}_a; Y_{h_2}, \mathcal{I}_a; \dots; Y_{h_{t-1}}, \mathcal{I}_a; O) U^{\otimes t} (\rho_{h_0}, \rho_{a_1}; Y_{h_1}, \rho_{a_2}; Y_{h_2}, \rho_{a_3}; \dots; Y_{h_{t-1}}, \rho_{a_t}) (U^\dagger)^{\otimes t}] \end{aligned} \quad (\text{A71})$$

$$\begin{aligned} &= \sum_{\mathbf{X}_{h_{t-1}}, \mathbf{Y}_{h_{t-1}}} \int d\mu(U) \text{Tr}[(X_{h_1}, \mathcal{I}_a; X_{h_2}, \mathcal{I}_a; \dots; X_{h_{t-1}}, \mathcal{I}_a; O; Y_{h_1}, \mathcal{I}_a; Y_{h_2}, \mathcal{I}_a; \dots; Y_{h_{t-1}}, \mathcal{I}_a; O) U^{\otimes 2t} \\ & \quad \cdot (\rho_{h_0}, \rho_{a_1}; X_{h_1}, \rho_{a_2}; X_{h_2}, \rho_{a_3}; \dots; X_{h_{t-1}}, \rho_{a_t}; \rho_{h_0}, \rho_{a_1}; Y_{h_1}, \rho_{a_2}; Y_{h_2}, \rho_{a_3}; \dots; Y_{h_{t-1}}, \rho_{a_t}) (U^\dagger)^{\otimes 2t}] \end{aligned} \quad (\text{A72})$$

$$\begin{aligned} &= \frac{1}{(d_a d_h)^{2t}} \left(\sum_{\mathbf{X}_{h_{t-1}}, \mathbf{Y}_{h_{t-1}}} \left(\sum_{\sigma \in P_{d_a d_h}(S_{2t})} \text{Tr}[(X_{h_1}, \mathcal{I}_a; X_{h_2}, \mathcal{I}_a; \dots; X_{h_{t-1}}, \mathcal{I}_a; O; Y_{h_1}, \mathcal{I}_a; Y_{h_2}, \mathcal{I}_a; \dots; Y_{h_{t-1}}, \mathcal{I}_a; O) \sigma] \right. \right. \\ & \quad \cdot \text{Tr}[(\rho_{h_0}, \rho_{a_1}; X_{h_1}, \rho_{a_2}; X_{h_2}, \rho_{a_3}; \dots; X_{h_{t-1}}, \rho_{a_t}; \rho_{h_0}, \rho_{a_1}; Y_{h_1}, \rho_{a_2}; Y_{h_2}, \rho_{a_3}; \dots; Y_{h_{t-1}}, \rho_{a_t}) \sigma^{-1}] \\ & \quad + \sum_{\sigma \in P_{d_a d_h}(S_{2t})} c_{\sigma, \pi} \text{Tr}[(X_{h_1}, \mathcal{I}_a; X_{h_2}, \mathcal{I}_a; \dots; X_{h_{t-1}}, \mathcal{I}_a; O; Y_{h_1}, \mathcal{I}_a; Y_{h_2}, \mathcal{I}_a; \dots; Y_{h_{t-1}}, \mathcal{I}_a; O) \sigma] \\ & \quad \left. \cdot \text{Tr}[(\rho_{h_0}, \rho_{a_1}; X_{h_1}, \rho_{a_2}; X_{h_2}, \rho_{a_3}; \dots; X_{h_{t-1}}, \rho_{a_t}; \rho_{h_0}, \rho_{a_1}; Y_{h_1}, \rho_{a_2}; Y_{h_2}, \rho_{a_3}; \dots; Y_{h_{t-1}}, \rho_{a_t}) \pi] \right) \end{aligned} \quad (\text{A73})$$

$$= \frac{1}{(d_a d_h)^{2t}} \left(\sum_{\sigma \in P_{d_a d_h}(S_{2t})} g_\sigma^{(2)}(O) \right) \cdot (1 + \mathcal{O}((d_a d_h)^{-1})), \quad (\text{A74})$$

where in the second equality we use the identity $\text{Tr}[A \otimes B] = \text{Tr}[A] \text{Tr}[B]$, in the third one the Lemma 1, and in the last one the fact that the prefactors $c_{\sigma, \pi} \in \mathcal{O}((d_a d_h)^{-1})$ are exponentially small in numbers of qubits, where we also define

$$\begin{aligned} g_\sigma^{(2)}(O) &:= \sum_{\mathbf{X}_{h_{t-1}}, \mathbf{Y}_{h_{t-1}}} \text{Tr}[(X_{h_1}, \mathcal{I}_a; \dots; X_{h_{t-1}}, \mathcal{I}_a; O; Y_{h_1}, \mathcal{I}_a; \dots; Y_{h_{t-1}}, \mathcal{I}_a; O) \sigma] \\ & \quad \cdot \text{Tr}[(\rho_{h_0}, \rho_{a_1}; X_{h_1}, \rho_{a_2}; \dots; X_{h_{t-1}}, \rho_{a_t}; \rho_{h_0}, \rho_{a_1}; Y_{h_1}, \rho_{a_2}; \dots; Y_{h_{t-1}}, \rho_{a_t}) \sigma^{-1}]. \end{aligned} \quad (\text{A75})$$

Using the same arguments as before, here we identify two types of leading terms that maximize the scaling in d_a and d_h . First, the one containing $\text{Tr}[O^2]$ will be induced by the symmetric group element $s = ((1)(2) \dots (t-1)(t, 2t)(t+1)(t+2) \dots (2t-1))$, such that the permutation only swaps the t -th and $2t$ -th spaces and applies identity for the rests. This

contributes to the second moment by:

$$g_\sigma^{(2)}(O) = \sum_{\mathbf{X}_{h_{t-1}}, \mathbf{Y}_{h_{t-1}}} \text{Tr}[X_{h_1}]^2 \cdots \text{Tr}[X_{h_{t-2}}]^2 \text{Tr}[Y_{h_1}]^2 \cdots \text{Tr}[Y_{h_{t-2}}]^2 \text{Tr}[X_{h_{t-1}}] \text{Tr}[Y_{h_{t-1}}] \text{Tr}[X_{h_{t-1}} Y_{h_{t-1}}] \text{Tr}[I_{d_a}]^{2(t-1)} \text{Tr}[O^2] \quad (\text{A76})$$

$$= d_a^{2t-2} \sum_{\mathbf{X}_{h_{t-1}}, \mathbf{Y}_{h_{t-1}}} \text{Tr}[X_{h_1}]^2 \cdots \text{Tr}[X_{h_{t-2}}]^2 \text{Tr}[Y_{h_1}]^2 \cdots \text{Tr}[Y_{h_{t-2}}]^2 \text{Tr}[X_{h_{t-1}}] \text{Tr}[Y_{h_{t-1}}] \text{Tr}[X_{h_{t-1}} Y_{h_{t-1}}] \text{Tr}[O^2] \quad (\text{A77})$$

$$= d_a^{2t-2} \sum_{\substack{i_1, j_1, \dots, i_{t-1}, j_{t-1} \in \{1, \dots, d_h\} \\ k_1, l_1, \dots, k_{t-1}, l_{t-1} \in \{1, \dots, d_h\}}} \text{Tr}[|i_1\rangle\langle j_1|]^2 \cdots \text{Tr}[|i_{t-2}\rangle\langle j_{t-2}|]^2 \text{Tr}[|k_1\rangle\langle l_1|]^2 \cdots \text{Tr}[|k_{t-2}\rangle\langle l_{t-2}|]^2 \text{Tr}[|i_{t-1}\rangle\langle j_{t-1}|] \text{Tr}[|k_{t-1}\rangle\langle l_{t-1}|] \text{Tr}[|i_{t-1}\rangle\langle j_{t-1}|k_{t-1}\rangle\langle l_{t-1}|] \text{Tr}[O^2] \quad (\text{A78})$$

$$= d_a^{2t-2} d_h^{4(t-1)-2(t-2)-3} \text{Tr}[O^2] \quad (\text{A79})$$

$$= d_a^{2t-2} d_h^{2t-3} \text{Tr}[O^2], \quad (\text{A80})$$

where in the first line we drop the traces of states which equal 1.

Another type of potential leading term contains $\text{Tr}[O]^2$ and is given by the symmetric group element $s = ((1)(2)\cdots(2t))$, such that the permutation applies identity $\mathcal{I}_a \otimes \mathcal{I}_h$ in all spaces. This leads to:

$$g_\sigma^{(2)}(O) = \sum_{\mathbf{X}_{h_{t-1}}, \mathbf{Y}_{h_{t-1}}} \text{Tr}[X_{h_1}]^2 \cdots \text{Tr}[X_{h_{t-2}}]^2 \text{Tr}[Y_{h_1}]^2 \cdots \text{Tr}[Y_{h_{t-2}}]^2 \text{Tr}[X_{h_{t-1}}]^2 \text{Tr}[Y_{h_{t-1}}]^2 \text{Tr}[I_{d_a}]^{2(t-1)} \text{Tr}[O]^2 \quad (\text{A81})$$

$$= d_a^{2t-2} \sum_{\mathbf{X}_{h_{t-1}}, \mathbf{Y}_{h_{t-1}}} \text{Tr}[X_{h_1}]^2 \cdots \text{Tr}[X_{h_{t-2}}]^2 \text{Tr}[Y_{h_1}]^2 \cdots \text{Tr}[Y_{h_{t-2}}]^2 \text{Tr}[X_{h_{t-1}}]^2 \text{Tr}[Y_{h_{t-1}}]^2 \text{Tr}[O]^2 \quad (\text{A82})$$

$$= d_a^{2t-2} \sum_{\substack{i_1, j_1, \dots, i_{t-1}, j_{t-1} \in \{1, \dots, d_h\} \\ k_1, l_1, \dots, k_{t-1}, l_{t-1} \in \{1, \dots, d_h\}}} \text{Tr}[|i_1\rangle\langle j_1|]^2 \cdots \text{Tr}[|i_{t-2}\rangle\langle j_{t-2}|]^2 \text{Tr}[|k_1\rangle\langle l_1|]^2 \cdots \text{Tr}[|k_{t-2}\rangle\langle l_{t-2}|]^2 \text{Tr}[|i_{t-1}\rangle\langle j_{t-1}|]^2 \text{Tr}[|k_{t-1}\rangle\langle l_{t-1}|]^2 \text{Tr}[O]^2 \quad (\text{A83})$$

$$= d_a^{2t-2} d_h^{4(t-1)-2(t-1)} \text{Tr}[O]^2 \quad (\text{A84})$$

$$= d_a^{2t-2} d_h^{2t-2} \text{Tr}[O]^2. \quad (\text{A85})$$

Insert Eq. (A85) and (A80) into Eq. (A74), we obtain

$$\mathbb{E}_{\mathbb{U}(d_a d_h)} [\langle O \rangle_t^2] = \left(\frac{\text{Tr}[O^2]}{d_a^2 d_h^3} + \frac{\text{Tr}[O]^2}{d_a^2 d_h^2} \right) \left(1 + \mathcal{O}\left(\frac{1}{d_a d_h}\right) \right). \quad (\text{A86})$$

We now subtract the square of first moment as in Eq. (A70) and obtain output's variance over reservoirs sampled from Haar measure on $\mathbb{U}(d_a d_h)$:

$$\text{Var}_{\mathbb{U}(d_a d_h)} [\langle O \rangle_t^2] = \frac{\text{Tr}[O^2]}{d_a^2 d_h^3} \left(1 + \mathcal{O}\left(\frac{1}{d_a d_h}\right) \right). \quad (\text{A87})$$

Finally, by applying the Chebyshev's tail bound with the average and the variance, we obtain the statement of probabilistic exponential concentration as claimed in Eq. (A27). \square

4. Proof of Theorem 2: Exponential memory decay

By using the QRP output form presented in Supplemental Proposition 1, we prove Theorem 2 in the main text, which shows the the exponential tight upper bound of memory indicators for an arbitrary ensemble of early state (see

Definition 3 and 2 of the memory indicators). However, before going to the proof of the theorem, we present the following simplified result where the input states are also extremely scrambled. This provides a guideline and exemplify some key steps in more simple setting for the proof of Theorem 2.

Supplemental Proposition 2 (Decay of memory indicator with scrambling initial states). *For extreme scrambling reservoirs and also an ensemble of extreme scrambling inputs $\mathcal{S}_a = \{V|0\rangle\langle 0|V^\dagger\}$ with V drawn from the scrambling ensemble, we have*

$$\mathcal{M}_a(t; \mathcal{S}_a, \mathcal{U}) := \mathbb{E}_{U \sim \mathcal{U}} \left[\text{Var}_{\rho_{a\tau} \sim \mathcal{S}_a} \left[\langle O \rangle_{(t+\tau)} \right] \right] = \frac{1}{d_h d_a^t} \left(1 + \mathcal{O} \left(\frac{1}{d_h} \right) \right). \quad (\text{A88})$$

Similarly, for extreme scrambling initial reservoir states $\mathcal{S}_h = \{V|0\rangle\langle 0|V^\dagger : V \in \nu(\mathbb{U}(d_h))\}$, we have

$$\mathcal{M}_h(t; \mathcal{S}_h, \mathcal{U}) := \mathbb{E}_{U \sim \mathcal{U}} \left[\text{Var}_{\rho_{h0} \sim \mathcal{S}_h} [\langle O \rangle_t] \right] = \frac{1}{d_h d_a^t} \left(1 + \mathcal{O} \left(\frac{1}{d_h} \right) \right). \quad (\text{A89})$$

Proof: We recall the expression in Eq. (A8) from Supplemental Proposition 1 and identify the term containing the initial state ρ_{h0} over hidden qubits:

$$\langle O \rangle_t = \sum_{\mathbf{X}_{h_{t-1}} \in \{|r\rangle\langle r'|_h\}} \text{Tr} \left[(X_{h_1}, \mathcal{I}_a; X_{h_2}, \mathcal{I}_a; \dots; X_{h_{t-1}}, \mathcal{I}_a; O) U^{\otimes t} (\rho_{h_0}, \rho_{a_1}; X_{h_1}, \rho_{a_2}; X_{h_2}, \rho_{a_3}; \dots; X_{h_{t-1}}, \rho_{a_t}) (U^\dagger)^{\otimes t} \right] \quad (\text{A90})$$

$$= \sum_{\mathbf{X}_{h_{t-1}} \in \{|r\rangle\langle r'|_h\}} \text{Tr} \left[(X_{h_1}, \mathcal{I}_a; X_{h_2}, \mathcal{I}_a; \dots; X_{h_{t-1}}, \mathcal{I}_a; O) U^{\otimes t} (\rho_{h_0}, \rho_{a_1}; X_{h_1}, \rho_{a_2}; X_{h_2}, \rho_{a_3}; \dots; X_{h_{t-1}}, \rho_{a_t}) (U^\dagger)^{\otimes t} \right] \quad (\text{A91})$$

$$= \sum_{\mathbf{X}_{h_{t-1}}} \text{Tr} \left[(X_{h_1}, \mathcal{I}_a) U (\rho_{h_0}, \rho_{a_1}) U^\dagger \right] \cdot \text{Tr} \left[(X_{h_2}, \mathcal{I}_a; \dots; X_{h_{t-1}}, \mathcal{I}_a; O) U^{\otimes(t-1)} (X_{h_1}, \rho_{a_2}; X_{h_2}, \rho_{a_3}; \dots; X_{h_{t-1}}, \rho_{a_t}) (U^\dagger)^{\otimes(t-1)} \right]. \quad (\text{A92})$$

Here, “,” denotes the tensor products of operators in accessible and hidden space, and “;” denotes the tensor products of composite operators in different copies of the composite space.

We next assume the initial state ρ_{h0} is obtained via a random unitary U_0 such that $\rho_{h0} = U_0 |0\rangle\langle 0| U_0^\dagger$. We calculate the expectation values over U_0 sampled from Haar measure. The first moment is

$$\mathbb{E}_{\rho_{h0}} [\langle O \rangle_t] = \sum_{\mathbf{X}_{h_{t-1}}} \mathbb{E}_{U_0 \sim \mathbb{U}(d_h)} \left[\text{Tr} \left[(X_{h_1}, \mathcal{I}_a) U (U_0 |0\rangle\langle 0| U_0^\dagger, \rho_{a_1}) U^\dagger \right] \right] \cdot \text{Tr} \left[(X_{h_2}, \mathcal{I}_a; \dots; X_{h_{t-1}}, \mathcal{I}_a; O) U^{\otimes(t-1)} (X_{h_1}, \rho_{a_2}; X_{h_2}, \rho_{a_3}; \dots; X_{h_{t-1}}, \rho_{a_t}) (U^\dagger)^{\otimes(t-1)} \right], \quad (\text{A93})$$

where

$$\mathbb{E}_{U_0 \sim \mathbb{U}(d_h)} \left[\text{Tr} \left[(X_{h_1}, \mathcal{I}_a) U (U_0 |0\rangle\langle 0| U_0^\dagger, \rho_{a_1}) U^\dagger \right] \right] = \text{Tr} \left[(X_{h_1}, \mathcal{I}_a) U \left[\left(\int_{\mathbb{U}(d_h)} dU_0 U_0 |0\rangle\langle 0| U_0^\dagger \right), \rho_{a_1} \right] U^\dagger \right] \quad (\text{A94})$$

$$= \text{Tr} \left[(X_{h_1}, \mathcal{I}_a) U \left(\frac{\mathcal{I}_h}{d_h}, \rho_{a_1} \right) U^\dagger \right]. \quad (\text{A95})$$

The second moment is

$$\begin{aligned} & \mathbb{E}_{\rho_{h0}} [\langle O \rangle_t^2] \\ &= \sum_{\mathbf{X}_{h_{t-1}}} \sum_{\mathbf{Y}_{h_{t-1}}} \mathbb{E}_{\rho_{h0}} \left[\text{Tr} \left[(X_{h_1}, \mathcal{I}_a) U (\rho_{h_0}, \rho_{a_1}) U^\dagger \right] \text{Tr} \left[(Y_{h_1}, \mathcal{I}_a) U (\rho_{h_0}, \rho_{a_1}) U^\dagger \right] \right] \\ & \quad \cdot \text{Tr} \left[(X_{h_2}, \mathcal{I}_a; \dots; X_{h_{t-1}}, \mathcal{I}_a; O; Y_{h_2}, \mathcal{I}_a; \dots; Y_{h_{t-1}}, \mathcal{I}_a; O) U^{\otimes t} (X_{h_1}, \rho_{a_2}; X_{h_2}, \rho_{a_3}; \dots; X_{h_{t-1}}, \rho_{a_t}; Y_{h_1}, \rho_{a_2}; Y_{h_2}, \rho_{a_3}; \dots; Y_{h_{t-1}}, \rho_{a_t}) (U^\dagger)^{\otimes t} \right], \end{aligned} \quad (\text{A96})$$

where

$$\begin{aligned} & \mathbb{E}_{\rho_{h_0}} \left[\text{Tr}[(X_{h_1}, \mathcal{I}_a)U(\rho_{h_0}, \rho_{a_1})U^\dagger] \text{Tr}[(Y_{h_1}, \mathcal{I}_a)U(\rho_{h_0}, \rho_{a_1})U^\dagger] \right] \\ &= \text{Tr} \left[(X_{h_1}, \mathcal{I}_a; Y_{h_1}, \mathcal{I}_a)U^{\otimes 2} \left(\int_{\mathcal{U}(d_h)} dU_0 U_0^{\otimes 2} |0\rangle\langle 0|^{\otimes 2} (U_0^\dagger)^{\otimes 2} \otimes \rho_{a_1}^{\otimes 2} \right) (U^\dagger)^{\otimes 2} \right] \end{aligned} \quad (\text{A97})$$

$$= \frac{1}{d_h(d_h + 1)} \text{Tr}[(X_{h_1}, \mathcal{I}_a; Y_{h_1}, \mathcal{I}_a)U^{\otimes 2} [(\mathcal{I}_h^{\otimes 2} + \text{SWAP}_{h,h}) \otimes \rho_{a_1}^{\otimes 2}] (U^\dagger)^{\otimes 2}] \quad (\text{A98})$$

$$\begin{aligned} &= \frac{1}{d_h(d_h + 1)} \text{Tr}[(X_{h_1}, \mathcal{I}_a)U(I, \rho_{a_1})U^\dagger] \text{Tr}[(Y_{h_1}, \mathcal{I}_a)U(I, \rho_{a_1})U^\dagger] \\ &\quad + \frac{1}{d_h(d_h + 1)} \text{Tr}[(X_{h_1}, \mathcal{I}_a; Y_{h_1}, \mathcal{I}_a)U^{\otimes 2} (\text{SWAP}_{h,h} \otimes \rho_{a_1}^{\otimes 2}) (U^\dagger)^{\otimes 2}]. \end{aligned} \quad (\text{A99})$$

Here in the last equality the SWAP operator is applied on the two copies of hidden spaces, i.e. $\text{SWAP}_{h,h} = \sum_{i,j=0}^{d_h-1} |i\rangle\langle j| \otimes |j\rangle\langle i|$. We next combine the expressions of the first and second moment to calculate the variance of initial state:

$$\text{Var}_{\rho_{h_0}} \langle O \rangle_t = \mathbb{E}_{\rho_{h_0}} [\langle O \rangle_t^2] - \mathbb{E}_{\rho_{h_0}} [\langle O \rangle_t]^2 \quad (\text{A100})$$

$$\begin{aligned} &= \sum_{\mathbf{X}_{h_{t-1}}} \sum_{\mathbf{Y}_{h_{t-1}}} \left(\frac{1}{d_h(d_h + 1)} \text{Tr}[(X_{h_1}, \mathcal{I}_a)U(\mathcal{I}_h, \rho_{a_1})(U^\dagger)] \text{Tr}[(Y_{h_1}, \mathcal{I}_a)U(\mathcal{I}_h, \rho_{a_1})(U^\dagger)] \right. \\ &\quad + \frac{1}{d_h(d_h + 1)} \text{Tr}[(X_{h_1}, \mathcal{I}_a; Y_{h_1}, \mathcal{I}_a)U^{\otimes 2} (\text{SWAP}_{h,h} \otimes \rho_{a_1}^{\otimes 2}) (U^\dagger)^{\otimes 2}] \\ &\quad \left. - \text{Tr}[(X_{h_1}, \mathcal{I}_a)U\left(\frac{\mathcal{I}_h}{d_h}, \rho_{a_1}\right)U^\dagger] \text{Tr}[(Y_{h_1}, \mathcal{I}_a)U\left(\frac{\mathcal{I}_h}{d_h}, \rho_{a_1}\right)U^\dagger] \right) \\ &\quad \cdot \text{Tr}[(X_{h_2}, \mathcal{I}_a; \dots; X_{h_{t-1}}, \mathcal{I}_a; O; Y_{h_2}, \mathcal{I}_a; \dots; Y_{h_{t-1}}, \mathcal{I}_a; O) U^{\otimes t} (X_{h_1}, \rho_{a_2}; \dots; X_{h_{t-1}}, \rho_{a_t}; Y_{h_1}, \rho_{a_2}; \dots; Y_{h_{t-1}}, \rho_{a_t}) (U^\dagger)^{\otimes t}] \end{aligned} \quad (\text{A101})$$

$$\begin{aligned} &= \frac{1}{d_h(d_h + 1)} \sum_{\mathbf{X}_{h_{t-1}}} \sum_{\mathbf{Y}_{h_{t-1}}} \left(\text{Tr}[(X_{h_1}, \mathcal{I}_a; Y_{h_1}, \mathcal{I}_a)U^{\otimes 2} (\text{SWAP}_{h,h} \otimes \rho_{a_1}^{\otimes 2}) (U^\dagger)^{\otimes 2}] \right. \\ &\quad \left. - \frac{1}{d_h} \text{Tr}[(X_{h_1}, \mathcal{I}_a)U(\mathcal{I}_h, \rho_{a_1})(U^\dagger)] \text{Tr}[(Y_{h_1}, \mathcal{I}_a)U(\mathcal{I}_h, \rho_{a_1})(U^\dagger)] \right) \\ &\quad \cdot \text{Tr}[(X_{h_2}, \mathcal{I}_a; \dots; X_{h_{t-1}}, \mathcal{I}_a; O; Y_{h_2}, \mathcal{I}_a; \dots; Y_{h_{t-1}}, \mathcal{I}_a; O) U^{\otimes 2(t-1)} \\ &\quad (X_{h_1}, \rho_{a_2}; \dots; X_{h_{t-1}}, \rho_{a_t}; Y_{h_1}, \rho_{a_2}; \dots; Y_{h_{t-1}}, \rho_{a_t}) (U^\dagger)^{\otimes 2(t-1)}]. \end{aligned} \quad (\text{A102})$$

We then decompose the SWAP operator using its definition and obtain

$$\begin{aligned} \text{Var}_{\rho_{h_0}} \langle O \rangle_t &= \frac{1}{d_h(d_h+1)} \sum_{\mathbf{X}_{h_{t-1}}} \sum_{\mathbf{Y}_{h_{t-1}}} \\ &\left(\sum_{i,j=0}^{d_h-1} \text{Tr} \left[(X_{h_1}, \mathcal{I}_a; X_{h_2}, \mathcal{I}_a; \dots; X_{h_{t-1}}, \mathcal{I}_a; O; Y_{h_1}, \mathcal{I}_a; Y_{h_2}, \mathcal{I}_a; \dots; Y_{h_{t-1}}, \mathcal{I}_a; O) U^{\otimes 2t} \right. \right. \\ &\quad \left. \left. (|i\rangle\langle j|, \rho_{a_1}; X_{h_1}, \rho_{a_2}; \dots; X_{h_{t-1}}, \rho_{a_t}; |j\rangle\langle i|, \rho_{a_1}; Y_{h_1}, \rho_{a_2}; \dots; Y_{h_{t-1}}, \rho_{a_t}) (U^\dagger)^{\otimes 2t} \right] \right. \\ &\quad \left. - \frac{1}{d_h} \text{Tr} \left[(X_{h_1}, \mathcal{I}_a; X_{h_2}, \mathcal{I}_a; \dots; X_{h_{t-1}}, \mathcal{I}_a; O; Y_{h_1}, \mathcal{I}_a; Y_{h_2}, \mathcal{I}_a; \dots; Y_{h_{t-1}}, \mathcal{I}_a; O) U^{\otimes 2t} \right. \right. \\ &\quad \left. \left. (\mathcal{I}_h, \rho_{a_1}; X_{h_1}, \rho_{a_2}; \dots; X_{h_{t-1}}, \rho_{a_t}; \mathcal{I}_h, \rho_{a_1}; Y_{h_1}, \rho_{a_2}; \dots; Y_{h_{t-1}}, \rho_{a_t}) (U^\dagger)^{\otimes 2t} \right] \right), \quad (\text{A103}) \end{aligned}$$

where in the last equality we obtain the standard form for Haar integral over reservoirs U . This quantity gives the input dependence of QRP for a fix reservoir. To find the averaged input dependence given an ensemble of reservoirs, we further calculate the expectation value of the variance, and here over Haar random reservoirs. We use again Lemma 1 to find the dominant term of the memory indicator:

$$\begin{aligned} \mathbb{E}_U[\text{Var}_{\rho_{h_0}} \langle O \rangle_t] &= \frac{1}{d_h(d_h+1)} \frac{1}{d_a^{2t} d_h^{2t}} \left(1 + \mathcal{O}\left(\frac{1}{d_a d_h}\right) \right) \sum_{\mathbf{X}_{h_{t-1}}} \sum_{\mathbf{Y}_{h_{t-1}}} \sum_{\sigma \in P_{d_a d_h}(\mathcal{S}_t)} \\ &\text{Tr} \left[(X_{h_1}, \mathcal{I}_a; X_{h_2}, \mathcal{I}_a; \dots; X_{h_{t-1}}, \mathcal{I}_a; O; Y_{h_1}, \mathcal{I}_a; Y_{h_2}, \mathcal{I}_a; \dots; Y_{h_{t-1}}, \mathcal{I}_a; O) \sigma \right] \\ &\left(\sum_{i,j=0}^{d_h-1} \text{Tr} \left[(|i\rangle\langle j|, \rho_{a_1}; X_{h_1}, \rho_{a_2}; \dots; X_{h_{t-1}}, \rho_{a_t}; |j\rangle\langle i|, \rho_{a_1}; Y_{h_1}, \rho_{a_2}; \dots; Y_{h_{t-1}}, \rho_{a_t}) \sigma^{-1} \right] \right. \\ &\quad \left. - \frac{1}{d_h} \text{Tr} \left[(I, \rho_{a_1}; X_{h_1}, \rho_{a_2}; \dots; X_{h_{t-1}}, \rho_{a_t}; I, \rho_{a_1}; Y_{h_1}, \rho_{a_2}; \dots; Y_{h_{t-1}}, \rho_{a_t}) \sigma^{-1} \right] \right). \quad (\text{A104}) \end{aligned}$$

Here we observe that the final expression is given by the difference of two Haar integrals. We compare the terms therein and find that all the terms with $P_{d_a d_h}(\sigma^{-1})$ containing identity operators on the first or $(t+1)$ -th space will be cancelled, as $\sum_{i,j} \text{Tr}[|i\rangle\langle j|] g(|j\rangle\langle i|) = g(\mathcal{I})$ for arbitrary function g . Among all the rest terms, we identify the leading term corresponding to the permutation $\otimes_{\tau=1}^t \text{SWAP}_{\tau, t+\tau}$ and obtain the initial state dependence for QRP with Haar random initial state and reservoir:

$$\mathbb{E}_U[\text{Var}_{\rho_{h_0}} \langle O \rangle_t] = \frac{1}{d_h(d_h+1)} \frac{1}{d_a^{2t} d_h^{2t}} \left(1 + \mathcal{O}\left(\frac{1}{d_h}\right) \right) \sum_{\mathbf{X}_{h_{t-1}}} \sum_{\mathbf{Y}_{h_{t-1}}} \left(\sum_{i,j=0}^{d_h-1} \text{Tr}[|i\rangle\langle j|] g(|j\rangle\langle i|) \right) \left(\prod_{\tau=1}^{t-1} \text{Tr}[X_\tau Y_\tau]^2 \text{Tr}[I_a] \right) \text{Tr}[O^2] \quad (\text{A105})$$

$$= \frac{1}{d_h d_a^t} \left(1 + \mathcal{O}\left(\frac{1}{d_h}\right) \right). \quad (\text{A106})$$

To calculate the memory indicator, we use the same approach. We first calculate the output's variance over the input state at an arbitrary time step. Compared with Eq. (A103) the only difference is that the Haar integral is taken over unitaries in accessible space instead of hidden space. That is, we view the objective input step as the first step and

consider the ensemble of input states $\{\rho_{a_1} = V\rho_0 V^\dagger : V \in \mathcal{U}(d_a)\}$. Thus we obtain:

$$\begin{aligned} \text{Var}_{\rho_{a_1}} \langle O \rangle_t &= \frac{1}{d_a(d_a + 1)} \sum_{\mathbf{X}_{h_{t-1}}} \sum_{\mathbf{Y}_{h_{t-1}}} \\ &\left(\sum_{i,j=0}^{d_a-1} \text{Tr} \left[(X_{h_1}, \mathcal{I}_a; X_{h_2}, \mathcal{I}_a; \dots; X_{h_{t-1}}, \mathcal{I}_a; O; Y_{h_1}, \mathcal{I}_a; Y_{h_2}, \mathcal{I}_a; \dots; Y_{h_{t-1}}, \mathcal{I}_a; O) U^{\otimes 2t} \right. \right. \\ &\quad \left. \left. (\rho_{h_0}, |i\rangle\langle j|; X_{h_1}, \rho_{a_2}; \dots; X_{h_{t-1}}, \rho_{a_t}; \rho_{h_0}, |j\rangle\langle i|; Y_{h_1}, \rho_{a_2}; \dots; Y_{h_{t-1}}, \rho_{a_t}) (U^\dagger)^{\otimes 2t} \right] \right. \\ &\quad \left. - \frac{1}{d_a} \text{Tr} \left[(X_{h_1}, \mathcal{I}_a; X_{h_2}, \mathcal{I}_a; \dots; X_{h_{t-1}}, \mathcal{I}_a; O; Y_{h_1}, \mathcal{I}_a; Y_{h_2}, \mathcal{I}_a; \dots; Y_{h_{t-1}}, \mathcal{I}_a; O) U^{\otimes 2t} \right. \right. \\ &\quad \left. \left. (\rho_{h_0}, \mathcal{I}_a; X_{h_1}, \rho_{a_2}; \dots; X_{h_{t-1}}, \rho_{a_t}; \rho_{h_0}, \mathcal{I}_a; Y_{h_1}, \rho_{a_2}; \dots; Y_{h_{t-1}}, \rho_{a_t}) (U^\dagger)^{\otimes 2t} \right] \right). \end{aligned} \quad (\text{A107})$$

Finally we average this quantity over Haar random reservoirs and find that the leading term is given by the same permutation as before:

$$\begin{aligned} \mathbb{E}_U[\text{Var}_{\rho_{a_1}} \langle O \rangle_t] &= \frac{1}{d_a(d_a + 1)} \frac{1}{d_a^{2t} d_h^{2t}} \left(1 + \mathcal{O}\left(\frac{1}{d_a d_h}\right) \right) \sum_{\mathbf{X}_{h_{t-1}}} \sum_{\mathbf{Y}_{h_{t-1}}} \sum_{\sigma \in P_{d_a d_h}(\mathcal{S}_t)} \\ &\text{Tr} \left[(X_{h_1}, \mathcal{I}_a; X_{h_2}, \mathcal{I}_a; \dots; X_{h_{t-1}}, \mathcal{I}_a; O; Y_{h_1}, \mathcal{I}_a; Y_{h_2}, \mathcal{I}_a; \dots; Y_{h_{t-1}}, \mathcal{I}_a; O) \sigma \right] \\ &\left(\sum_{i,j=0}^{d_a-1} \text{Tr} \left[(\rho_{h_0}, |i\rangle\langle j|; X_{h_1}, \rho_{a_2}; \dots; X_{h_{t-1}}, \rho_{a_t}; \rho_{h_0}, |j\rangle\langle i|; Y_{h_1}, \rho_{a_2}; \dots; Y_{h_{t-1}}, \rho_{a_t}) \sigma^{-1} \right] \right. \\ &\quad \left. - \frac{1}{d_a} \text{Tr} \left[(\rho_{h_0}, \mathcal{I}_a; X_{h_1}, \rho_{a_2}; \dots; X_{h_{t-1}}, \rho_{a_t}; \rho_{h_0}, \mathcal{I}_a; Y_{h_1}, \rho_{a_2}; \dots; Y_{h_{t-1}}, \rho_{a_t}) \sigma^{-1} \right] \right) \end{aligned} \quad (\text{A108})$$

$$= \frac{1}{d_a(d_a + 1)} \frac{1}{d_a^{2t} d_h^{2t}} \left(1 + \mathcal{O}\left(\frac{1}{d_h}\right) \right) \sum_{\mathbf{X}_{h_{t-1}}} \sum_{\mathbf{Y}_{h_{t-1}}} \left(\sum_{i,j=0}^{d_a-1} \text{Tr}[|i\rangle\langle j| \langle j| \langle i|] \right) \left(\prod_{\tau=1}^{t-1} \text{Tr}[X_\tau Y_\tau]^2 \text{Tr}[I_a] \right) \text{Tr}[O^2] \quad (\text{A109})$$

$$= \frac{1}{d_h d_a^{2t}} \left(1 + \mathcal{O}\left(\frac{1}{d_h}\right) \right). \quad (\text{A110})$$

□

We are now ready for the main proof of Theorem 2. Here, we consider an arbitrary ensemble of input states instead of Haar random inputs. That is, ρ_{a_1} is sampled from an ensemble \mathcal{S}_a with a measure $d\nu(\rho_{a_1})$ and the average of input states is $\bar{\rho} := \int_{\rho_{a_1}} d\nu(\rho_{a_1}) \rho_{a_1}$. Similarly we consider an initial state ensemble \mathcal{S}_h with the measure $d\nu(\rho_{h_0})$ and the averaged initial state $\bar{\rho}_{h_0}$.

We restate the theorem again below for readers' convenience. In addition, we note that complementary to Fig 3 in the main text, further numerical simulation is provided in Fig. 10. In particular, it shows the scaling of $\mathcal{M}_h(t; \mathcal{S}_h, \mathcal{U})$ which is found to be in an agreement with the theoretical prediction, further supporting Theorem 2.

Theorem 2 (Upper bound of memory indicator for arbitrary input and state ensemble). *For extreme scrambling reservoirs and an arbitrary ensemble of inputs \mathcal{S}_a , we have*

$$\mathcal{M}_a(t; \mathcal{S}_a, \mathcal{U}) \in \mathcal{O}\left(\frac{1}{d_h d_a^t}\right). \quad (\text{A111})$$

Similarly, for an arbitrary ensemble of initial reservoir states \mathcal{S}_h , we have

$$\mathcal{M}_h(t; \mathcal{S}_h, \mathcal{U}) \in \mathcal{O}\left(\frac{1}{d_h d_a^t}\right). \quad (\text{A112})$$

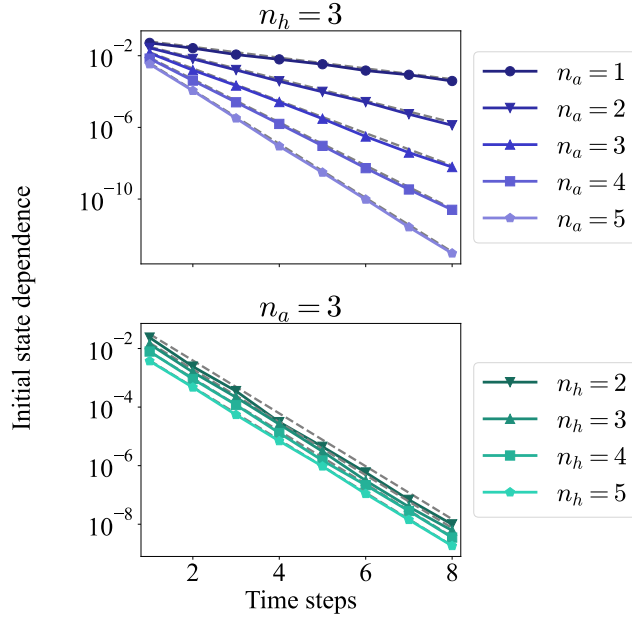


Figure 10. **Initial reservoir state dependence.** The dependence of outputs on initial state of hidden qubits of $\mathcal{M}_h(t; \mathcal{S}_a, \mathcal{U})$ are plotted for different qubit numbers. Here both the reservoirs and initial states are Haar random. The grey lines indicate the bounds given in Theorem 2.

Proof: Using the similar approach as before, we obtain

$$\begin{aligned}
 \text{Var}_{\rho_{a_1} \sim \mathcal{S}_a} \langle O \rangle_t &= \sum_{\mathbf{x}_{h_{t-1}}} \sum_{\mathbf{y}_{h_{t-1}}} \\
 &\left(\int d\nu(\rho_{a_1}) \rho_{a_1} \text{Tr} \left[(X_{h_1}, \mathcal{I}_a; X_{h_2}, \mathcal{I}_a; \dots; X_{h_{t-1}}, \mathcal{I}_a; O; Y_{h_1}, \mathcal{I}_a; Y_{h_2}, \mathcal{I}_a; \dots; Y_{h_{t-1}}, \mathcal{I}_a; O) U^{\otimes 2t} \right. \right. \\
 &\quad \left. \left. (\rho_{h_0}, \rho_{a_1}; X_{h_1}, \rho_{a_2}; \dots; X_{h_{t-1}}, \rho_{a_t}; \rho_{h_0}, \rho_{a_1}; Y_{h_1}, \rho_{a_2}; \dots; Y_{h_{t-1}}, \rho_{a_t}) (U^\dagger)^{\otimes 2t} \right] \right. \\
 &\quad \left. - \text{Tr} \left[(X_{h_1}, \mathcal{I}_a; X_{h_2}, \mathcal{I}_a; \dots; X_{h_{t-1}}, \mathcal{I}_a; O; Y_{h_1}, \mathcal{I}_a; Y_{h_2}, \mathcal{I}_a; \dots; Y_{h_{t-1}}, \mathcal{I}_a; O) U^{\otimes 2t} \right. \right. \\
 &\quad \left. \left. (\rho_{h_0}, \bar{\rho}; X_{h_1}, \rho_{a_2}; \dots; X_{h_{t-1}}, \rho_{a_t}; \rho_{h_0}, \bar{\rho}; Y_{h_1}, \rho_{a_2}; \dots; Y_{h_{t-1}}, \rho_{a_t}) (U^\dagger)^{\otimes 2t} \right] \right), \quad (\text{A113})
 \end{aligned}$$

where $\bar{\rho} := \int_{\rho_{a_1}} d\nu(\rho_{a_1}) \rho_{a_1}$. We average the variance over Haar random reservoirs and obtain

$$\begin{aligned} \mathbb{E}_U[\text{Var}_{\rho_{a_1} \sim \mathcal{S}_a} \langle O \rangle_t] &= \frac{1}{d_a^{2t} d_h^{2t}} \left(1 + \mathcal{O}\left(\frac{1}{d_a d_h}\right) \right) \sum_{\mathbf{X}_{h_{t-1}}} \sum_{\mathbf{Y}_{h_{t-1}}} \sum_{\sigma \in P_{d_a d_h}(\mathcal{S}_t)} \\ &\quad \text{Tr} \left[(X_{h_1}, \mathcal{I}_a; X_{h_2}, \mathcal{I}_a; \dots; X_{h_{t-1}}, \mathcal{I}_a; O; Y_{h_1}, \mathcal{I}_a; Y_{h_2}, \mathcal{I}_a; \dots; Y_{h_{t-1}}, \mathcal{I}_a; O) \sigma \right] \\ &\quad \left(\int d\nu(\rho_{a_1}) \text{Tr} \left[(\rho_{h_0}, \rho_{a_1}; X_{h_1}, \rho_{a_2}; \dots; X_{h_{t-1}}, \rho_{a_t}; \rho_{h_0}, \rho_{a_1}; Y_{h_1}, \rho_{a_2}; \dots; Y_{h_{t-1}}, \rho_{a_t}) \sigma^{-1} \right] \right. \\ &\quad \left. - \text{Tr} \left[(\rho_{h_0}, \bar{\rho}; X_{h_1}, \rho_{a_2}; \dots; X_{h_{t-1}}, \rho_{a_t}; \rho_{h_0}, \bar{\rho}; Y_{h_1}, \rho_{a_2}; \dots; Y_{h_{t-1}}, \rho_{a_t}) \sigma^{-1} \right] \right) \end{aligned} \quad (\text{A114})$$

$$= \frac{1}{d_a^{2t} d_h^{2t}} \left(1 + \mathcal{O}\left(\frac{1}{d_h}\right) \right) \sum_{\mathbf{X}_{h_{t-1}}} \sum_{\mathbf{Y}_{h_{t-1}}} \left(\int d\nu(\rho_{a_1}) \text{Tr}[\rho_{a_1}^2] - \text{Tr}[\bar{\rho}^2] \right) \left(\prod_{\tau=1}^{t-1} \text{Tr}[X_\tau Y_\tau]^2 \text{Tr}[\mathcal{I}_a] \right) \text{Tr}[O^2] \quad (\text{A115})$$

$$= \frac{1}{d_h d_a^{2t}} \left(1 + \mathcal{O}\left(\frac{1}{d_h}\right) \right) (1 - \text{Tr}[\bar{\rho}^2]) \quad (\text{A116})$$

$$\leq \frac{1}{d_h d_a^{2t}} \left(1 + \mathcal{O}\left(\frac{1}{d_h}\right) \right). \quad (\text{A117})$$

Here in the third equality, the term $\text{Tr}[\bar{\rho}^2]$ is the purity of the averaged input states. The limit of this purity, as the distribution of inputs approaches Haar measure, equals $1/d_a$, which can also be identified in Eq. (A108) and (A107).

Using the same approach, we also upper bound the initial state dependence for an arbitrary ensemble of initial state. We obtain

$$\mathbb{E}_U[\text{Var}_{\rho_{h_0} \sim \mathcal{S}_h} \langle O \rangle_t] = \frac{1}{d_h d_a^{2t}} \left(1 + \mathcal{O}\left(\frac{1}{d_h}\right) \right) (1 - \text{Tr}[\bar{\rho}_{h_0}^2]) \quad (\text{A118})$$

$$\leq \frac{1}{d_h d_a^{2t}} \left(1 + \mathcal{O}\left(\frac{1}{d_h}\right) \right), \quad (\text{A119})$$

which completes the proof. \square

Appendix B: Practical consequences of exponential concentration on QRP

1. Preliminaries: Hypothesis testing

We first provide some standard results of statistical indistinguishability of probability distributions using hypothesis testing tools

Lemma 2. Consider two probability distributions \mathcal{P} and \mathcal{Q} over some finite set of outcomes \mathcal{I} . Suppose we are given a single sample S drawn from either \mathcal{P} or \mathcal{Q} with equal probability, and we have the following two hypotheses:

- Null hypothesis \mathcal{H}_0 : S is drawn from \mathcal{P} ,
- Alternative hypothesis \mathcal{H}_1 : S is drawn from \mathcal{Q} .

The probability of correctly deciding the true hypothesis is upper bounded as

$$\Pr[\text{“right decision between } \mathcal{H}_0 \text{ and } \mathcal{H}_1\text{”}] \leq \frac{1}{2} + \frac{\|\mathcal{P} - \mathcal{Q}\|_1}{4}, \quad (\text{B1})$$

where we denote $\|\mathcal{P} - \mathcal{Q}\|_1 = \sum_{s \in \mathcal{I}} |p(s) - q(s)|$ as the 1-norm between the probability vectors ($2 \times$ the total variation distance).

Proof. There exists a region \mathcal{A} such that $p(s) > q(s)$ for all $s \in \mathcal{A}$. The optimal decision making strategy is to choose that the given sample S is drawn from \mathcal{P} if it falls in the region i.e., $S \in \mathcal{A}$ and choose \mathcal{Q} , otherwise. The probability of making the right decision can be expressed as

$$\Pr[\text{“right decision between } \mathcal{H}_0 \text{ and } \mathcal{H}_1\text{”}] = \Pr(S \in \mathcal{A} | S \sim \mathcal{P})\Pr(S \in \mathcal{P}) + \Pr(S \notin \mathcal{A} | S \sim \mathcal{Q})\Pr(S \in \mathcal{Q}) \quad (\text{B2})$$

$$= \frac{1}{2} [\Pr(S \in \mathcal{A} | S \sim \mathcal{P}) + \Pr(S \notin \mathcal{A} | S \sim \mathcal{Q})] \quad (\text{B3})$$

$$= \frac{1}{2} \left[\sum_{s \in \mathcal{A}} p(s) + \sum_{s \notin \mathcal{A}} q(s) \right], \quad (\text{B4})$$

where the second equality is due to the sample being equally likely to be drawn from either \mathcal{P} or \mathcal{Q} . In the last equality, we use the fact that given that the sample is from \mathcal{P} , the probability that this sample takes any value within the region \mathcal{A} is simply $\sum_{s \in \mathcal{A}} p(s)$, and similarly for $s \notin \mathcal{A}$.

The 1-norm between probability vectors can be written as

$$\|\mathcal{P} - \mathcal{Q}\|_1 = \sum_{s \in \mathcal{I}} |p(s) - q(s)| \quad (\text{B5})$$

$$= \sum_{s \in \mathcal{A}} (p(s) - q(s)) + \sum_{s \notin \mathcal{A}} (q(s) - p(s)), \quad (\text{B6})$$

where we have separated terms in the sum based on the region \mathcal{A} . Lastly, we notice that

$$\frac{2 + \|\mathcal{P} - \mathcal{Q}\|_1}{2} = \frac{1}{2} \left(\sum_{s \in \mathcal{I}} p(s) + \sum_{s \in \mathcal{I}} q(s) + \|\mathcal{P} - \mathcal{Q}\|_1 \right) \quad (\text{B7})$$

$$= \sum_{s \in \mathcal{A}} p(s) + \sum_{s \notin \mathcal{A}} q(s), \quad (\text{B8})$$

where in the second line we have used Eq. (B6). Substituting this back to Eq. (B4), we obtain the desired result. \square

Lemma 3. Consider two binary probability distributions $\mathcal{P}_0 = (p_0, 1 - p_0)$ and $\mathcal{P}_\varepsilon = (p_\varepsilon, 1 - p_\varepsilon)$ where $p_\varepsilon = p_0 + \varepsilon$. Suppose we are given N samples (denoted as \mathcal{M}) drawn from either \mathcal{P}_0 or \mathcal{P}_ε with equal probability, and we have the following two hypotheses:

- Null hypothesis \mathcal{H}_0 : \mathcal{M} is drawn from \mathcal{P}_0 ,
- Alternative hypothesis \mathcal{H}_1 : \mathcal{M} is drawn from \mathcal{P}_ε .

The probability of correctly deciding the true hypothesis is upper bounded as

$$\Pr[\text{“right decision between } \mathcal{H}_0 \text{ and } \mathcal{H}_1\text{”}] \leq \frac{1}{2} + \frac{N|\varepsilon|}{2}. \quad (\text{B9})$$

Proof. We remark that the combination of the standard upper bound

$$\|\mathcal{P}^{\otimes N} - \mathcal{Q}^{\otimes N}\|_1 \leq N\|\mathcal{P} - \mathcal{Q}\|_1, \quad (\text{B10})$$

along with Lemma 2 gives success probability

$$\Pr[\text{“right decision between } \mathcal{H}_0 \text{ and } \mathcal{H}_1\text{”}] \leq \frac{1}{2} + \frac{N\|\mathcal{P}_0 - \mathcal{P}_\varepsilon\|_1}{4} \quad (\text{B11})$$

and explicit evaluation shows that $\|\mathcal{P}_0 - \mathcal{P}_\varepsilon\|_1 = 2|\varepsilon|$. \square

2. Main results: Statistical indistinguishability in QRP

In the presence of concentration, the QRP predictions estimated with a polynomial number of measurement shots become indistinguishable from random variables that are insensitive to input data. This result is indeed the interplay between the concentration and the polynomial measurement shots. In what follows, we formally show that statistical estimates of these expectations as well as model predictions are indistinguishable from some data-independent random variables.

a. Setting

To rigorously see the practical implications of the concentration, we consider observables $\{O_k\}_{k=1}^M$ to be Pauli operators and the measurements are made in the respective eigen basis. For the Pauli operator O_k , after polynomial number of measurements N , the statistical estimate of the expectation can be obtained by

$$\widehat{O}_{k;t} = \frac{1}{N} \sum_{i=1}^N \lambda_i, \quad (\text{B12})$$

where λ_i is the i^{th} measurement outcome which takes the value $+1$ with the probability $p_{k;t}^{(+)}$ and the value -1 with the probability $p_{k;t}^{(-)}$. That is, each sample is drawn from a distribution

$$\mathcal{P}_{k;t} = \{p_{k;t}^{(+)}, p_{k;t}^{(-)}\}. \quad (\text{B13})$$

Next, we assume the exponentially vanishing variance over the instances of quantum reservoir

$$\text{Var}_U[\langle O_k \rangle_t] \leq \beta, \quad \beta \in \mathcal{O}(1/b^n), \quad (\text{B14})$$

for all k and some constant $b > 1$. By using Chebyshev's inequality, the vanishing variance leads to the exponential concentration as in Definition 1 with the concentration point being the average over the reservoirs i.e., $\mu = \mathbb{E}_U[\langle O_k \rangle_t]$. We further assume that this concentration point is zero

$$\mathbb{E}_U[\langle O_k \rangle_t] = 0. \quad (\text{B15})$$

Now, the concentration in expectation values also implies the concentration in probability outcomes (when measured in eigen basis) which is formalized in the following proposition

Supplemental Proposition 3. *Given the concentration of the expectation value of some observable O_k according to Eq. (B14) and Eq. (B15), the outcome probabilities when measuring in eigen basis also concentrate with*

$$\text{Var}_U[p_{k;t}^{(+)}], \text{Var}_U[p_{k;t}^{(-)}] \in \mathcal{O}(1/b^n), \quad (\text{B16})$$

where $p_{k;t}^{(+)}$ and $p_{k;t}^{(-)}$ are the probabilities of obtaining $+1$ and -1 respectively. In addition, the concentration points are $1/2$ i.e.,

$$\mathbb{E}_U[p_{k;t}^{(+)}] = \mathbb{E}_U[p_{k;t}^{(-)}] = \frac{1}{2}. \quad (\text{B17})$$

Proof. Let us first decompose the expectation into the eigen basis

$$\langle O_k \rangle_t = p_{k;t}^{(+)} - p_{k;t}^{(-)}, \quad (\text{B18})$$

where the eigenvalues for a Pauli operators are +1 and -1 respectively. By using Eq. (B15) and Eq. (B18) together with the normalization condition on the outcome probabilities i.e., $p_{k;t}^{(+)} + p_{k;t}^{(-)} = 1$, we have the concentration points to be

$$\mathbb{E}_U [p_{k;t}^{(+)}] = \mathbb{E}_U [p_{k;t}^{(-)}] = \frac{1}{2}. \quad (\text{B19})$$

Similarly, by using the same conditions, the variances of the outcome probabilities can be expressed as

$$\text{Var}_U [(O_k)_t] = \text{Var}_U [p_{k;t}^{(+)}] + \text{Var}_U [p_{k;t}^{(-)}] - 2\text{Cov}_U [p_{k;t}^{(+)}, p_{k;t}^{(-)}], \quad (\text{B20})$$

$$0 = \text{Var}_U [p_{k;t}^{(+)}] + \text{Var}_U [p_{k;t}^{(-)}] + 2\text{Cov}_U [p_{k;t}^{(+)}, p_{k;t}^{(-)}], \quad (\text{B21})$$

which leads to

$$\text{Var}_U [p_{k;t}^{(+)}], \text{Var}_U [p_{k;t}^{(-)}] \in \mathcal{O}(1/b^n). \quad (\text{B22})$$

This completes the proof. \square

b. Statistical indistinguishability with QRP

We formally introduce the concepts of statistical indistinguishability at the levels of distributions and of outcomes.

Definition 4 (Statistical indistinguishability (of distributions)). *Two probability distributions \mathcal{P} and \mathcal{Q} are statistically indistinguishable with N samples if a binary hypothesis test cannot be passed with probability at least 0.51. That is, given a set of N samples \mathcal{M} drawn from either \mathcal{P} or \mathcal{Q} (with an equal probability), consider the following hypotheses*

- Null hypothesis \mathcal{H}_0 : \mathcal{M} is drawn from \mathcal{P} ,
- Alternative hypothesis \mathcal{H}_1 : \mathcal{M} is drawn from \mathcal{Q} ,

where \mathcal{P} and \mathcal{Q} are statistically indistinguishable (with N samples) if for any algorithm the probability of correctly identifying the correct hypothesis, $\Pr[\text{“right decision between } \mathcal{H}_0 \text{ and } \mathcal{H}_1\text{”}]$, satisfies:

$$\Pr[\text{“right decision between } \mathcal{H}_0 \text{ and } \mathcal{H}_1\text{”}] \leq 0.51. \quad (\text{B23})$$

Note that the threshold 0.51 in the definition is arbitrary chosen to be close to that of random guessing.

Definition 5 (Statistical indistinguishability (of outputs)). *Consider a map $\Phi: \mathbb{R}^N \rightarrow \mathbb{R}^M$ (with M being the dimension of the output) and two distributions \mathcal{P} and \mathcal{Q} which are statistically indistinguishable under N samples according to Definition 4. Draw N respective samples from \mathcal{P} and \mathcal{Q} , which we respectively denote as $\mathcal{M}_{\mathcal{P}}$ and $\mathcal{M}_{\mathcal{Q}}$. We say that $\Phi(\mathcal{M}_{\mathcal{P}})$ and $\Phi(\mathcal{M}_{\mathcal{Q}})$ are statistically indistinguishable outputs.*

The formal formal version of Proposition 1 in the main text which shows the statistical indistinguishability of the QRP output is stated formally below. We note that it is also stated in a more general manner which includes exponential concentration from any other sources (not just the extreme scrambling reservoirs).

Supplemental Theorem 1. *[Statistical indistinguishability of an expectation value] Suppose that the expectation value of some Pauli operator O_k exponentially concentrates towards zero according to Eq. (B14) and Eq. (B15). For any reservoir instance U , we consider estimating the expectation value in the respective eigen basis. That is, samples are drawn from the distribution $\mathcal{P}_{k;t}$ in Eq. (B13). Then, for polynomial number of samples $N \in \mathcal{O}(\text{poly}(n))$, $\mathcal{P}_{k;t}$ is indistinguishable from the uniform distribution $\mathcal{P}_{\text{unif}} = \{1/2, 1/2\}$ according to Definition 4. In particular, let \mathcal{M} be a polynomial sized set of samples drawn either from $\mathcal{P}_{k;t}$ or $\mathcal{P}_{\text{unif}}$ (with an equal probability). We then perform a hypothesis test with:*

- Null hypothesis \mathcal{H}_0 : \mathcal{M}_s is drawn from the uniform distribution $\mathcal{P}_{\text{unif}}$,

- *Alternative hypothesis \mathcal{H}_s : \mathcal{M} is drawn from $\mathcal{P}_{k;t}$.*

With probability at least $1 - \delta$ over the choice of reservoir U regardless of the input signals we have that

$$\Pr[\text{“right decision between } \mathcal{H}_s \text{ and } \mathcal{H}_0\text{”}] \leq \frac{1}{2} + \epsilon, \quad (\text{B24})$$

with $\delta \in \mathcal{O}(c^{-n})$ for some $c > 1$ and $\epsilon \in \mathcal{O}(c'^{-n})$ for some $c' > 1$. In addition, with high probability exponentially close to 1, the statistical estimate of $\langle O_k \rangle_t$ is indistinguishable from a input-independent random variable of the form

$$\widehat{O}_{\text{rand}} = \frac{1}{N} \sum_{i=1}^N z_i, \quad (\text{B25})$$

where each z_i is drawn from $\mathcal{P}_{\text{unif}}$.

Consequently, Supplemental Theorem 1 leads to poor performance of QRP on unseen input sequences. In particular, while training the model with estimated QRP outputs is guaranteed to minimize the training loss thanks to the convex optimization with the hard coded training labels, the trained QRP model generalizes poorly. The following statement captures this subtlety.

Supplemental Corollary 1 (Impact of concentration on trainability and generalization). *Under the same setting as Supplemental Theorem 1, consider the loss in Eq. (5) with the training dataset \mathcal{S}_{tr} . Given that each QRP output (necessarily for estimating the loss and making prediction on unseen input) is estimated with polynomial measurement shots $N \in \mathcal{O}(\text{poly}(n))$, then after training the QRP model we have:*

- *With high probability $1 - \delta$ with $\delta' \in \mathcal{O}(c'^{-n})$ and $c' > 1$, the optimal weights $\hat{\boldsymbol{\eta}}^*$ are statistically indistinguishable from an input-independent random vector of the form*

$$\boldsymbol{\eta}_{\text{rand}} = (R_0^T R_0)^{-1} R_0^T \mathbf{y}, \quad (\text{B26})$$

where R_0 is an input-independent random matrix of the dimensions $N_{\text{tr}} \times M$ whose elements are instances of $\widehat{O}_{\text{rand}}$ defined in Eq. (B25) and \mathbf{y} is a vector whose elements corresponding to the training labels of the dimension N_{tr} . Here, $N_{\text{tr}} = D_{\text{tr}} |\mathcal{T}_{\text{tr}}|$ corresponds to the number of terms in the training loss, and M is the number of observables.

- *The empirical training loss evaluated with $\boldsymbol{\eta}^*$ is at the global minimum (given those estimated QRP outputs).*
- *For an unseen input sequence $\boldsymbol{\rho}_{a_\tau} \notin \mathcal{S}_{\text{tr}}$, with high probability $1 - \delta'$ with $\delta' \in \mathcal{O}(c'^{-n})$, the estimated QRP prediction is independent of $\boldsymbol{\rho}_{a_\tau}$ and statistically indistinguishable from*

$$\hat{\mathbf{f}}_{\text{rand}} = \mathbf{O}_{\text{rand}}^T \boldsymbol{\eta}_{\text{rand}}, \quad (\text{B27})$$

where \mathbf{O}_{rand} is an input-independent vector of length M whose elements are instances of $\widehat{O}_{\text{rand}}$.

3. Proofs of analytical results

a. Proof of Supplemental Theorem 1

Proof. First, recall that the concentration of $\langle O_k \rangle_t$ implies the concentration of outcome probabilities as in Proposition 3. Our proof strategy is to show that, due to exponential concentration in outcome probabilities, $\Delta_p^{(+)} = |p_{k;t}^{(+)} - 1/2|$ and $\Delta_p^{(-)} = |p_{k;t}^{(-)} - 1/2|$ are very likely (i.e., with probability exponentially close to 1) to be exponentially small for any given reservoir U . This exponentially small value corresponds to an exponentially small perturbation from the uniform distribution $\mathcal{P}_{\text{unif}}$. Combining this observation with Lemma 3 we can then establish that it is hard to decide the correct hypothesis with polynomial resources.

More explicitly, we first note that it follows from Lemma 3 that

$$\Pr\left(\text{“right decision between } \mathcal{H}_s \text{ and } \mathcal{H}_0\text{”} \mid \Delta_p^{(+)} = s, \Delta_p^{(+)} = s'\right) \leq \left(\frac{1}{2} + \frac{N(s+s')}{4}\right). \quad (\text{B28})$$

For $s, s' \in \mathcal{O}(c'^{-n})$ for some $c' > 1$ and $N \in \mathcal{O}(\text{poly}(n))$ we have $\epsilon \in \mathcal{O}(c'^{-n})$ as claimed. It remains to determine with what probability we have $s, s' \in \mathcal{O}(c'^{-n})$. By invoking Proposition 3, for $p_{k;t}^{(+)}$ we have

$$\Pr_U \left[\left| p_{k;t}^{(+)} - \frac{1}{2} \right| \geq \delta_c \right] \leq \frac{\beta}{\delta_c^2}, \quad (\text{B29})$$

with

$$\beta \in \mathcal{O}(1/b^n), \quad (\text{B30})$$

for some $b, b' > 1$. We then choose $\delta_c = \beta^{1/4}$ and invert the inequality of Eq. (B29), leading to (with $\Delta_p^{(+)} = |p_{k;t}^{(+)} - 1/2|$)

$$\Pr_U [\Delta_p^{(+)} \leq \beta^{1/4}] \geq 1 - \sqrt{\beta}. \quad (\text{B31})$$

It follows that $\Delta_p^{(+)}$ takes value between $-\beta^{1/4}$ and $\beta^{1/4}$ (which are exponentially small) with probability at least $1 - \sqrt{\beta}$ (which is exponentially close to 1). By following the identical steps, one can show that $\Delta_p^{(-)}$ is exponentially small with high probability. This completes the proof of the first part. To show the indistinguishability of the statistical estimate to $\widehat{\mathcal{O}}_{\text{rand}}$, we can prove by contradiction. Basically, if they were distinguishable, we could have used this as a quantity to distinguish the distributions. \square

b. Proof of Supplemental Corollary 1

Proof. We first recall the training procedure of the QRP model. The loss function in Eq. (5) can be written in a compact form as

$$\mathcal{L}(\boldsymbol{\eta}) = \frac{1}{N_{\text{tr}}} \sum_{l, \tau} \left(f_{\tau}(\boldsymbol{\rho}_{a_{\tau}}^{(l)}; \boldsymbol{\eta}) - y_{\tau}^{(l)} \right)^2, \quad (\text{B32})$$

where $N_{\text{tr}} = D_{\text{tr}} |\mathcal{T}_{\text{tr}}|$. Minimizing this loss over $\boldsymbol{\eta}$ corresponds to doing a least square fitting and has an analytical closed-form solution [8]

$$\boldsymbol{\eta}^* = (R^T R)^{-1} R \mathbf{y}, \quad (\text{B33})$$

where R is a matrix whose elements are the appropriate QRP outputs $\langle O_k \rangle_{\tau}^{(l)}$ with dimensions $N_{\text{tr}} \times M$, and \mathbf{y} is a vector corresponding to the training labels in an appropriated order of the dimension N_{tr} . The exact forms of R and \mathbf{y} are not necessary for the proof². What crucial here is that for a given estimate of R (done by measuring associated QRP outputs with quantum computers), estimating the optimal parameters with Eq. (B33) guarantees to minimize the empirical training loss. This happens regardless whether the QRP faces the concentration. This proves the second point of the corollary.

In the presence of concentration, Supplemental Theorem 1 indicates that a single attempt to estimate a QRP output with polynomial measurement shots is statistically indistinguishable from $\widehat{\mathcal{O}}_{\text{rand}}$ in Eq (B25) with high probability exponentially close to 1. To prove the first and the last points of the corollary, it is sufficient to show that the statistical

² and left as an exercise for the readers

indistinguishability pertains with a polynomial number of attempts. This is because estimating optimal parameters and making prediction requires at most polynomial number of QRP outputs.

More concretely, consider estimating the total of N_a QRP outputs (that exponentially concentrate) with $N_a \in \mathcal{O}(\text{poly}(n))$, and denote o_k as a statistical estimate of the k^{th} output (with polynomial measurement shots). Let E_k be the event that o_k is statistically indistinguishable from $\widehat{\mathcal{O}}_{\text{rand}}$. From Supplemental Theorem 1, we have

$$\Pr[E_k] \geq 1 - \delta_k \ ; \ \forall o_k \ , \quad (\text{B34})$$

with $\delta \in \mathcal{O}(c^{-n})$ with some positive constant $c > 1$ and the total qubits n . Now the probability that all E_k occurs can be bounded using the union bound as

$$\Pr\left[\bigcap_k E_k\right] = 1 - \Pr\left[\bigcup_k \bar{E}_k\right] \quad (\text{B35})$$

$$\geq 1 - \sum_{k=1}^{N_a} \Pr[\bar{E}_k] \quad (\text{B36})$$

$$\geq 1 - \frac{N_a \delta}{2} \ , \quad (\text{B37})$$

where \bar{E}_k is a conjugate event of E_k , we use the union bound in the second line and use $\Pr[\bar{E}_k] \leq \delta$ by reversing the final inequality in Eq. (B34). Since $N_a \in \mathcal{O}(\text{poly}(n))$, we have that the probability that each of the estimates are statistically indistinguishable is $1 - \delta'$ with $\delta' := N_a \delta_k / 2 \in \mathcal{O}(\tilde{c}^{-n})$ for some $\tilde{c} > 1$.

Crucially, since the estimates are all indistinguishable, post-processing them also leads to the statistical indistinguishability. That is, for some map $\Phi(\cdot)$, we have that $\Phi(\{o_k\}_{k=1}^{N_a})$ is also indistinguishable from $\Phi(\{o_{\text{rand};k}\}_{k=1}^{N_a})$ where $\{o_{\text{rand};k}\}_{k=1}^{N_a}$ are different instances of $\widehat{\mathcal{O}}_{\text{rand}}$. Hence, by replacing QRP outputs with the instances of $\widehat{\mathcal{O}}_{\text{rand}}$ in Eq. (B33) and the model prediction in Eq. (4), with high probability we have that the optimal parameters are indistinguishable from

$$\boldsymbol{\eta}_{\text{rand}} = (R_0^T R_0)^{-1} R_0^T \mathbf{y} \ , \quad (\text{B38})$$

where R_0 is an input-independent random matrix of the dimensions $N_{\text{tr}} \times M$ whose elements are instances of $\widehat{\mathcal{O}}_{\text{rand}}$, and the model prediction on unseen data is indistinguishable from

$$\hat{f}_{\text{rand}} = \mathbf{O}_{\text{rand}}^T \boldsymbol{\eta}_{\text{rand}} \ , \quad (\text{B39})$$

where \mathbf{O}_{rand} is an input-independent vector of length M whose elements are instances of $\widehat{\mathcal{O}}_{\text{rand}}$. This completes the proof. \square

Appendix C: Role of noise in output concentration and memory retention in QRP

In this appendix, we analyse two distinct noise sources in QRP: (i) input-data encoding noise and (ii) noise acting during reservoir evolution. We derive recursive relations in the time step t , and obtain, respectively, an *output-concentration bound* induced by noisy input-data encodings, and a *memory-forgetting bound* that quantifies how noisy reservoir dynamics washes out information about early inputs and the initial state.

1. Preliminaries on noise channels

We consider *local* noise, which can be modelled by single-qubit channels. In general, any single-qubit channel \mathcal{N} admits the following decomposition [66, 87]

$$\mathcal{N} = \mathcal{U} \circ \mathcal{M} \circ \mathcal{V} \ , \quad (\text{C1})$$

where $\mathcal{U} = U(\cdot)U^\dagger$ and $\mathcal{V} = V(\cdot)V^\dagger$ are unitary channels and \mathcal{M} is a channel in *normal form*, i.e. a quantum operation that captures the non-unitary components of the noise. Given a single-qubit state $\sigma := \frac{1}{2}(I + \sum_{P \in \{X,Y,Z\}} r_P P)$, we have

$$\mathcal{M}(\sigma) = \frac{1}{2} \left(I + \sum_{P \in \{X,Y,Z\}} (D_P r_P + t_P) P \right). \quad (\text{C2})$$

The vectors $\mathbf{D} = (D_X, D_Y, D_Z)$ and $\mathbf{t} = (t_X, t_Y, t_Z)$ are called *normal form parameters*. A quantum channel is *unital* if it maps the maximally mixed state onto itself, and otherwise it is called *non-unital*. Specifically, a single-qubit channel is unital if it satisfies $\mathbf{t} = (0, 0, 0)$.

An important property of unital noise is that the associated normal form channel \mathcal{M} can be expressed as a Pauli channel, i.e. as a probabilistic mixture of Pauli unitaries, i.e.

$$\mathcal{M}(\cdot) = \sum_{P \in \{I,X,Y,Z\}} p_P P(\cdot) P, \quad (\text{C3})$$

where $p_P \geq 0$ and $\sum_{P \in \{I,X,Y,Z\}} p_P = 1$. A channel \mathcal{M} expressed as in Eq. (C3) is commonly referred as *Pauli noise* in the literature.

Unital channels can be further classified in *depolarizing-like* and *dephasing-like*. Depolarizing-like noise satisfies $\max_P |D_P| < 1$, while dephasing-like noise satisfies $\min_P |D_P| < \max_P |D_P| = 1$. Importantly, depolarizing-like noise drives any state towards the maximally mixed state, thereby increasing its entropy. In contrast, dephasing-like noise and non-unital noise do not necessarily increase the entropy of a quantum state. In order to show that generic local noise can cause QRP to lose memory of initial states or inputs, we follow two distinct strategies:

- for **depolarizing-like** noise, we will employ entropy accumulation tools, such as those introduced in Refs. [63, 88, 89],
- for **dephasing-like** and **non-unital** noise, we will study the effect of noise on *typical* reservoirs, such as those composed by local Haar-random unitaries. Our analysis extends to quantum reservoir processing the techniques introduced in Refs. [67, 68, 90] in the context of random quantum circuits.

2. Noisy input-data encoding induces concentration in the output

In this section, we additionally study the scenario where classical data encoding strategy is noisy, generalizing the concentration upper bound induced by noisy embedding from QELM [51] to QRP with arbitrary number of steps. Similar to the noise model we discussed for QELMs [51], here we also consider a L -layered encoding subject to local noise for each time step. Then the embedded state will be

$$\rho_{a_\tau} = \mathcal{N}^{\otimes n} \circ \mathcal{U}_L(\mathbf{s}_{\tau,L}) \circ \mathcal{N}^{\otimes n} \circ \dots \circ \mathcal{N}^{\otimes n} \circ \mathcal{U}_1(\mathbf{s}_{\tau,1}) \circ \mathcal{N}^{\otimes n}(\rho_0), \quad (\text{C4})$$

where $\mathcal{U}_i(\mathbf{s}_\tau)(\cdot) = U_i(\mathbf{s}_{\tau,i})(\cdot)U_i(\mathbf{s}_{\tau,i})^\dagger$ and $\{\mathbf{s}_{\tau,i}\}_{i=1}^L$ are some functions of \mathbf{s}_τ . We assume the noise to be depolarizing-like, i.e. the associated normal form parameters \mathbf{D} and \mathbf{t} satisfy

$$\max_P |D_P| < 1 \quad (\text{C5})$$

$$t_X = t_Y = t_Z = 0. \quad (\text{C6})$$

Finally let us define the characteristic noise parameter $q = \max\{|D_X|, |D_Y|, |D_Z|\}$. We will make use of the following lemma.

Lemma 4 (Sandwiched 2-Rényi relative entropy contraction, Supplementary Lemma 6 in Ref. [63] and Corollary 5.6 in Ref. [91]). *Let \mathcal{N} be a single-qubit noise channel with normal form parameters \mathbf{D}, \mathbf{t} as defined above. Assume that $\mathbf{t} = (0, 0, 0)$ (i.e. \mathcal{N} is unital)*

$$S_2 \left(\mathcal{N}^{\otimes n}(\rho) \left\| \frac{I^{\otimes n}}{2^n} \right\| \right) \leq q^b S_2 \left(\rho \left\| \frac{I^{\otimes n}}{2^n} \right\| \right) \quad (\text{C7})$$

where $q := \max_P |D_P|$, $b = 1/\ln 2$ and $S_2(\cdot \|\cdot)$ denotes the sandwiched 2-Rényi relative entropy.

Then, the following theorem holds true.

Supplemental Theorem 2 (Noisy encoding induced concentration). *Suppose a L -layered encoding as defined in Eq. (C4), with $q < 1$. Then, for each $t \in \mathbb{N}$, the expectation value of the observable will concentrate towards an input-independent quantity $\mu_t = \text{Tr}[\Omega_t O]$ where $\Omega_t = U(\mathcal{I}/2^{n_a} \otimes \text{Tr}_a[\Omega_{t-1}])U^\dagger$ with $\Omega(0) = \rho_0$:*

$$|\langle O \rangle_t - \mu_t| \leq \|O\|_\infty \sqrt{t} \left[2 \ln 2q^{b(L+1)} S_2\left(\rho_0 \left\| \frac{\mathcal{I}_a}{2^{n_a}} \right\| \right) \right]^{1/2}, \quad (\text{C8})$$

where $b = 1/\ln 2$, and $S_2(\cdot\|\cdot)$ denotes the sandwiched 2-Rényi relative entropy.

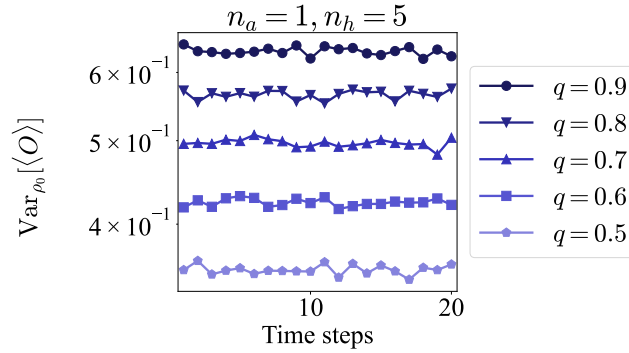


Figure 11. **Noisy encoding induced concentration.** The variance of outputs over randomly selected input series are plotted.

This upper bound indicates that if the number of encoding layers $L \in \mathcal{O}(n_a)$, then the deviation of the observable from an input-independent value will concentrate exponentially with respect to the number of the accessible qubits.

Proof: We compute the deviation of the expectation value for time-step t ,

$$|\langle O \rangle_t - \mu_t| = \left| \text{Tr} \left[\left(\rho_t - \Omega_t \right) O \right] \right| \quad (\text{C9})$$

$$\leq \|\rho_t - \Omega_t\|_1 \|O\|_\infty \quad (\text{C10})$$

$$\leq \|O\|_\infty \sqrt{2 \ln 2} S_2\left(\rho_t \left\| \Omega_t \right\| \right)^{1/2}, \quad (\text{C11})$$

where the first inequality is achieved by using the Hölder's inequality, in the second inequality we combine Pinsker's inequality and $S(\cdot\|\cdot) \leq S_2(\cdot\|\cdot)$. Now, we find the recursive relation for the term $S_2\left(\rho_t \left\| \Omega_t \right\| \right)$,

$$S_2\left(\rho_t \left\| \Omega_t \right\| \right) = S_2\left(\rho_{a_t} \otimes \rho_{h_{t-1}} \left\| \frac{\mathcal{I}_a}{2^{n_a}} \otimes \text{Tr}_a[\Omega_{t-1}] \right\| \right) \quad (\text{C12})$$

$$= S_2\left(\rho_{a_t} \left\| \frac{\mathcal{I}_a}{2^{n_a}} \right\| \right) + S_2\left(\rho_{h_{t-1}} \left\| \text{Tr}_a[\Omega_{t-1}] \right\| \right) \quad (\text{C13})$$

$$\leq S_2\left(\rho_{a_t} \left\| \frac{\mathcal{I}_a}{2^{n_a}} \right\| \right) + S_2\left(\rho_{t-1} \left\| \Omega_{t-1} \right\| \right), \quad (\text{C14})$$

where we use the unitary invariance of relative entropy in the first equality and the additivity in the second equality. The last inequality is obtained using data processing inequality. Next, by applying this recursive relation t -times we obtain

$$S_2\left(\rho_t \parallel \Omega_t\right) \leq \sum_{i=1}^t S_2\left(\rho_i \parallel \frac{\mathcal{I}_a}{2^{n_a}}\right) \quad (\text{C15})$$

$$\leq tq^{b(L+1)} S_2\left(\rho_0 \parallel \frac{\mathcal{I}_a}{2^{n_a}}\right), \quad (\text{C16})$$

where in the last inequality we apply the noise inequality in Lemma 4 for all $1 \leq i \leq t$. Finally, by combining Eq. (C11) and (C16), we obtain

$$|\langle O \rangle_t - \mu_t| \leq \|O\|_\infty \sqrt{t} \left[2 \ln 2 q^b S_2\left(\rho_0 \parallel \frac{\mathcal{I}_a}{2^{n_a}}\right) \right]^{1/2}. \quad (\text{C17})$$

□

3. Memory erasure induced by reservoir with depolarizing-like noise

We now prove that adding noisy layers between each reservoir iteration can also erase memory of the initial condition and early inputs exponentially quickly.

Theorem 3 (Memory erasure induced by Pauli noise in the reservoir). *Consider a QRP with noisy layers between reservoir evolutions as defined in Eq. (C4), with $q < 1$. Then, for each $t \in \mathbb{N}$, the expectation value of the observable will become independent of the initial condition and early inputs, exponentially in number of steps t . Formally, given two initial states of hidden qubits ρ_{h_0} and σ_{h_0} , given two inputs ρ_{a_1} and σ_{a_1} at the first time step, given the same series of input states $[\rho_{a_k}]_{k=2}^t = [\sigma_{a_k}]_{k=2}^t$ from the second step, then the deviation of the corresponding outputs*

$$\Delta O \leq \|O\|_\infty \sqrt{2 \ln 2 q^{b(t-1)}} \left(S_2\left(\rho_{a_1} \parallel \sigma_{a_1}\right) + S_2\left(\rho_{h_0} \parallel \sigma_{h_0}\right) \right)^{1/2}, \quad (\text{C18})$$

where $\Delta O = |\langle O \rangle_t^{(\rho_{h_0}, \rho_{a_1})} - \langle O \rangle_t^{(\sigma_{h_0}, \sigma_{a_1})}|$, $b = 1/\ln 2$ and $S_2(\cdot \parallel \cdot)$ denotes the sandwiched 2-Rényi relative entropy.

Proof: We similarly upper bounds the deviation of the expectation values using 2-Rényi relative entropy,

$$\Delta O = \left| \text{Tr} \left[\left(\rho_t - \sigma_t \right) O \right] \right| \quad (\text{C19})$$

$$\leq \|\rho_t - \sigma_t\|_1 \|O\|_\infty \quad (\text{C20})$$

$$\leq \|O\|_\infty \sqrt{2 \ln 2} S_2\left(\rho_t \parallel \sigma_t\right)^{1/2}, \quad (\text{C21})$$

where the first inequality is achieved by using the Hölder's inequality, in the second inequality we combine Pinsker's

inequality and $S(\|\cdot\|) \leq S_2(\|\cdot\|)$. Next, we find the recursive relation for the term $S_2\left(\rho_t \parallel \sigma_t\right)$,

$$S_2\left(\rho_t \parallel \sigma_t\right) = S_2\left(\rho_{a_t} \otimes \mathcal{N}(\rho_{h_{t-1}}) \parallel \rho_{a_t} \otimes \mathcal{N}(\sigma_{h_{t-1}})\right) \quad (\text{C22})$$

$$= S_2\left(\rho_{a_t} \parallel \rho_{a_t}\right) + S_2\left(\mathcal{N}(\rho_{h_{t-1}}) \parallel \mathcal{N}(\sigma_{h_{t-1}})\right) \quad (\text{C23})$$

$$= 0 + q^b S_2\left(\rho_{h_{t-1}} \parallel \sigma_{h_{t-1}}\right) \quad (\text{C24})$$

$$\leq q^b S_2\left(\rho_{t-1} \parallel \sigma_{t-1}\right). \quad (\text{C25})$$

By applying this recursive relation $(t-1)$ times, we obtain

$$S_2\left(\rho_t \parallel \sigma_t\right) \leq q^{b(t-1)} S_2\left(\rho_1 \parallel \sigma_1\right) \quad (\text{C26})$$

$$= q^{b(t-1)} S_2\left(\rho_{a_1} \otimes \rho_{h_0} \parallel \rho_{a_1} \otimes \sigma_{h_0}\right) \quad (\text{C27})$$

$$= q^{b(t-1)} \left(S_2\left(\rho_{a_1} \parallel \sigma_{a_1}\right) + S_2\left(\rho_{h_0} \parallel \sigma_{h_0}\right) \right) \quad (\text{C28})$$

Finally, by combining the last inequality with Eq. (C21), we obtain the statement. \square

4. Memory erasure induced by reservoir with arbitrary noise

Let \mathcal{N} be an arbitrary single-qubit noise channel. We assume that the reservoir \mathcal{U} is composed of a sequence of random unitary channels interleaved by local noise of the form $\mathcal{N}^{\otimes n}$:

$$\mathcal{U} = \mathcal{U}_L \circ \mathcal{N}^{\otimes n} \circ \mathcal{U}_{L-1} \circ \dots \circ \mathcal{N}^{\otimes n} \circ \mathcal{U}_1 \circ \mathcal{N}^{\otimes n}. \quad (\text{C29})$$

We define the average contraction coefficient as

$$\chi := \sqrt{\frac{1}{3} \left(\|\mathbf{D}\|_2^2 + \|\mathbf{t}\|_2^2 \right)}, \quad (\text{C30})$$

where \mathbf{D} and \mathbf{t} are the normal form parameters defined in Section II of Ref. [68]. Notably, $\eta < 1$ if and only if \mathcal{N} is non-unitary, as shown in Lemma 18 in Ref. [67]. While our analysis encompasses all non-unitary local noise channels, we will make some additional assumptions on the reservoir dynamics.

- **Random circuit layers.** We assume that the unitary \mathcal{U}_j are independently sampled from a locally scrambled distribution \mathcal{D} up to the second moment, i.e. for any pair of Hermitian operators O, O' we have

$$\mathbb{E}_{\mathcal{U}_j \sim \mathcal{D}} \left\{ \mathcal{U}_j^{\otimes 2} (O \otimes O') \right\} = \mathbb{E}_{\mathcal{U}_j \sim \mathcal{D}} \mathbb{E}_{V_1, V_2, \dots, V_{n_h} \sim \text{Cl}(2)} \left\{ \mathcal{U}_j^{\otimes 2} \left(\bigotimes_{j=1}^{n_h} V_j^{\otimes 2} [O \otimes O'] \bigotimes_{j=1}^{n_h} V_j^{\dagger \otimes 2} \right) \right\}, \quad (\text{C31})$$

where V_1, V_2, \dots, V_{n_h} are single-qubit unitaries sampled independently and uniformly from the Clifford group. In other terms, each layer \mathcal{U}_j is invariant under post-processing by randomly sampled single-qubit Clifford gates, up to the second moment. In particular, this assumption is satisfied by Brickwork circuits with Haar-random gates.

- **Linear-depth reservoir.** We assume that the depth L in Eq. (C29) is at least linear in system size, i.e. $L \in \Omega(n_h + n_a)$.

As a preliminary step, we restate a result from Ref. [68] within our notation.

Lemma 5 (Adapted from Theorem 7 in Ref. [68]). *Let O be a traceless Hermitian operator independent of \mathcal{U} . Then*

$$\mathbb{E}_{\mathcal{U}} \|\mathcal{U}^\dagger(O)\|_2 \leq \chi^L \|O\|_2. \quad (\text{C32})$$

The lemma above states that the Schatten 2-norm of an operator O is suppressed by the noisy reservoir in the adjoint picture, on average over the random unitary layers. However, a potential issue arises in the analysis of reservoir dynamics, where we often deal with observables $O_{\mathcal{U}}$ that depend on the reservoir. As a result, the above statement is not immediately applicable. To address this, we derive a refined version that accounts for operators that explicitly depend on the reservoir.

Supplemental Corollary 2. *It holds that*

$$\mathbb{E}_{\mathcal{U}} \left\{ \max_H \frac{\|\mathcal{U}(H)\|_1}{\|H\|_2} \right\} \leq (d_h d_a)^{\frac{3}{2}} \chi^L, \quad (\text{C33})$$

where the maximization is over traceless Hermitian operators.

Proof. Given a Hermitian operator H and a channel \mathcal{U} , we expand $\mathcal{U}(H)$ in the Pauli basis:

$$\mathcal{U}(H) = \frac{1}{d_h d_a} \sum_{P \in \{I, X, Y, Z\}^{\otimes(n_h+n_a)}} \text{Tr}[\mathcal{U}(H)P] P = \frac{1}{d_h d_a} \sum_{P \in \{I, X, Y, Z\}^{\otimes(n_h+n_a)} \setminus \{I^{\otimes(n_h+n_a)}\}} \text{Tr}[H\mathcal{U}^\dagger(P)] P, \quad (\text{C34})$$

where we noted that $\text{Tr}[I^{\otimes(n_h+n_a)}\mathcal{U}(H)] = \text{Tr}[\mathcal{U}(H)] = \text{Tr}[H] = 0$ since \mathcal{U} is trace-preserving. We can upper bound the trace norm $\|\mathcal{U}(H)\|_1$ via Minkowski's inequality:

$$\|\mathcal{U}(H)\|_1 \leq \frac{1}{d_h d_a} \sum_{P \in \{I, X, Y, Z\}^{\otimes(n_h+n_a)} \setminus \{I^{\otimes(n_h+n_a)}\}} |\text{Tr}[H\mathcal{U}^\dagger(P)]| \|P\|_1 \quad (\text{C35})$$

$$\leq \sum_{P \in \{I, X, Y, Z\}^{\otimes(n_h+n_a)} \setminus \{I^{\otimes(n_h+n_a)}\}} |\text{Tr}[H\mathcal{U}^\dagger(P)]| \quad (\text{C36})$$

$$\leq \sum_{P \in \{I, X, Y, Z\}^{\otimes(n_h+n_a)} \setminus \{I^{\otimes(n_h+n_a)}\}} \|\mathcal{U}^\dagger(P)\|_2 \|H\|_2 \quad (\text{C37})$$

We obtain the desired result taking the maximum over H and averaging over \mathcal{U} .

$$\mathbb{E}_{\mathcal{U}} \left\{ \max_H \frac{\|\mathcal{U}(H)\|_1}{\|H\|_2} \right\} \leq \mathbb{E}_{\mathcal{U}} \max_H \frac{\|H\|_2}{\|H\|_2} \left\{ \sum_{P \in \{I, X, Y, Z\}^{\otimes(n_h+n_a)} \setminus \{I^{\otimes(n_h+n_a)}\}} \|\mathcal{U}^\dagger(P)\|_2 \right\} \quad (\text{C38})$$

$$\leq (d_h d_a)^2 \mathbb{E}_{\mathcal{U}} \|\mathcal{U}^\dagger(P)\|_2 \leq (d_h d_a)^2 \chi^L \|P\|_2 \quad (\text{C39})$$

$$= (d_h d_a)^{\frac{3}{2}} \chi^L. \quad (\text{C40})$$

□

Repeatedly applying Supplementary Corollary 2, we found that average-case noisy reservoirs lead to memory erasure that is exponentially fast in both the system size and the number of iterations.

Theorem 4 (Memory erasure induced by non-unital noise in the reservoir). *Assume that the reservoir \mathcal{U} consists in a random circuit interspersed by local noise as in Eq. (C29), and let χ with average contraction coefficient defined in Eq. (C30). Let the reservoir depth L be at least*

$$L \geq \frac{\frac{3}{2}(n_a + n_h) + \log_2(1/\epsilon) + \log(1/\delta)}{\log_2(1/\chi)}. \quad (\text{C41})$$

Given two initial states of hidden qubits ρ_{h_0} and σ_{h_0} , given two inputs ρ_{a_1} and σ_{a_1} at the first time step, given the same series of input states $[\rho_{a_k}]_{k=2}^t = [\sigma_{a_k}]_{k=2}^t$ from the second step, the corresponding output states satisfies

$$\|\rho_t - \sigma_t\|_1 \leq \epsilon^{t-1} \|\rho_{a_1} - \sigma_{a_1}\|_1, \quad (\text{C42})$$

with probability at least $1 - \delta$ over the randomness of the reservoir. In particular, if $L \geq c \cdot n$ for a sufficiently large constant $c > 0$, then with obtain

$$\|\rho_t - \sigma_t\|_1 \in \exp(-\Omega((n_a + n_h)t)), \quad (\text{C43})$$

with probability at least $1 - \exp(-\Omega(n_a + n_h))$.

Proof. First, we use Markov's inequality to derive a probabilistic statement from Corollary 2,

$$\Pr_{\mathcal{U}} \{ \forall H : \|\mathcal{U}(H)\|_1 \leq \epsilon \|H\|_1 \} \geq 1 - \frac{(d_h d_a)^{\frac{3}{2}} \chi^L}{\epsilon} \geq 1 - \delta, \quad (\text{C44})$$

where last inequality follows from the fact that $L \geq \frac{\frac{3}{2}(n_a + n_h) + \log_2(1/\epsilon) + \log(1/\delta)}{\log_2(1/\chi)}$. In the following of this proof, we condition on the event $E := \{ \forall H : \|\mathcal{U}(H)\|_1 \leq \epsilon \|H\|_1 \}$ happening.

Thus, we can find the recursive relation for the term $\|\rho_t - \sigma_t\|_1$,

$$\|\rho_t - \sigma_t\|_1 = \mathbb{E}_{\mathcal{U}} \|\mathcal{U}(\rho_{a_t} \otimes \rho_{h_{t-1}} - \rho_{a_t} \otimes \sigma_{h_{t-1}})\|_1 \quad (\text{C45})$$

$$\leq \epsilon \|\rho_{a_t} \otimes \rho_{h_{t-1}} - \rho_{a_t} \otimes \sigma_{h_{t-1}}\|_1 \quad (\text{C46})$$

$$= \epsilon \|\rho_{h_{t-1}} - \sigma_{h_{t-1}}\|_1 \quad (\text{C47})$$

$$\leq \epsilon \|\rho_{t-1} - \sigma_{t-1}\|_1. \quad (\text{C48})$$

By applying this recursive relation $t - 1$ times, we obtain the desired result

$$\|\rho_t - \sigma_t\|_1 \leq \epsilon \|\rho_{t-1} - \sigma_{t-1}\|_1 \leq \epsilon^2 \|\rho_{t-2} - \sigma_{t-2}\|_1 \leq \dots \leq \epsilon^{t-1} \|\rho_1 - \sigma_1\|_1. \quad (\text{C49})$$

□

Appendix D: Memory indicators, and relations to standard metrics for reservoir computing

In this appendix, we provide a pedagogical discussion of our *memory indicators* \mathcal{M}_a and \mathcal{M}_h for quantum reservoir processing (QRP), and relate these quantities to the common metrics used in reservoir computing literature, namely the *Echo State Property* (ESP) and the *Fading Memory Property* (FMP). However, we emphasize that our definitions capture these properties *on average*, and *not* in the deterministic or topological sense as in mathematical foundations of reservoir computing [60, 61]. These quantities are thus better viewed as *FMP-like* and *ESP-like* characteristics, which nonetheless provide quantitative measures of how old inputs and initial reservoir states become irrelevant, due to *exponential concentration*, in typical scenarios for QRP with finite measurement shots. While these concentration-induced memory characteristics resonate with the essence of FMP or ESP in mathematical RC, we do not claim a strict equivalence to the mathematical definitions used in formal universality results. Finally, we discuss the effects that exponential concentration have on reservoir universality.

1. Background: echo state and fading memory properties in reservoir computing

In *classical* Reservoir Computing (RC) [14–16, 92], one uses a fixed dynamical system (the *reservoir*) to process sequential data (time-series) $\{s_t\}$. At each time step t , the reservoir's hidden state \mathbf{x}_t evolves under the current input s_t and the previous state \mathbf{x}_{t-1} through a fixed (nonlinear) map $f(s_t, \mathbf{x}_{t-1}) = \mathbf{x}_t$. Only a simple *readout* (often, for simplicity, a linear map on \mathbf{x}_t) is trained to produce the output y_t .

Two fundamental dynamical properties, informally stated, that are necessary for classical reservoir computing to be well-defined (though by themselves insufficient to guarantee strong predictive performance) are:

1. *Fading Memory Property (FMP)*: A reservoir has FMP if the influence of inputs fed *far in the past* on the present output *fades away* in time. In other words, perturbations in the input $s_{t-\tau}$ for large τ cause only a negligible difference in the current output y_t . FMP ensures that the reservoir focuses on the relevant recent history of the input and is not overwhelmed by far past information.
2. *Echo State Property (ESP)*: A reservoir has ESP if its internal state \mathbf{x}_t at large t depends only on the driving inputs $\{s_t\}$ and *not* on the reservoir's initial state \mathbf{x}_0 . ESP thus guarantees that, after a long washout (burn-in) period, the reservoir state becomes a function of only recent inputs, and not on how the reservoir was initially prepared. Without ESP, the output could spuriously depend on arbitrary past state preparations, making the system ill-defined for consistent time series processing.

When both properties are satisfied, the reservoir map f defines a *causal time-invariant filter* on semi-infinite inputs³, guaranteeing that outputs are primarily driven by recent inputs [60]. Moreover, by optimizing the readout layer (via linear regression) and by properly choosing a reservoir (such as a sufficiently large Echo State Network (ESN)), certain systems with such properties can achieve a *universal approximation* of fading memory maps and possess short-term sequence-modeling capabilities [60, 61].

How \mathcal{M}_a and \mathcal{M}_h in our QRP framework relate to FMP and ESP. While mathematical RC defines FMP and ESP using rigorous deterministic statements [60], our memory indicators \mathcal{M}_a and \mathcal{M}_h are *ensemble-averaged* quantities. We consider how quickly the variance of outputs decays under perturbations (in either past inputs or initial states). This approach captures an *operational* sense of early input forgetting and early state forgetting in the *typical behavior* of a quantum reservoir. Unlike statements that universally work for each input or each initial reservoir instance in mathematical RC, our probabilistic statements reflect the common use of ensemble averaging in theoretical models (e.g., Haar random unitaries or noise channels, as used in the main text) which enables a rigorous study of exponential concentration in QRP, and the essential role of dissipation and noise in open quantum systems [38, 55, 56, 58]. Thus, our results do not necessarily imply the same universal approximation theorems proven by classical references [60, 61], but does capture the essence of FMP-like and ESP-like behaviors relevant to QRP with finite measurement shots. The formalization of ESP and FMP in QRP is an active area of research, with recent proposals adapting classical concepts to quantum contexts [38, 54, 55, 93, 94].

2. Exponential decay of $\mathcal{M}_a(t)$ implies Fading Memory Property (FMP)-like characteristics in QRP

Setting. Fix an initial time step τ , such that an input state ρ_{a_τ} is injected into the reservoir's *accessible* qubits. The reservoir then evolves for t more steps (with subsequent inputs $\rho_{a_{\tau+1}}, \rho_{a_{\tau+2}}, \dots$) until time $(\tau + t)$. Denote the reservoir's measurement outcome at that final time by

$$\langle O \rangle_{(\tau+t)}^{(\rho_{a_\tau})} = \text{Tr}[O \rho_{\tau+t}], \quad (\text{D1})$$

where $\rho_{\tau+t}$ is the resulting reservoir state (accessible and hidden qubits together).

As in Definition 2 of the main text, we define

$$\mathcal{M}_a(t; \mathcal{S}_a, \mathcal{U}) = \mathbb{E}_{U \sim \mathcal{U}} \left[\text{Var}_{\rho_{a_\tau} \sim \mathcal{S}_a} (\langle O \rangle_{\tau+t}) \right], \quad (\text{D2})$$

where $\text{Var}_{\rho_{a_\tau} \sim \mathcal{S}_a}(\cdot)$ is the variance of $\langle O \rangle_{\tau+t}$ over the distribution of possible inputs ρ_{a_τ} at the *initial time* τ . If $\mathcal{M}_a(t)$ is large, then changing the initial input can significantly influence the final output at the subsequent time step t . Conversely, if $\mathcal{M}_a(t)$ is small, the reservoir effectively *forgets* that earlier input.

³ In many treatments, inputs $\{s_t\}$ are defined for all integer time $t \leq 0$, called a *left-infinite* or *semi-infinite* input sequence. Intuitively, we let the reservoir receives the input data from $-\infty$ up to the present so that any dependence on an arbitrarily chosen initial reservoir state $\mathbf{x}_{-\infty}$ is washed out at large times. This ensures well-defined behavior of the map f .

Supplemental Theorem 3 (FMP-like behavior from exponentially decaying $\mathcal{M}_a(t)$). Assume there exist constants $c > 0$ and $\alpha > 0$ such that

$$\mathcal{M}_a(t; \mathcal{S}_a, \mathcal{U}) \leq c e^{-\alpha t}, \quad \forall t \in \mathbb{N}. \quad (\text{D3})$$

Then the reservoir exhibits FMP-like fading of old inputs on average over random pairs of inputs. Concretely, for two different initial states ρ_{a_τ} and σ_{a_τ} drawn from \mathcal{S}_a (with all subsequent inputs in the time series fixed), the outputs at time $(\tau + t)$ satisfy

$$\mathbb{E}_{U, \rho_{a_\tau}, \sigma_{a_\tau}} \left[\left(\langle O \rangle_{\tau+t}^{(\rho_{a_\tau})} - \langle O \rangle_{\tau+t}^{(\sigma_{a_\tau})} \right)^2 \right] \leq 4 c e^{-\alpha t}. \quad (\text{D4})$$

Hence, on average, older inputs ρ_{a_τ} for large τ fade exponentially from the reservoir's subsequent outputs.

Implications from exponential concentrations:

- **Reservoir's dimension-based decays:** For Haar random reservoirs, $\mathcal{M}_a(t) \in \mathcal{O}(1/[d_h d_a^t])$, see Theorem 2 in the main text, and then $\alpha \in \mathcal{O}(n_a)$.
- **Reservoir's noise-based decays:** For local Pauli noise with $0 < q < 1$, one typically gets $\mathcal{M}_a(t) \propto \sqrt{q}^{bt}$, see Theorem 3 in the main text, so $\alpha \in \mathcal{O}(1)$. More generally, non-unital noise can also induce local-scrambling exponentials.

Proof. By (D2) and (D3), we have

$$\mathcal{M}_a(t; \mathcal{S}_a, \mathcal{U}) = \mathbb{E}_U \left[\text{Var}_{\rho_{a_\tau} \sim \mathcal{S}_a} (\langle O \rangle_{\tau+t}) \right] \leq c e^{-\alpha t}. \quad (\text{D5})$$

Thus, on average over the Haar random reservoir U , the variance of the output with respect to the random input ρ_{a_τ} is at most $c e^{-\alpha t}$.

We next draw two i.i.d. states $(\rho_{a_\tau}, \sigma_{a_\tau})$ from the same distribution \mathcal{S}_a , representing two possible early inputs at time τ . Our goal is to bound

$$\left(\langle O \rangle_{\tau+t}^{(\rho_{a_\tau})} - \langle O \rangle_{\tau+t}^{(\sigma_{a_\tau})} \right)^2 \quad (\text{D6})$$

on average over both U and $(\rho_{a_\tau}, \sigma_{a_\tau})$.

First, fix the reservoir U . For each possible input $\rho_{a_\tau} \in \mathcal{S}_a$, define

$$X(\rho_{a_\tau}) = \langle O \rangle_{\tau+t}^{(\rho_{a_\tau})} - \mathbb{E}_{\rho'_{a_\tau} \sim \mathcal{S}_a} [\langle O \rangle_{\tau+t}^{(\rho'_{a_\tau})}], \quad (\text{D7})$$

thus centering the random variable $\langle O \rangle_{\tau+t}^{(\rho_{a_\tau})}$ by subtracting its mean value (averaged over $\rho'_{a_\tau} \sim \mathcal{S}_a$). Given two distinct inputs $(\rho_{a_\tau}, \sigma_{a_\tau})$, one can rewrite the difference

$$\langle O \rangle_{\tau+t}^{(\rho_{a_\tau})} - \langle O \rangle_{\tau+t}^{(\sigma_{a_\tau})} = (X(\rho_{a_\tau}) - X(\sigma_{a_\tau})) + \Delta_\mu, \quad (\text{D8})$$

where $\Delta_\mu = \mathbb{E}_{\rho'_{a_\tau} \sim \mathcal{S}_a} [\langle O \rangle_{\tau+t}^{(\rho'_{a_\tau})}] - \mathbb{E}_{\sigma'_{a_\tau} \sim \mathcal{S}_a} [\langle O \rangle_{\tau+t}^{(\sigma'_{a_\tau})}] = 0$ since the two initial states are drawn from the same ensemble \mathcal{S}_a and the rest of the sequence are identical. We will use the usual inequality $(x \pm y)^2 \leq 2x^2 + 2y^2$ (see the footnote ⁴). From $(x - y)^2 \leq 2x^2 + 2y^2$, one obtains

$$\left(\langle O \rangle_{\tau+t}^{(\rho_{a_\tau})} - \langle O \rangle_{\tau+t}^{(\sigma_{a_\tau})} \right)^2 = (X(\rho_{a_\tau}) - X(\sigma_{a_\tau}))^2 \leq 2X(\rho_{a_\tau})^2 + 2X(\sigma_{a_\tau})^2. \quad (\text{D9})$$

⁴ A quick way to see the inequality is to first expand $(x \pm y)^2 = x^2 \pm 2xy + y^2$. Then, note that $\pm 2xy \leq x^2 + y^2$, since $0 \leq (x \mp y)^2 = x^2 \mp 2xy + y^2$. Therefore, $(x \pm y)^2 \leq x^2 + y^2 + (x^2 + y^2) = 2x^2 + 2y^2$.

We now take expectations *first* over the random pair $(\rho_{a_\tau}, \sigma_{a_\tau})$ drawn i.i.d. from \mathcal{S}_a , and *then* over the random reservoir U . Observe that

$$\mathbb{E}_{\rho_{a_\tau}}[X(\rho_{a_\tau})^2] = \text{Var}_{\rho_{a_\tau} \sim \mathcal{S}_a}(\langle O \rangle_{\tau+t}^{(\rho_{a_\tau})}), \quad (\text{D10})$$

by definition of variance. The same argument applies to σ_{a_τ} . Hence, all terms inside that expectation in the RHS of (D9) are precisely

$$\mathbb{E}_U[\text{Var}_{\rho_{a_\tau} \sim \mathcal{S}_a}(\langle O \rangle_{\tau+t}^{(\rho_{a_\tau})})],$$

which is indeed $\mathcal{M}_a(t)$. Therefore, taking all the expectations together on both sides of (D9) yields

$$\mathbb{E}_{U, \rho_{a_\tau}, \sigma_{a_\tau}}[(\langle O \rangle_{\tau+t}^{(\rho_{a_\tau})} - \langle O \rangle_{\tau+t}^{(\sigma_{a_\tau})})^2] \leq 4\mathcal{M}_a(t). \quad (\text{D11})$$

Thus, on average, old inputs cause at most an exponentially small deviation in the output, once $\mathcal{M}_a(t)$ is exponentially small in t . \square

Note that inequality (D11) implies that once $\mathcal{M}_a(t)$ decays as $ce^{-\alpha t}$, any small change in the input at time τ leads to an *exponentially small* difference in the outputs at time $(\tau + t)$, *on average* over the reservoir ensemble and pairs of inputs. This reflects an *FMP-like* characteristic, such that old inputs are effectively forgotten at a rate set by α . By contrast, mathematical RC typically uses a more stringent, deterministic definition of FMP that requires *all* possible input variations to vanish in time [60]. In our QRP framework, the exponential concentration phenomena leads to the difference between outputs shrinking *exponentially* fast in t .

3. Exponential decay of $\mathcal{M}_h(t)$ implies Echo State Property (ESP)-like characteristics in QRP

Setting. Let ρ_{h_0} be the hidden qubits' initial state, while keeping all subsequent inputs $\rho_{a_1}, \rho_{a_2}, \dots$ in the accessible qubits fixed. After t steps of evolution, an observable O is measured, giving

$$\langle O \rangle_t^{(\rho_{h_0})} = \text{Tr}[O \rho_t], \quad (\text{D12})$$

where ρ_t is the resulting reservoir state (accessible and hidden qubits together). As in Definition 3 of the main text, we define

$$\mathcal{M}_h(t; \mathcal{S}_h, \mathcal{U}) = \mathbb{E}_U[\text{Var}_{\rho_{h_0} \sim \mathcal{S}_h}(\langle O \rangle_t)], \quad (\text{D13})$$

If $\mathcal{M}_h(t)$ is small, then $\langle O \rangle_t^{(\rho_{h_0})}$ barely depends on how the hidden qubits were initially prepared, implying the reservoir *forgets* its own initial condition. If one starts the reservoir in two distinct hidden-qubit states ρ_{h_0} and σ_{h_0} at the outset, the reservoir's outputs should eventually converge, given the *same* subsequent sequence of inputs. As discussed earlier, this intuitive ESP-like requirement guarantees the reservoir is well-defined on average, since one does not want the final outputs to spuriously depend on arbitrary preparation procedures from long in the past.

Supplemental Theorem 4 (ESP-like behavior from exponentially decaying $\mathcal{M}_h(t)$). *Suppose there exist constants $c' > 0$ and $\alpha' > 0$ such that*

$$\mathcal{M}_h(t; \mathcal{S}_h, \mathcal{U}) \leq c' e^{-\alpha' t} \quad \forall t \in \mathbb{N}. \quad (\text{D14})$$

Then the reservoir exhibits an ESP-like behavior: on average, the influence of the reservoir's initial hidden state decays exponentially. Specifically, consider two runs of the reservoir with the same time-series inputs $\{\rho_{a_1}, \dots, \rho_{a_t}, \dots\}$, but different reservoir's hidden-qubit initial states ρ_{h_0} and σ_{h_0} . Denote their final outcomes at time t by

$$\langle O \rangle_{(t)}^{(\rho_{h_0})} \quad \text{and} \quad \langle O \rangle_{(t)}^{(\sigma_{h_0})}. \quad (\text{D15})$$

Then, on average over random draws $\rho_{h_0}, \sigma_{h_0} \sim \mathcal{S}_h$ and $U \sim \mathcal{U}$,

$$\mathbb{E}_{U, \rho_{h_0}, \sigma_{h_0}} \left[\left(\langle O \rangle_{(t)}^{(\rho_{h_0})} - \langle O \rangle_{(t)}^{(\sigma_{h_0})} \right)^2 \right] \leq 4c'e^{-\alpha't}. \quad (\text{D16})$$

Hence, the two output trajectories converge exponentially quickly, irrespective of distinct hidden-state preparations in the far past. In other words, old initial conditions of the reservoir state are washed away, and the final outputs does echo the recent input signals.

Proof. The argument fully parallels the proof for FMP in Theorem 3. First, the assumption (D14) tells us that

$$\mathcal{M}_h(t) \equiv \mathbb{E}_U \left[\text{Var}_{\rho_{h_0} \sim \mathcal{S}_h} (\langle O \rangle_{(t)}) \right] \leq c'e^{-\alpha't}. \quad (\text{D17})$$

For any *fixed* reservoir evolution U , define the centered random variable

$$Y(\rho_{h_0}) \equiv \langle O \rangle_{(t)}^{(\rho_{h_0})} - \mathbb{E}_{\rho'_{h_0} \sim \mathcal{S}_h} [\langle O \rangle_{(t)}^{(\rho'_{h_0})}]. \quad (\text{D18})$$

One sees that $\mathbb{E}_{\rho_{h_0}} [Y(\rho_{h_0})] = 0$ and $\mathbb{E}_{\rho_{h_0}} [Y(\rho_{h_0})^2] = \text{Var}_{\rho_{h_0} \sim \mathcal{S}_h} (\langle O \rangle_{(t)})$. Next, let us compare two distinct initial hidden states, ρ_{h_0} and σ_{h_0} . Their outputs differ by

$$\langle O \rangle_{(t)}^{(\rho_{h_0})} - \langle O \rangle_{(t)}^{(\sigma_{h_0})} = (Y(\rho_{h_0}) - Y(\sigma_{h_0})) + \Delta_\mu, \quad (\text{D19})$$

where $\Delta_\mu \equiv \mathbb{E}_{\rho'_{h_0} \sim \mathcal{S}_h} [\langle O \rangle_{(t)}^{(\rho'_{h_0})}] - \mathbb{E}_{\sigma'_{h_0} \sim \mathcal{S}_h} [\langle O \rangle_{(t)}^{(\sigma'_{h_0})}]$. Since ρ_{h_0}, σ_{h_0} are *both* drawn from the same distribution \mathcal{S}_h , then $\Delta_\mu = 0$. Applying the usual inequalities $(x - y)^2 \leq 2(x^2 + y^2)$ to the squared of the previous equation yields

$$\left(\langle O \rangle_{(t)}^{(\rho_{h_0})} - \langle O \rangle_{(t)}^{(\sigma_{h_0})} \right)^2 \leq 2[Y(\rho_{h_0})^2 + Y(\sigma_{h_0})^2]. \quad (\text{D20})$$

Finally, taking the expectation over the i.i.d. draws $\rho_{h_0}, \sigma_{h_0} \sim \mathcal{S}_h$ and over $U \sim \mathcal{U}$, we get

$$\begin{aligned} \mathbb{E}_{U, \rho_{h_0}, \sigma_{h_0}} \left[\left(\langle O \rangle_{(t)}^{(\rho_{h_0})} - \langle O \rangle_{(t)}^{(\sigma_{h_0})} \right)^2 \right] &\leq 2 \mathbb{E}_{U, \rho_{h_0}, \sigma_{h_0}} [Y(\rho_{h_0})^2 + Y(\sigma_{h_0})^2] \\ &= 4 \mathbb{E}_U \left[\text{Var}_{\rho_{h_0} \sim \mathcal{S}_h} (\langle O \rangle_{(t)}) \right] = 4\mathcal{M}_h(t) \leq 4c'e^{-\alpha't}. \end{aligned} \quad (\text{D21})$$

This completes the proof of Eq. (D16). \square

Once $\mathcal{M}_h(t)$ decays as $c'e^{-\alpha't}$, any difference in the reservoir's initial hidden state ρ_{h_0} results in an *exponentially small* difference in outputs at time t *on average*, over both hidden-state pairs and the reservoir ensemble. This signifies an ESP-like characteristic: the system forgets initial conditions at a rate determined by α' . Note that mathematical RC typically adopts a more demanding, deterministic form of ESP [60]. It is important to emphasize again that in our QRP framework, the *exponential concentration* phenomena typically induce this rapid forgetting, exponentially fast in t .

4. Discussions on reservoir universality and the role of dissipation

In mathematical RC, if a sufficiently rich reservoir deterministically satisfies formal definitions of ESP and FMP (often via topological continuity or uniform state convergence), one can prove *universal approximation* of fading-memory filters [60, 61]. In our QRP framework, however, the memory indicators $\mathcal{M}_a(t)$ and $\mathcal{M}_h(t)$ yield a *probabilistic* statement on the exponential decay of old inputs and initial states, *on average*. While this forgetting is essential for operative QRP, it does *not* directly imply the deterministic criteria required by classical universality theorems. Whether there is a direct link to formal universality would require additional analysis beyond the scope of this work. Instead, our findings

emphasize that, under finite measurement shots, practical QRP faces a tension between scaling up the reservoir to handle more complex memory tasks and avoiding exponential concentration of outputs.

Moreover, realistic QRP platforms harness dissipation and decoherence as *resources* for RC scheme: they wash out old inputs or initial states to enforce FMP-like and ESP-like behaviors [38, 55, 56, 95, 96]. Such dissipative or measurement processes are useful for short-term time-series prediction. Hence, although existing universal approximation proofs typically rely on stronger deterministic definitions, our analysis highlights how dissipation and measurement can induce exponential concentration phenomena that realize decaying memory properties in QRP.